REGULATION OF THE ANAPHASE-PROMOTING COMPLEX BY PHOSPHORYLATION

Matthew Phillip Torres

A dissertation submitted to the faculty of the University of North Carolina at Chapel Hill in partial fulfillment of the requirements for the degree of Doctor of Philosophy in the Department of Biochemistry and Biophysics.

Chapel Hill
2007

Approved by,

Advisor: Dr. Christoph Borchers

Reader: Dr. William Marzluff

Reader: Dr. Henrik Dohlman

Reader: Dr. Yue Xiong

Reader: Dr. Robert Duronio

ABSTRACT

MATTHEW P. TORRES: Regulation of the anaphase-promoting complex by phosphorylation

(Under the direction of Dr. Christoph H. Borchers)

Regulation of the eukaryotic cell cycle is accomplished in large part by well-timed and targeted destruction of proteins that inhibit or activate passage through cell cycle transitions. Ubiquitin-mediated proteolysis is well established as the primary mechanism through which this occurs, and the anaphase-promoting complex (APC), an E3 ubiquitin ligase, is a vital regulatory component of this system. The APC is a multi-subunit complex required for cell cycle transitions that include progression through anaphase, exit from mitosis, as well as many events throughout meiosis. Two APC subunits, Apc2 and Apc11, are necessary for catalytic transfer of ubiquitin to target substrates, while the remaining subunits participate in a variety of regulatory mechanisms that coordinate APC activity with other cell cycle events. The primary mechanisms of APC regulation include co-activator protein association and phosphorylation of specific subunits in the complex. In budding yeast, two proteins, Mnd2 and Swm1, were identified by mass spectrometry after co-purification with the APC subunit, Cdc27. Here, I show that the APC co-purifies with epitope-tagged Mnd2 or Swm1 and that both proteins are present on the APC at stoichiometric levels throughout the mitotic cell cycle. Mnd2 that co-purifies with the APC is phosphorylated in a cell cycle dependent manner. Using a variety of mass spectrometry techniques, I found that phosphorylation occurs on a least 8 serine or threonine residues within the Mnd2 primary structure. Yeast

strains that harbor alanine phosphorylation site mutations in Mnd2 progress normally through pre-meiotic S phase, but are unable to progress efficiently through the first nuclear division of meiosis. In contrast, yeast harboring aspartic acid phosphorylation site mutations display a partial recovery of the wild type meiosis phenotype. Alanine phosphorylation site mutants also displayed low levels of the APC^{Ama1} meiotic substrate, Clb5. Taken together, these results demonstrate that Mnd2 is a stoichiometric component of the APC during mitosis and that Mnd2 phosphorylation is necessary for APC-mediated progression beyond the first meiotic nuclear division.

ACKNOWLEDGEMENTS

This thesis represents a great deal of time and hard work for which I cannot take all the credit. I am indebted to all those who have helped me throughout the process, some of whom I am aware, and others of who I am not. I am grateful to Dr. Christoph Borchers for providing me with the opportunity to work under his direction. I am also grateful to my committee members, Drs. Dohlman, Marzluff, Xiong, and Duronio, for their careful consideration of my research. In particular, I would like to single out Dr. Marzluff, who has always found time to speak with me about my work and my progress. I would also like to mention Dr. Dohlman for his selfless donation of time and support towards the end of my Ph.D. career.

Many others have contributed to my growth as a scientist as well. I thank Dr. Evgeniy Petrotchenko for his ever-stimulating conversation regarding my research and other worldly topics. I also thank *soon-to-be-Dr*. Mike Dial, who has been a good friend and ally during our time together in the lab. I am particularly grateful to Dr. Mark Hall, whose level of scientific professionalism I can only hope to reach one day.

I thank my family, especially my mother and father, for learning to grow with me over the course of my training. Most importantly, I am forever grateful to my wife Katie, who has been a wonderful and sturdy companion through all of our years together. Thanks also to my daughter, Lindsay, whose beautiful and generous smile lifts my spirit with every new day that passes. Anything done in their absence simply wouldn't be worth doing.

CONTENTS

LIST OF TABLES

LIST OF FIGURES

LIST OF ABBREVIATIONS AND SYMBOLS

AP	Alkaline phosphatase
APC	Anaphase-promoting complex
CDK	Cyclin-dependant kinase
Co-IP	Co-immunoprecipitation
Da	Daltons
E1	Ubiquitin activating enzyme
E2	Ubiquitin conjugating enzyme
E3	Ubiquitin ligating enzyme
ESI	Electrospray ionization
FACS	Flourescence activated cell sorter
G0	Quiescent phase of the cell cycle
G1	Gap 1 phase of the cell cycle between M phase and S phase
G2	Gap 2 phase of the cell cycle between S phase and M phase
GST	Glutathione-S-transferase
HPLC	High performance liquid chromatography
LC	Liquid chromatography
M	Mitosis phase in the cell cycle
MALDI	Matrix assisted laser desorption/ionization
MS	Mass spectrometry
MS/MS	Tandem mass spectrometry
m/z	mass-to-charge ratio
PAGE	Polyacrylamide gel electrophoresis

PSP	Pre-sporulation medium
PTM	Post-translational modification
S	DNA synthesis phase of the cell cycle
SCF	SKP1/CUL1/F-box complex
SDS	Sodium dodecyl sulfate
SPM	sporulation medium
TOF	Time-of-flight
Ub	Ubiquitin
Δ	Deleted
λP	Lambda phosphatase

CHAPTER I

INTRODUCTION

Cell cycle regulation, cyclin-dependent kinases, and ubiquitin-mediated proteolysis

The eukaryotic cell cycle is a highly coordinated sequence of molecular events in which one cell duplicates and divides its genetic content to produce two identical cells. Mis-regulating the molecular mechanisms responsible for cell cycle progression can lead to cell death, uncontrolled cell growth, or other forms of irreparable damage (McDonald and El-Deiry, 2001; Michalides et al., 2002; Pray et al., 2002; Yam et al., 2002). Consequently, eukaryotic cell survival depends on numerous molecular events that are precisely timed and tightly coordinated at the transitions between each cell cycle stage. Naturally, research that elucidates how these mechanisms work is fundamental to our understanding of disease biology, and most notably, cancer.

The eukaryotic cell cycle is divided into two major phases: S phase, during which the cell duplicates its genome by DNA synthesis; and mitosis or M phase, during which the duplicated genome is equivalently divided into two progeny cells. These two major events in the cell cycle are separated by two gap or growth stages/phases known as G1 and G2. M phase is further divided into sub-phases that involve the organization of replicated chromosomes (during Prophase and Metaphase) and their equivalent distribution into two progeny cells (during Anaphase and Telophase/Cytokinesis). Timely progression of the cell cycle is governed by regulating passage between cell cycle phases or sub-phases, and requires the coordination of molecular events that must occur before the cell can pass through each transition (Figure 1.1 A).

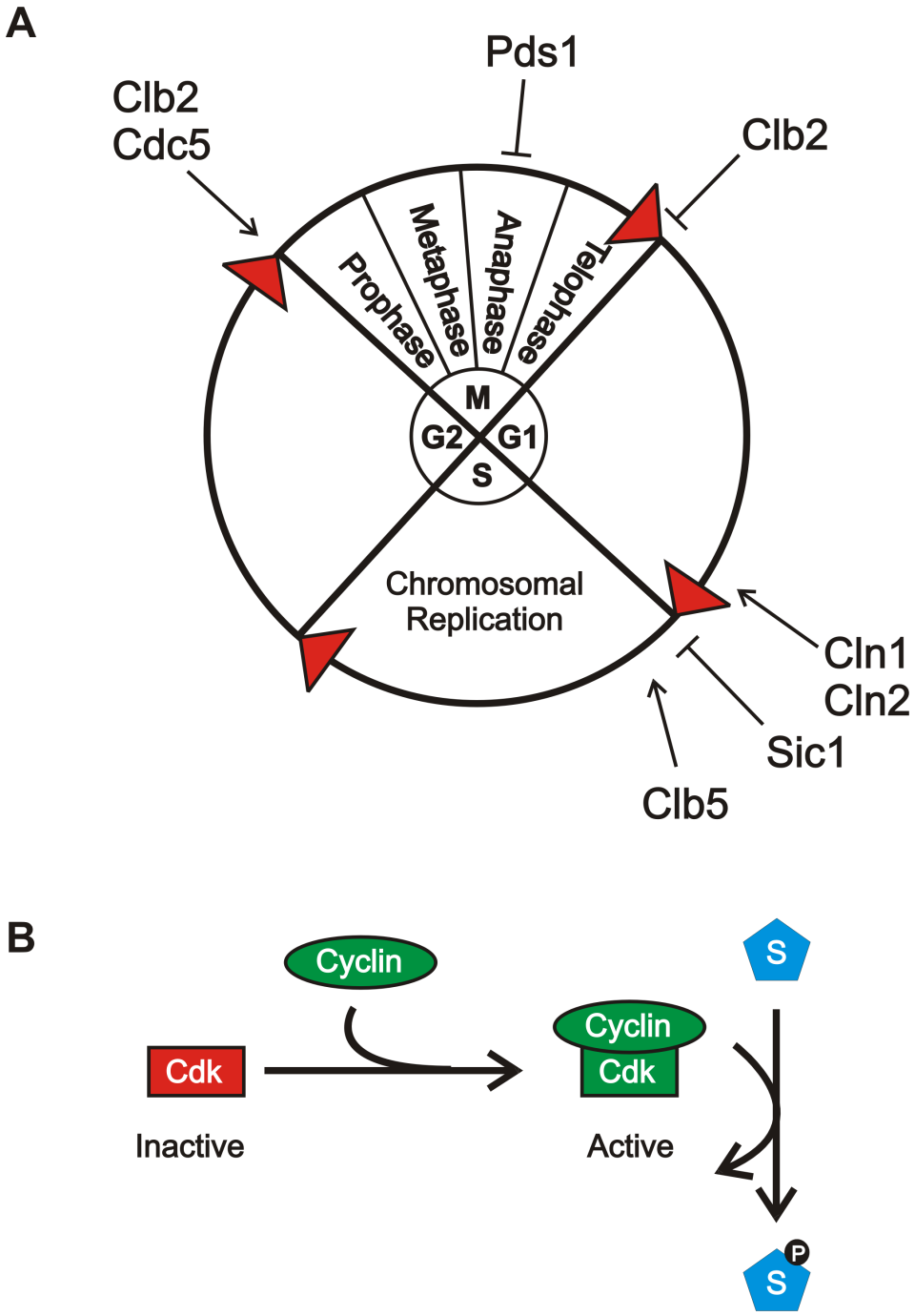

Figure 1.1. The cell cycle and major transition regulators. (A) Schematic diagram of the eukaryotic cell cycle and major regulators of cell cycle transitions including: B-type (Clb) and G1 (Cln) cyclins, the polo-like kinase (Cdc5), the CDK inhibitor (Sic1), and the anaphase inhibitor (Pds1). (B) CDKs are regulated by controlling the association of different cyclins, which activate the CDK and provide substrate specificity.

Reversible protein phosphorylation is a predominant post-translational modification (PTM) necessary for cell cycle progression. Proteins modified by phosphorylation may be affected in various ways such as allosteric activation, interaction specificity, binding affinity, or enzymatic activity (Johnson et al., 1987). Altering these fundamental characteristics of protein biochemistry often results in significant changes to protein function. Depending on the protein or protein complex involved, phosphorylation dependent changes may be manifested through alterations in sub-cellular localization, protein-protein interactions, or in the reactant/product ratios of a catalytic event. Thus, investigating phosphorylation-specific function for any given protein requires careful consideration of these possibilities.

Cyclin-dependent kinases (CDK) are two-component enzymes that drive the cell cycle by phosphorylating specific proteins at precise times (Mendenhall et al., 1987; Wittenberg and Reed, 1988) (Figure 1.1 B). In budding yeast, there is a single CDK, Cdc28, to which bind at least nine distinct cyclins during different times in the cell cycle (Murray, 2004). Binding of the cyclin activates the kinase and also confers kinase specificity. Regulating specific CDKs is accomplished by controlling the availability of cyclins through expression, degradation, localization, and through direct inhibition by CDK inhibitor proteins. Originally named for their cyclical appearance and disappearance in growing cells, the abundance of cyclins oscillates in harmony with the cell cycle (Evans et al., 1983). In budding yeast, the transition from G1 phase to S phase depends on G1 cyclins, Cln1 and Cln2, which bind and activate Cdc28 that in turn phosphorylates substrates necessary for S phase entry. An increase in Cln/Cdk activity throughout G1 phase results in increased phosphorylation and subsequent removal of the S phase Clb5/Cdk inhibitor, Sic1 (Dirick et al., 1995; Feldman et al., 1997; Mendenhall, 1993; Mendenhall et al., 1995; Schwob et al., 1994; Tyers, 1996). Once

released from inhibition, Clb5/Cdk can phosphorylate additional substrates that promote the initiation of chromosomal replication (Kuntzel et al., 1996; Schwob and Nasmyth, 1993). Similar to S phase entry, the transitions into and during M phase also require CDK. In this case B-type cyclins Clb1 and Clb2 activate Cdc28, and phosphorylate substrates necessary to promote M phase entry and progression through anaphase (Amon et al., 1993; Harper et al., 2002; Peters, 2002). Finally, transition from M phase back into G1 phase requires the removal of Clb2, which otherwise inhibits mitotic exit by phosphorylating proteins that maintain the mitotic state (Chang et al., 2004; Ghislain et al., 1993; Murray, 1989; Murray and Kirschner, 1989; Murray et al., 1989; Seufert et al., 1995).

While multiple CDKs are responsible for promoting cell cycle progression, passage through the transitions between cell cycle phases is regulated in large part by the destruction of proteins that inhibit cell cycle progression from one stage to the next. For example, the well-timed destruction of Pds1 (called *securin* in humans), which binds and inhibits the anaphase activator protein Esp1 (called *separase* in humans), is the initial trigger for chromosome segregation during anaphase (Ciosk et al., 1998; Cohen-Fix and Koshland, 1997; Cohen-Fix et al., 1996). Similarly, the well timed destruction of the CDK inhibitor, Sic1, at the end of G1 phase, allows cells to enter S phase (Marshall et al., 1998; Schwob et al., 1994).

Polyubiquitin-mediated proteolysis

The most common way in which cells degrade proteins in a time-resolved fashion is through polyubiquitin-mediated proteolysis (Figure 1.2). Polyubiquitin-mediated proteolysis is a 4-step enzymatic process ending in covalent modification of a target protein with

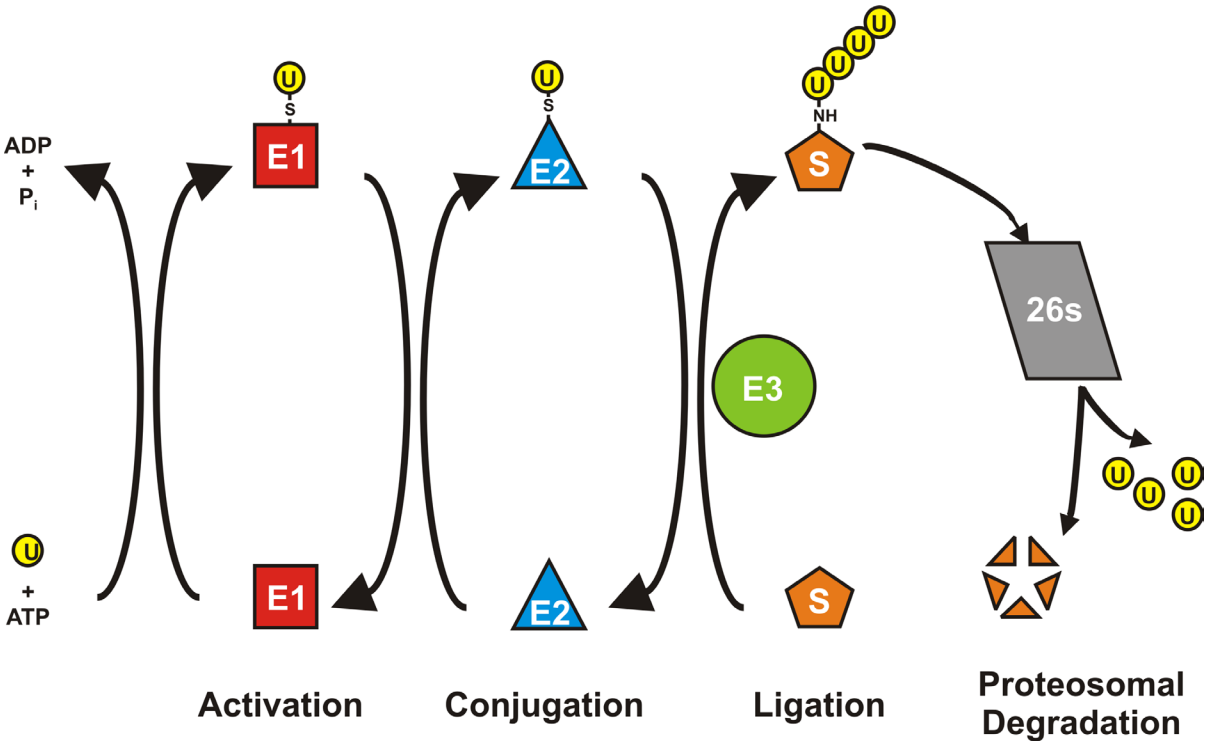

Figure 1.2. Polyubiquitin-mediated proteolysis. Note that the E3 in this case is of the RING family, and indirectly catalyzes the transfer of ubiquitin from the E2 to the substrate, which is different from the HECT E3 ligases that form a covalent intermediate with ubiquitin before transfer. The polyubiquitinated protein is recognized by specialized cap proteins in the 26s proteosome and deubiquitinated before degradation. The ubiquitin has a long half life and is recycled for additional round of ubiquitin ligation.

polymeric ubiquitin chains and subsequent degradation of the protein by the 26s proteosome (Pickart, 2001). In the first step, a ubiquitin-activating enzyme (E1) begins by hydrolyzing ATP to form a high energy thio-ester bond with the C-terminal glycine of ubiquitin, a small 8 kDa protein found in all eukaryotes. Second, the E1 transfers the ubiquitin to a cysteine residue on one of many possible ubiquitin-conjugating enzymes (E2). Third, the E2 enzyme associates with an ubiquitin ligase enzyme (E3), which catalyzes transfer of ubiquitin from the E2 to the ε-amino groups of lysine residues on the target substrate. Fourth, additional rounds of ubiquitination target Lys-48 within the previous ubiquitin itself, resulting in the formation of polyubiquitin chains that are recognized by the 26s proteosome (Chau et al., 1989; Harper et al., 2002; Henry et al., 1989; Scheffner et al., 1995; Thrower et al., 2000). The polyubiquitinated protein is selectively bound by the 19s caps that exist at either end of the proteosome, and then unfolded and thread through the 20s cylindrical structure in an ATP-dependent process. The protein is then cleaved into small peptide fragments by the proteolytic active sites lining the inner surface of the 20s sub-complex (Baumeister et al., 1998). The peptide remnants of the protein are released from the opposite end of the proteosome, and recycled by the cell. Ubiquitin is unconjugated from the protein by deubiquitinating enzymes before entering the 20s structure (Swaminathan et al., 1999; Zhu et al., 2005), and can be reused in the ubiquitination process.

Monoubiquitin-mediated proteolysis

Whereas polyubiquitination serves as a signal for proteosomal degradation of intracellular proteins, monoubiquitination has been found to serve as a signal for the internalization and trafficking of transmembrane proteins to the lysosome for degradation (Haglund et al., 2003;

Hicke, 2001a; Hicke, 2001b; Ho et al., 2002; Katzmann et al., 2002; Lucero et al., 2000; Raiborg et al., 2003; Sigismund et al., 2004; Terrell et al., 1998). Monoubiquitinated proteins are not efficiently targeted by the 26S proteosome (Beal et al., 1996). Rather, they are recognized by a series of receptors that contain specific monubiquitin-binding domains (Swanson et al., 2006) that trigger internalization of the transmembrane protein. Upon internalization, monoubiquitin serves as a signal for sorting proteins into multivesicular bodies (MVB), which in turn fuse with the lysosome (Haigler et al., 1979). Inside the lysosome, the small internal vesicles of the MVB, consisting of internalized transmembrane proteins, are degraded by proteases and lipases (Hurley and Emr, 2006; Katzmann and Wendland, 2005).

HECT and RING E3 ubiquitin ligases

The E3 ligase is of particular scientific interest because it is responsible for the specificity and timing of polyubiquitin-mediated proteolysis, and therefore a primary target for regulatory control by the cell. Two protein families constitute most known E3 ubiquitin ligases: HECT domain (homologous to E6-AP carboxy terminus) ligases or RING (really interesting new gene) ligases; and the two families differ in their mechanism of substrate ubiquitination (Scheffner et al., 1993; Scheffner et al., 1995). Whereas HECT domain ligases form a covalent thioester intermediate with ubiquitin before transfer to the substrate (Huibregtse et al., 1995), RING ligases catalyze the transfer of ubiquitin directly from the E2 to the substrate and without the formation of a covalent intermediate. HECT domain E3 ligases consist of a ~350-residue region that contains a strictly conserved cysteine residue positioned approximately 35 residues upstream from the C-terminus of the protein

(Huibregtse et al., 1995; Scheffner et al., 1993). The thiol side chain of this cysteine forms the thioester intermediate with ubiquitin. Substrate specificity of HECT domain ligases is provided by the unique N-terminus of each ligase, while the C-terminal HECT domain mediates E2 binding and ubiquitination (Huibregtse et al., 1993; Huibregtse et al., 1997; Olsen et al., 2006).

RING ligases belong to the RING finger family of proteins that contain zinc finger tertiary structures in which a series of histidine and cysteine residues are spaced in close proximity so as to allow coordination of two zinc ions (Borden and Freemont, 1996). Although the zinc finger itself is catalytically inert, it functions in concert with non-zinc finger regions (or proteins) to bind activated E2 enzyme and facilitate the conjugation of ubiquitin to the substrate. The crystal structure of the c-Cbl RING finger protein complexed with the E2 protein, UbcH7, shows that the active site thiol of UbcH7 (to which ubiquitin would be conjugated) is directed away from the RING finger structure (Zheng et al., 2003), and supports a model in which RING finger proteins facilitate ubiquitin transfer by serving as molecular scaffolds (Borden, 2000) that properly position the activated E2 enzyme in close proximity to the substrate. RING ligases often exist in multi-protein complexes that contain non-RING finger subunits utilized for substrate binding and specificity; however, single-subunit RING ligases also exist and utilize non-RING finger domains within their structure to bind substrates with high specificity (Hochstrasser, 1996; Loo et al., 2005; Reggiori and Pelham, 2002).

RING E3 ligases regulate cell cycle transitions

Two major RING E3 ligases regulate cell cycle transitions in eukaryotes (Peters, 1998):

the Skp1/Cul1/F-Box (SCF) complex, which regulates progression through the G1/S transition (Feldman et al., 1997; Schwob et al., 1994); and the anaphase-promoting complex (APC), which regulates progression through anaphase (Agarwal and Cohen-Fix, 2002; Ciosk et al., 1998) and exit from mitosis (Harper et al., 2002; Morgan, 1999; Tyers and Jorgensen, 2000). Both the SCF and APC are multi-subunit RING E3 ligases whose catalytic cores consist of a cullin or cullin-like subunit in close association with a RING finger protein. In addition, both SCF and APC contain subunits that function as substrate targeting factors (specificity factors or co-activators), which are critical for regulating substrate specificity. The SCF targets phosphorylated substrates that are recognized by one of many possible F-box proteins. The F-box protein can simultaneously bind to the Cul1 adapter protein, Skp1, and in so doing, positions the target substrate in close proximity to the activated E2 enzyme that associates with the Cullin/RING finger protein complex (Maniatis, 1999). Various combinations of Skp1-like adapters and different F-box proteins are utilized at different times during the cell cycle to regulate the timing and substrate specificity of the SCF. In addition, Cul1 can be differentially modified by the ubiquitin-like molecule, NEDD8, which inhibits the association of the SCF inhibitor, CAND1 (Liu et al., 2002).

APC substrates do not require phosphorylation to be targeted for polyubiquitination. Rather, the targeted substrate is recruited by one of two different co-activator proteins through association with specific degradation motifs on the substrate (Glotzer et al., 1991; Pfleger et al., 2001). The co-activator can simultaneously bind the substrate and adapter proteins on the APC (Fang et al., 1998b; Schwab et al., 1997; Visintin et al., 1997), thereby bringing the substrate into close proximity to the activated E2 enzyme bound to the cullin-like Apc2 subunit and the RING finger protein, Apc11. Regulating substrate-specific APC

activity is accomplished by phosphorylation of APC subunits and co-activators at different times during the cell cycle (Golan et al., 2002; Kramer et al., 2000; Rudner et al., 2000; Rudner and Murray, 2000). APC co-activators are also subject to regulation through binding with inhibitory proteins (Fang et al., 1998a; Reimann et al., 2001a; Reimann et al., 2001b; Song et al., 2004; Sudakin et al., 2001).

The APC ubiquitin ligase

General structure and enzymatic mechanism

The APC is the largest known RING E3 ubiquitin ligase, consisting of 11 different subunits (Zachariae et al., 1998b; Zachariae et al., 1996), and at least 2 different co-activators (3 in budding yeast) (Cooper et al., 2000; Visintin et al., 1997), giving the entire yeast complex a total mass of approximately 1700 kDa (Passmore et al., 2005) (Table 1.1). Although the function and regulation of the co-activators has been researched extensively, the function of many individual subunits had not been assigned at the onset of my research (Harper et al., 2002; Peters, 2002). The subunit composition of the complex appears to remain constant during the mitotic cell cycle (Bonenfant et al., 2003). However, one report has suggested the existence of multiple APC isoforms that localize to different regions within cells from *Drosophila* (Oda et al., 1999), although no other reports have tested this hypothesis.

APC-mediated ubiquitination is accomplished through the simultaneous and proximal association of activated E2 enzyme and substrate protein. The E2 enzyme is recruited by two subunits in the complex, Apc2 and Apc11 (Gmachl et al., 2000; Shahgholi et al., 2001), while association of substrates is facilitated by co-activator proteins that bind to the APC and

Table 1.1
APC subunits and co-activators

***S. cerevisiae* Name**	**M.W. (kDa)**	**Deletion Viability**	**Known Motifs**	**Known Yeast PTMs**	**Vertebrate Name**	***S. pombe* Name**
Apc1	196	Inviable	Rpn1/Rpn2 homology[c]		Apc1/Tsg24	Cut4
Apc2	96	Inviable	Cullin homology domain		Apc2	
Cdc16	95	Inviable	Tetratricopeptide repeats[d]	Phosphorylation	Apc6/Cdc16	Cut9
Cdc27	85	Inviable	Tetratricopeptide repeats	Phosphorylation	Apc3/Cdc27	Nuc2
Apc5	77	Inviable			Apc5	
Apc4	73	Inviable			Apc4	Cut2/Lid1
Cdc23	70	Inviable	Tetratricopeptide repeats	Phosphorylation	Apc8/Cdc23	Cut23
Apc9	30	Viable				
Apc10/Doc1	26	Viable[a]	DOC homology domain		Apc10	Apc10
Apc11	19	Inviable	RING-H2 finger domain		Apc11	Apc11
Cdc26	14	Viable			Cdc26	Hcn1
Co-activators		Viable				
Cdc20	67	Inviable	WD40 repeats	Phosphorylation	Cdc20	Slp1
Cdh1	63	Viable	WD40 repeats	Phosphorylation	Cdh1	Srw1/Ste90
Ama1	67	Viable[b]	WD40 repeats	Phosphorylation		

[a]Although viable, *apc10Δ* strains exhibit severely compromised growth rates due to low APC processivity (Carol et al., 2002; Passmore et al., 2003).

[b]Deletion of *AMA1* displays a meiotic arrest phenotype.

[c]Apc1 shares homology with a structural motif found in the 19s proteosome cap proteins, Rpn1 and Rpn2, which can bind multiubiquitin-binding proteins.

[d]Note that vertebrate APC contains an additional subunit not found in yeast, called Apc7, which also contains tetratricopeptide repeats.

position substrates in close proximity to the activated E2 enzyme (Eytan et al., 2006; Visintin et al., 1997; Zachariae, 2004). The APC may contribute more than just scaffolding for the co-activator/substrate and E2/ubiquitin since cryo-electron microscopic (cryo-EM) analysis shows a large conformational change in the human APC upon binding of the co-activator, Cdh1 (Dube et al., 2005). Furthermore, multimerization of the APC may also contribute to ubiquitination activity. Studies with budding yeast APC support this hypothesis, showing that monomer and dimer forms can be purified from cell extracts, with the dimer exhibiting greatly enhanced ubiquitination processivity (Passmore et al., 2005).

Subunits and co-activators of the APC

Apc2 and Apc11. Apc2 and Apc11 constitute the catalytic core of the APC, and are responsible for recruiting activated E2 enzyme to the complex (Gmachl et al., 2000; Shahgholi et al., 2001). Apc2 contains a cullin-homology domain similar to the cullin proteins found in all SCF complexes (Loo et al., 1992). Apc11, which is homologous with ROC1 of the SCF (Ohta et al., 1999), tightly associates with the cullin-homology domain of Apc2, and contains the RING finger domain that is necessary for recruitment of the E2 enzyme. Apc2 and Apc11 have been shown to be the minimal subunit requirement for ubiquitination *in vitro*, although this activity does not display substrate specificity (Leverson et al., 2000). *In vitro*, Apc11 alone can bind to the E2, Ubc4, and promote ubiquitination of substrates, while binding to another E2, Ubch10, requires both Apc11 and the C-terminal cullin-homology domain of Apc2 (Shahgholi et al., 2001).

Tetratricopeptide repeat containing proteins: Cdc16, Cdc27, and Cdc23. Three yeast APC subunits, (Cdc16, Cdc27, and Cdc23) contain tetratricopeptide repeat (TPR) motifs that are

critical for the function of the APC (Dube et al., 2005; Thornton et al., 2006; Vodermaier et al., 2003). The TPR is a degenerate 34 amino acid sequence found in tandem arrays of 3 – 16 motifs that often provides scaffolding for protein-protein interactions (Das et al., 1998). Assembly of human APC sub-complexes lacking TPR subunits can assemble poly-ubiquitin chains, but are incapable of binding to the co-activator protein Cdh1. In comparison, assembly of a sub-complex lacking only Apc2 and Apc11 can bind Cdh1, but does not exhibit ubiquitin ligase activity (Vodermaier et al., 2003).

Although the TPR subunits have been clearly shown to mediate co-activator binding, the specific functional roles of each TPR subunit is currently unclear. Recent studies have shown that TPR subunits act as docking sites for APC co-activator proteins. In particular, Cdc27 has been implicated as the primary docking site for the co-activator Cdh1 (Kraft et al., 2005; Vodermaier et al., 2003), and also possibly Cdc20 (Kraft et al., 2005). However, APC purified from *cdc27Δ* cells retains some level of ubiquitin ligase activity, while APC lacking *cdc16* is completely inactive (Thornton et al., 2006), suggesting that co-activators can bind subunits other than Cdc27 in a productive fashion. In addition, each TPR subunit is phosphorylated in a manner that affects co-activator association (Rudner et al., 2000; Rudner and Murray, 2000) (discussed below).

Apc10/Doc1. Apc10 is a 26 kDa subunit containing a 'DOC' domain that is also found in cullins and HECT domain proteins (Grossberger et al., 1999). Although deletion of Apc10 does not destabilize APC structure (Grossberger et al., 1999), the processivity of ubiquitination is significantly reduced in its absence, which may be due to slower rates of substrate dissociation (Carroll and Morgan, 2002). Apc10 may also be required for some degree of substrate recognition since the association of APC substrates, Clb2 and Hsl1, with

APC/co-activator complexes is lost when Apc10 is absent from the complex (Passmore et al., 2003). Interestingly, Apc10, like the APC co-activators, contains a C-terminal IR-tail (ILR in budding yeast) and binds to Cdc27 (Wendt et al., 2001) as well as Apc11 (Shahgholi et al., 2001). Therefore, it has been proposed that Apc10 may be involved in stabilizing sub-complexes of the APC in a conformational change during co-activator/substrate association (Castro et al., 2005; Thornton and Toczyski, 2006) (discussed below).

Apc1, Apc4, and Apc5. Apc1 is the largest of all the APC subunits, and at 196 kDa, is nearly twice the size of the next largest subunit. The function of Apc1 appears to be largely structural, acting as a scaffold upon which APC sub-complexes are arranged (Thornton et al., 2006). Interestingly, Apc1 shares a structural motif with the Rpn1 and Rpn2 subunits found in the 19s cap of the proteosome (Lupas et al., 1997), and is capable of binding to multi-ubiquitin-binding proteins (Seeger et al., 2003), although the functional significance is unclear. In addition to the TPR subunits, Apc1 is the only other yeast subunit known to be phosphorylated *in vivo* (Peters et al., 1996).

Apc4 and Apc5 may strictly be required to maintain the structural integrity of the APC as there have been no indications that either protein is directly involved in ubiquitination or APC regulation. However, both proteins are required for enzymatic activity, possibly through maintaining the link between Apc1 and the sub-complex containing the TPR subunits (Thornton et al., 2006; Vodermaier et al., 2003).

Apc9 and Cdc26. Both Apc9 and Cdc26 have been found in sub-complexes with the TPR subunits and Apc1, and are required for maintenance of APC structure (Thornton et al., 2006). Mutations to Apc9 exhibit only minor defects in substrate degradation in α-factor arrested cells, and delayed Clb2 (but not Pds1 or Clb5) degradation in cycling cells, which

suggests that it may be involved in substrate selectivity specifically mediated through Cdh1 during G1 phase of the cell cycle (Page et al., 2005). Cdc26 is the smallest APC subunit and has been described for both yeast (Zachariae et al., 1998b) and vertebrates (Gmachl et al., 2000). Cdc26 associates directly with Cdc16 (Thornton et al., 2006), and loss of Cdc26 results in loss of Cdc27 and Cdc16 that is potentially mediated through Apc9 (Schwickart et al., 2004).

Co-activator proteins Cdh1, Cdc20, and Ama1. In addition to the subunits that constitute the APC, there are three distinct co-activator proteins (Cdh1, Cdc20, and Ama1) that associate temporarily with the complex to facilitate APC substrate specificity and recruitment. The first indication of the existence of APC co-activators was found in *Drosophila*, when mutations to the gene encoding Cdc20 (known as Fizzy) blocked mitotic degradation of cyclins A, B, and B3 (Sigrist et al., 1995). Later studies in *Drosophila* discovered the existence of an additional co-activator with high homology to Fizzy, called Fizzy-related, which was required for G1 cyclin removal and is now known as Cdh1 (Sigrist and Lehner, 1997). Similar functions were ascribed for Cdc20 and Cdh1 in the budding yeast (Schwab et al., 1997; Visintin et al., 1997). Finally, a third co-activator with high homology to Cdc20, called Ama1, was found to be expressed only during meiosis in yeast by microarray analysis (Janek et al., 2001). Later, the AMA1 gene was found to contain an intron that required meiosis-specific splicing factors for proper protein expression (Cooper et al., 2000). At the onset of this report, Ama1 had been shown to be responsible for degradation of the meiosis-promoting cyclin Clb1 (Cooper et al., 2000).

APC co-activators belong to a conserved family of WD40 proteins, members of which contain a WD40 propeller domain that has been described for numerous proteins including

the Gβ subunits of trimeric G proteins (Henry et al., 1989), as well as F-box proteins of the SCF complex (Wu et al., 2003). The WD40 propeller domain consists of 4-8 blades, where each blade is constructed of a 4-stranded anti-parallel β-sheet that provides a platform for stable or reversible protein binding (Orlicky et al., 2003). In F-box proteins, the WD40 domain mediates substrate binding for the SCF ubiquitin ligase (Patton et al., 1998). Recent evidence in yeast suggests that APC co-activators also use the WD40 domain as a substrate receptor. Using photochemical crosslinking in combination with mutational analysis, an evolutionarily conserved region of the WD40 propeller structure of Cdh1 and Cdc20 was found to interact specifically with the APC substrates cyclin B and securin (Kraft et al., 2005). In addition, Cdh1 binding to cyclin A was found to be dependent on a short cyclin-binding motif (RVL) found in the WD40 domain and conserved across all co-activators (Ho et al., 2002).

While it appears that APC co-activators utilize the WD40 domain for substrate binding, association of the co-activator with the APC is dependent on two motifs found in the N- and C-terminus of the protein. Association of the co-activator with the APC is mediated through the TPR subunits, most notably Cdc27 and Cdc16 (Kraft et al., 2005; Thornton et al., 2006; Vodermaier et al., 2003), and depends on the presence of a C-terminal isoleucine-arginine dipeptide (IR-tail), as well as a short, seven amino acid N-terminal motif known as the C-box (DR(F/Y)IPxR) (Schwab et al., 2001; Vodermaier et al., 2003), which is conserved across all APC co-activators from yeast to vertebrates. Mutation of the C-box results in a complete loss of ligase activity, while mutation of the IR-tail results in reduced, but not eliminated activity (Vodermaier et al., 2003). Consistent with this data, others have shown that the IR-tail is dispensable for yeast viability and that the C-box is the primary functional interaction

site between Cdh1 and the APC (Thornton and Toczyski, 2006). The association of the co-activators with substrate and with the APC is heavily regulated by phosphorylation and by direct protein-protein interactions (discussed further below).

APC subunits are organized into sub-complexes. The ability to delete entire genes in yeast has led a few groups to look at APC structure in terms of sub-complex organization. Using a yeast strain in which the APC is rendered non-essential (*pds1Δ, clb5Δ, SIC1*^{10x}) (Thornton et al., 2004; Thornton and Toczyski, 2003), Thornton et al. purified Apc1 via a C-terminal TAP (tandem affinity purification) epitope tag in the absence of individual APC subunits (*apc2Δ, apc11Δ, cdc27Δ, cdc16Δ cdc23Δ, apc4Δ, apc5Δ*). Analysis of the resulting sub-complexes reveals a model of APC in which two main sub-complexes exist: one containing the TPR subunits (Cdc27, Cdc16, and Cdc23), as well as Apc9, Cdc26, Apc4, and Apc5; and the other, containing Apc2, Apc11, and Apc10. The two sub-complexes are bridged by the largest subunit, Apc1 (Figure 1.3). This recent model of APC subunit topology is supported by previous independent analyses (Schwickart et al., 2004; Vodermaier et al., 2003; Zachariae et al., 1998b). The model is particularly intriguing because it provides testable hypotheses that could explain the role of Apc10 as a potential mediator of APC conformational changes that have been observed at low resolution by cryo-EM (Dube et al., 2005).

Regulation of the APC

Regulation by co-activator proteins

Co-activator substrate specificity. The APC directs time-resolved ubiquitin-mediated proteolysis of a growing list of at least 15 known distinct substrates involved in anaphase

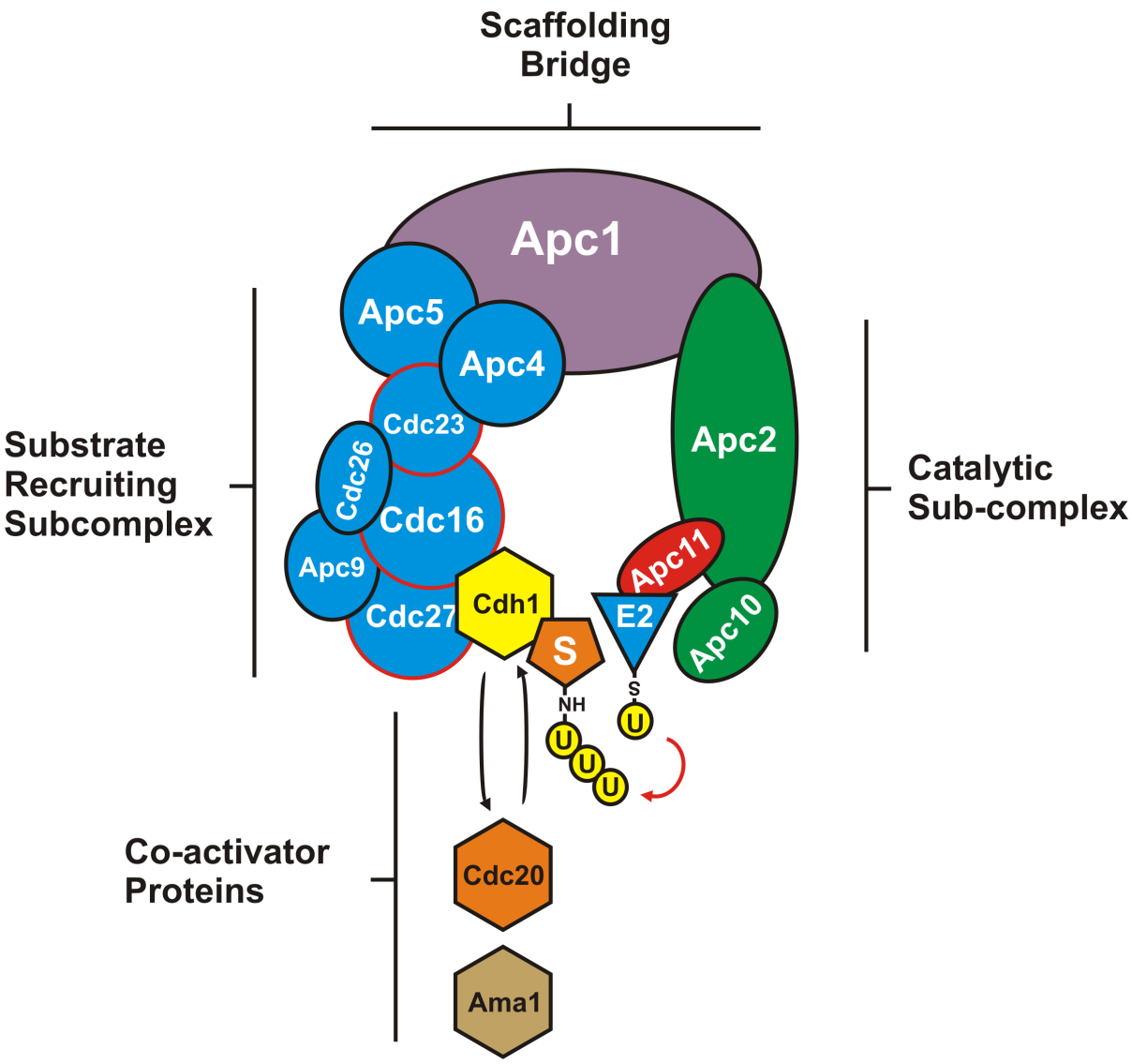

Figure 1.3. The APC ubiquitin ligase. Current model of the multisubunit APC E3 ligase showing two distinct sub-complexes connected by an Apc1 scaffold. The subcomplex shown in blue consists of the TPR proteins (outlined in red), which associate with the co-activator proteins to recruit substrates. The subcomplex shown in green and red consists of the catalytic subunits, Apc2 and Apc11, as well as the processivity factor, Apc10. Ubiquitination of substrates is accomplished through a mechanism in which the activated E2 enzyme is positioned in close proximity to the co-activator-bound substrate. (Figure adapted from Thornton et al., 2004).

inhibition, exit from mitosis, and other cell cycle events (Harper et al., 2002; Peters, 1999; Peters, 2002; Reed, 2003). Recruitment of substrates to the APC is accomplished through the temporary association of one of three different co-activator proteins, Cdc20, Cdh1, or Ama1, each of which display distinct substrate specificities (Pfleger et al., 2001; Sigrist et al., 1995; Sigrist and Lehner, 1997). Whereas the APC substrates, Pds1 and Clb5, can be recruited by Cdc20, they cannot be recruited by Cdh1 (Hilioti et al., 2001; Shirayama et al., 1999; Visintin et al., 1997). Conversely, the APC substrates Clb3 and Cdc5 appear to require Cdh1 for degradation (Schwab et al., 2001).

The substrate selectivity of different co-activators is due in-part to transposable degradation signals found in the primary sequence of the substrates. The first such degradation signal was found in cyclin B/Clb2 and called a destruction or 'Dbox', consisting of the 9 amino acid degenerate sequence that includes the consensus RxxL (Glotzer et al., 1991), and necessary for all Cdc20-dependent degradation (Eytan et al., 2006). A second degradation signal, called the KENbox is necessary for Cdh1-mediated degradation of Cdc20 (Pfleger and Kirschner, 2000), and was later found to exist in other substrates such as Aurora A, and Hsl1, which contain the KENbox in addition to a Dbox (Burton and Solomon, 2001; Castro et al., 2002a; Littlepage and Ruderman, 2002). While the Dbox is required for Cdc20 degradation, Cdh1 can target both Dbox and KENbox containing proteins (Pfleger and Kirschner, 2000; Zur and Brandeis, 2002). Mutation of the Dbox or KENbox can stabilize the associated protein (Pfleger and Kirschner, 2000). Furthermore, both boxes are transposable, such that addition of either box stimulates the degradation of any protein into which it is inserted (Pfleger and Kirschner, 2000; Zur and Brandeis, 2002). The co-activators are capable of binding to their substrates in the absence of the APC (Pfleger et al., 2001), and

binding of a substrate's Dbox or KENbox appears to enhance binding of the co-activator with the APC (Burton et al., 2005). In addition to the Dbox and KENbox, some proteins also contain a Dbox-activating-domain known as the Abox (Castro et al., 2002b; Littlepage and Ruderman, 2002), which has been found to regulate Dbox-dependent protein degradation in a phosphorylation-dependent fashion.

Inhibition of APC co-activators. APC co-activators are regulated through a variety of inhibition mechanisms that prevent substrate recruitment and APC activation. Co-activator inhibition is necessarily coordinated in a timely fashion with other cellular processes, such as cyclin accumulation and formation of the mitotic spindle assembly, to promote proper cell cycle progression. For instance, accumulation of the mitosis promoting factor cyclin B, which begins in S phase and increases through M phase, requires that the APC is maintained in an inactive state. Inactivating the APC from S through M phase is accomplished through direct inhibition of the Cdc20 co-activator, which is itself upregulated at the same time (Spellman et al., 1998). Cdc20 is inhibited by a sequence of multiple inhibitor proteins that are themselves regulated to promote cell cycle progression (Figure 1.4). During S and G2 phase, Cdc20 is inhibited by the F-box protein, Emi1 (early mitotic inhibitor 1), which is upregulated during S phase and then promptly degraded by ubiquitin-mediated proteolysis during mitosis (Reimann et al., 2001a). Emi1 can bind to Cdc20 and inhibit cyclin ubiquitination *in vitro*; and immunodepletion of Emi1 from *Xenopus* extracts creates a delay in cyclin B accumulation and the onset of mitosis (Reimann et al., 2001a). Recent evidence suggests that Emi1 acts as a pseudosubstrate inhibitor. Reimann et al. show that Emi1 can bind and inhibit Cdh1 from activating the APC (Reimann et al., 2001b) by acting as a pseudosubstrate that competes with true substrates for binding to the Dbox receptor sites of

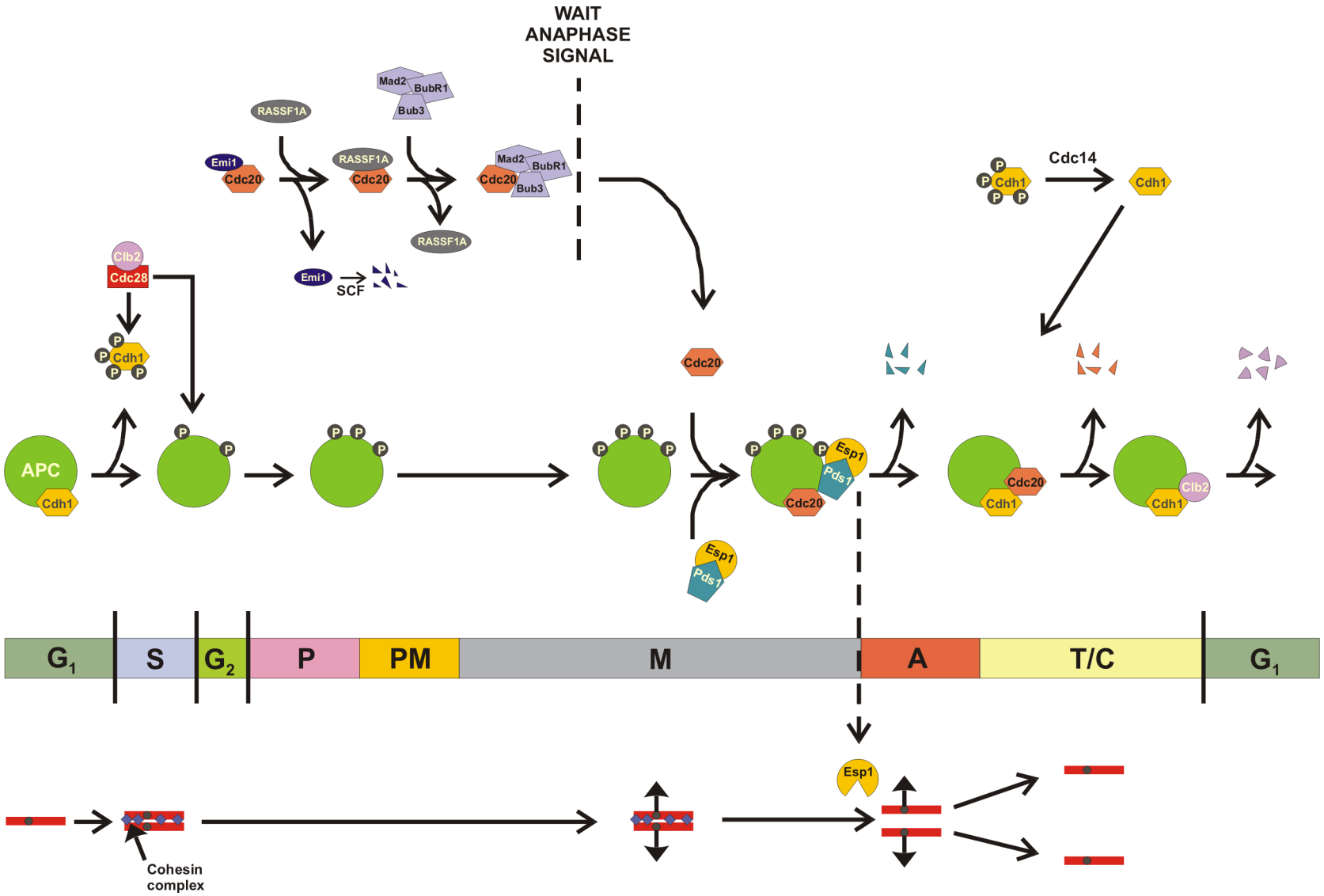
WAIT
ANAPHASE
SIGNAL
RASSF1A
Mad2
BubR1
Bub3
Emi1
Cdc20
SCF
Clb2
Cdc28
Cdh1
APC
Cdc14
Esp1
Pds1
G1
S
G2
P
PM
M
A
T/C
Cohesin
complex

Figure 1.4. APC regulation by co-activators and phosphorylation. Schematic diagram of the APC during the mitotic cell cycle, showing the major regulatory events including phosphorylation and direct inhibition by co-activator binding proteins. APC is increasingly phosphorylated by Clb2/Cdc28 CDK (and throughout S phase, G2 phase, and maximal during M phase. Phosphorylation of the APC is required for association of the co-activator, Cdc20, while phosphorylation of the co-activator, Cdh1, inhibits its association with the APC. Inhibition of Cdh1 allows accumulation of Cdc20 through G2/M phase, but the APC remains inactive by Cdc20 inhibition through association with Emi1, RASSF1A, and the spindle assembly checkpoint proteins, Mad2, BubR1, and Bub3. Cdc20 is inhibited by a "wait anaphase" signal that is generated by the spindle assembly checkpoint and is tightly linked with tension sensing mechanisms that communicate the status of chromosome/microtubule attachment. The "wait anaphase" signal is maintained until sister chromatids are properly aligned and attached to opposite spindle poles. Once released from inhibition, Cdc20 is free to activate the APC towards the anaphase inhibitor, Pds1 (also called securin), which is degraded by the ubiquitin machinery. Degradation of Pds1 frees the anaphase activator, Esp1 (also called separase), which proteolyses the cohesin subunit Scc1, thereby breaking cohesion between sister chromatids and resulting in anaphase. During telophase/cytokinesis, Cdh1 becomes dephosphorylated by the Cdc14 phosphatase that is released as part of a mitotic exit network mechanism. Dephosphorylated Cdh1 again activates the APC towards Cdc20 and Clb2, leading to exit from mitosis and completion of the cell cycle. The APC is also dephosphorylated at this time, possibly by multiple phosphatases including protein phosphatase 2A and Cdc14. Note that Emi1 and RASSF1A are human proteins with no known orthologues in yeast.

APC^{Cdh1} complexes (Craig et al., 1994). Moreover, they show that Emi1 contains a zinc-binding region that antagonizes APC E3 ligase activity (Craig et al., 1994). Once cells have progressed to prometaphase of mitosis, Emi1 is degraded and replaced by the inhibitor RASSF1A (Song et al., 2004), a tumor suppressor gene that is silenced in lung cancers and other sporadic tumors (Burbee et al., 2001; Dammann et al., 2000; Dreijerink et al., 2001; Shivakumar et al., 2002). Inhibition of APC^{Cdc20} by RASSF1A occurs through direct binding with Cdc20 and prevents premature degradation of cyclin B during prometaphase (Song and Lim, 2004). In addition, silencing of RASSF1A results in elevated levels of polyubiquitinated cyclin B and premature anaphase progression. Unlike Emi1, RASSF1A is strictly an APC^{Cdc20} inhibitor, and does not bind to Cdh1 or block cyclin ubiquitination by APC^{Cdh1} *in vitro* (Song et al., 2004). Neither Emi1 nor RASSF1A have a known orthologue in yeast.

As cells progress through prometaphase, Cdc20 becomes the target of the spindle assembly checkpoint mechanism, which inhibits the onset of anaphase until the kinetochores of sister chromatids are attached in a bi-oriented fashion to opposite spindle poles (Musacchio and Hardwick, 2002). Inhibition of Cdc20 by the spindle checkpoint is accomplished through formation of a mitotic checkpoint complex (MCC) consisting of the proteins Mad2, BubR1, Bub3, and Cdc20 (Fang et al., 1998a; Sudakin et al., 2001). Mad2, BubR1, and Bub3 localize to kinetochores during prometaphase, where they receive a "wait anaphase" signal that promotes formation of the MCC (including Cdc20) when there is either a lack of kinetochore/microtubule attachment or a lack of tension that exists when sister chromatids are improperly attached to opposite spindle poles (Stern and Murray, 2001). Although each component of the MCC can individually bind and inhibit Cdc20, the complex

is formed through cooperative binding that enhances the potency of Cdc20 inhibition (Fang, 2002). Coordinating Cdc20 inhibition with spindle assembly is critical to preserve Pds1, which binds and inhibits Esp1, a protease that eliminates sister chromatid cohesion by degrading the cohesin subunit Scc1 (Ciosk et al., 1998; McGrew et al., 1992; Tinker-Kulberg and Morgan, 1999; Uhlmann et al., 1999). Upon proper spindle attachment of each sister chromatid, Cdc20 is freed from the MCC, and recruits Pds1 to the APC where it is polyubiquitinated and subsequently degraded by the 26s proteosome (Ciosk et al., 1998; Tinker-Kulberg and Morgan, 1999). The removal of cohesion between sister chromatids, combined with the pulling force exerted on each chromatid by the spindle assembly, results in rapid separation of sister chromatids to opposite poles of the cell during anaphase (Musacchio and Hardwick, 2002). The mitotic spindle assembly checkpoint mechanism and the MCC exist and function similarly in budding yeast.

After anaphase, Cdc20 itself becomes a substrate of the APC, and is recruited by the Cdh1 co-activator (Shirayama et al., 1998). However, Cdh1 also targets other mitosis-promoting proteins such as the kinases Cdc5 and Clb2 (Kramer et al., 2000; Shirayama et al., 1998), and therefore, must be inhibited from premature APC activation in early mitosis. Cdh1 is inhibited by CDK phosphorylation that acts to block association with the APC (Blanco et al., 2000; Kramer et al., 2000; Zachariae et al., 1998a). Cdh1 phosphorylation occurs at the onset of S phase, mediated by Clb5/Cdk, Cln/Cdks, and Cdc5 (Amon et al., 1994; Hall et al., 2004; Oda et al., 1999; Yeong et al., 2001), and continues through M phase (Kramer et al., 2000) until late telophase when it becomes dephosphorylated by the phosphatase Cdc14 (Jaspersen et al., 1999; Visintin et al., 1998), which is sequestered in the nucleolus until then (Shou and Naidong, 2005; Visintin et al., 1999). After cells exit mitosis and undergo

cytokinesis, Cdh1 remains active during G1 phase and maintains low levels of B-type cyclins, thereby inhibiting premature S phase entry (Irniger and Nasmyth, 1997).

Regulation by Phosphorylation

A mechanism in which phosphorylation co-regulates APC activity in conjunction with the co-activator proteins has been suggested (Harper et al., 2002; Kotani et al., 1999; Page and Hieter, 1999; Peters, 2002; Zachariae and Nasmyth, 1999). Early experiments in *Xenopus* and clam revealed that interphase (G1) APC activity was stimulated by mitotic CDK (Felix et al., 1990; Hershko et al., 1994; Lahav-Baratz et al., 1995; Shteinberg et al., 1999). More thorough analyses with human APC exposed both activating and deactivating forms of phosphorylation by CDK, polo-like kinase (PLK, Cdc5 in budding yeast), and cAMP-dependent protein kinase A (PKA) *in vivo* (Kotani et al., 1998). Overexpressing PLK in human cells resulted in phosphorylation of Cdc16, Cdc27, and Apc1 and correlated with elevated APC activity, while constitutive activation of PKA by cyclic AMP resulted in phosphorylation of Apc1 and correlated with reduced APC activity *in vivo*. The same subunits were phosphorylated in the presence of both kinases but APC activity was suppressed (Kotani et al., 1998). In addition, alanine mutations of putative cyclin-dependant kinase (CDK) sites in the budding yeast APC subunits Cdc16, Cdc27, and Cdc23, resulted in compromised APC^{Cdc20} activity towards Clb2 and Pds1 *in-vivo*, as well as a delay in the onset of anaphase (Rudner et al., 2000; Rudner and Murray, 2000). CDK consensus sequences within Cdc16, Cdc27, and Cdc23 could also be phosphorylated *in vitro* by Cdc28 (Rudner et al., 2000; Rudner and Murray, 2000). However, mutation at these sites did not abrogate phosphorylation by PLK *in vitro*, and cells harboring mutated PLK displayed

reduced phosphorylation *in vivo*, indicating that additional non-CDK phosphorylation regulates APC activity. Later, mass spectrometric characterization of APC purified from HeLa cells revealed numerous phosphorylation sites on these same TPR subunits as well as Apc1, Apc4, Apc5, and Apc7, although only half could be recapitulated by Cdk1 or Plk1 *in vitro*, suggesting the involvement of additional kinases (Kraft et al., 2003). The most notable experimentally determined biophysical effect of APC phosphorylation is on the association of the Cdc20 co-activator during mitosis. Using APC purified from either interphase or M phase *Xenopus* oocytes or human cells, Kramer et al. demonstrated that only M phase APC could be activated by Cdc20 *in vitro* (Kramer et al., 2000). Moreover, phosphatase treatment of the M phase APC eliminated Cdc20 co-immunoprecipitation with Cdc27 and resulted in significantly lower ubiquitin ligase activity *in vitro*. In contrast, Cdh1 binding and activation of the APC was unaltered (Kramer et al., 2000).

The APC in meiosis

The bulk of current evidence on APC-mediated cell cycle regulation comes from research on mitotic cells. Comparatively, our understanding of pathways governing the passage through meiotic cell cycle transitions is just beginning. In this section, I describe the meiotic cell cycle as it pertains to budding yeast, and go further to describe what is known about the involvement of the APC in this process.

Meiosis in Saccharomyces cerevisiae

Meiosis is a specialized gametogenic cell cycle in which diploid cells (cells containing two copies of each chromosome; called homologous chromosomes with *2n* DNA content)

undergo one round of DNA replication followed by two successive nuclear divisions that result in the formation of four haploid progeny (each containing a single copy of each chromosome or *1n* DNA content). Meiosis is divided into two distinct nuclear divisions, meiosis I (MI) and meiosis II (MII), each of which consists of prophase (prophase I or II), metaphase (metaphase I or II), and anaphase (anaphase I or II).

Yeast undergo meiosis as a "protective" response to sub-optimal environmental levels of nitrogen and a fermentable carbon source (e.g. glucose) in a process called *sporulation*. Sporulation consists of two overlapping processes, meiotic nuclear division and spore morphogenesis, the completion of which results in the formation of four haploid spores (Clancy, 1998; Janek et al., 2001). The biological mechanisms involved in controlling the transitions through meiotic nuclear division are well conserved throughout eukaryotes, making yeast a very useful model organism for studying meiosis.

Meiosis I. The first nuclear division, MI, is commonly referred to as the meiotic division, and is fundamentally different from mitosis because homologous chromosomes, but not sister chromatids, are segregated to opposite spindle poles. This requires that microtubule attachment to the kinetochores of each homologous chromosome is mono-oriented (as opposed to bi-oriented), resulting in the segregation of sister chromatids to the same pole. This type of spindle attachment is only possible during MI, since mono-orientation of sister chromatids during mitosis would fail to generate the tension necessary to escape the spindle checkpoint mechanism. Even so, tension is also used as a signal for proper spindle assembly during MI, but is generated through two physical connections: cohesion between sister chromatids provided by a meiotic cohesin protein complex and *chiasmata*, which provide a DNA bridge between chromatids of neighboring homologous chromosomes (Petronczki et

al., 2003). During pre-meiotic S phase in budding yeast, as chromosomes are being replicated, a cohesin complex in which the mitosis-specific subunit Scc1 is replaced by the meiosis-specific subunit Rec8, links sister chromatids together along the entire length of their chromosome arms (Klein et al., 1999; Watanabe and Nurse, 1999). Induction of the meiotic program after mitotic DNA replication results in failed cohesion between homologous chromosomes during MI (Watanabe et al., 2001). Thus, the signal for cells to enter the meiotic program must occur before DNA replication so that the meiosis-specific rather than the mitosis specific cohesin complex is loaded onto chromosomes. After pre-meiotic S phase, cells undergo an elongated prophase (prophase I), during which homologous chromosomes are aligned adjacent to one another through formation of the synaptonemal complex: a repetitive series of protein complexes that join homologous chromosomes along the entire axis of a chromatid pair, thereby allowing genetic recombination in the event known as *crossover*. During crossover, genetic material from the chromatids of neighboring homologous chromosomes is exchanged in a process involving DNA double strand break repair through the formation of double Holliday junctions (Holliday, 1964; Schwacha and Kleckner, 1995). Resolution of the double Holliday junction by a yet to be discovered resolvase enzyme results in chiasmata. The completion of crossover recombination is monitored by the pachytene checkpoint, which inhibits exit from prophase I until all double-strand breaks are repaired (Borchers et al., 2004). Formation of chiasmata effectively links the cohesion between sister chromatids of one homologous chromosome pair to that of the other, and thereby links the homologous pair in what is called a *bivalent*. After dissolution of the synaptonemal complex that occurs near the end of prophase I, chiasmata and cohesin distal to the chiasmata provide the only physical link between homologous chromosomes.

Indeed, failure to form chiasmata results in random segregation of homologous chromosomes in MI that leads to aneuploidy and inviable progeny (Baudat et al., 2000; Romanienko and Camerini-Otero, 2000).

Once cells reach the metaphase/anaphase transition of MI, Rec8 is proteolyzed by Esp1 (Kitajima et al., 2003), which until that time is inhibited by Pds1 (Salah and Nasmyth, 2000). However, only the Rec8 along chromosome arms is degraded (Ho et al., 2002), while the Rec8 and consequential cohesion around centromeres is preserved until MII (Klein et al., 1999; Toth et al., 2000; Watanabe and Nurse, 1999). The elimination of arm cohesion and preservation of centromeric cohesion allows the segregation of homologous chromosomes, but not sister chromatids, to opposite spindle poles in MI. During anaphase I, centromeric Rec8 is protected from Esp1 proteolysis by associating with the conserved kinetochore protein, shugoshin (Sgo1) (Katis et al., 2004; Kitajima et al., 2004; Marston et al., 2004; Rabitsch et al., 2004).

Meiosis II. After MI, cells do not undergo a second S phase and so the second nuclear division is very similar to a mitotic nuclear division. In this case, sister chromatids are attached via their kinetochores, in a bi-oriented fashion, to opposing spindle poles (Petronczki et al., 2003). Similar to MI, MII requires the destruction Rec8 by Esp1 (Kitajima et al., 2003) during anaphase II, however, Sgo1 must be degraded before this can happen. How this happens is not clear, although the APC has been suggested as a potential mediator of timely Sgo1 destruction (Penkner et al., 2005).

The role of APC in yeast meiosis

The APC is necessary for both nuclear divisions during meiosis in yeast (Petronczki et al.,

2003; Salah and Nasmyth, 2000) (Figure 1.5), as well as spore morphogenesis (Blanco et al., 2001; Cooper et al., 2000). At the onset of anaphase I, the APC is activated by Cdc20, which recruits Pds1 for ubiquitination (Salah and Nasmyth, 2000), resulting in the release of Esp1 and degradation of chromosomal arm Rec8 (Kitajima et al., 2003) that is the trigger for anaphase I and the resolution of chiasmata (Kudo et al., 2006). APC^{Cdc20} is also necessary to trigger Pds1 at the metaphase/anaphase transition of MII that results in a second round of Esp1-mediated Rec8 degradation (Salah and Nasmyth, 2000). A role for Cdh1 co-activator in meiosis is unclear, although it has been shown that the meiosis-specific kinase, Ime2, when expressed in mitotic cells can negatively regulate APC activity by phosphorylating and inhibiting Cdh1 (Bolte et al., 2002). In budding yeast the APC is regulated in part by the meiosis-specific, Cdc20-like co-activator, Ama1 (Cooper et al., 2000). The AMA1 gene is expressed and spliced in prophase I, and shares similar but not completely overlapping functions with the mitotic co-activators Cdc20 and Cdh1 (Cooper et al., 2000). At the inception of this thesis, only one report described Ama1 function (Cooper et al., 2000), and showed that Ama1 could bind the APC *in vivo* and was necessary for degradation of the B-type cyclin Clb1 after the second nuclear division. The study further showed that deletion of *ama1* resulted in meiotic arrest before metaphase I, and that Ama1 protein is also required for late meiotic gene expression and spore formation (Cooper et al., 2000; McDonald et al., 2005).

Thesis summary

At the inception of my thesis (*2003*), our understanding of APC structure and regulation was just beginning to emerge. At that time, it was clear that the APC was an enormous

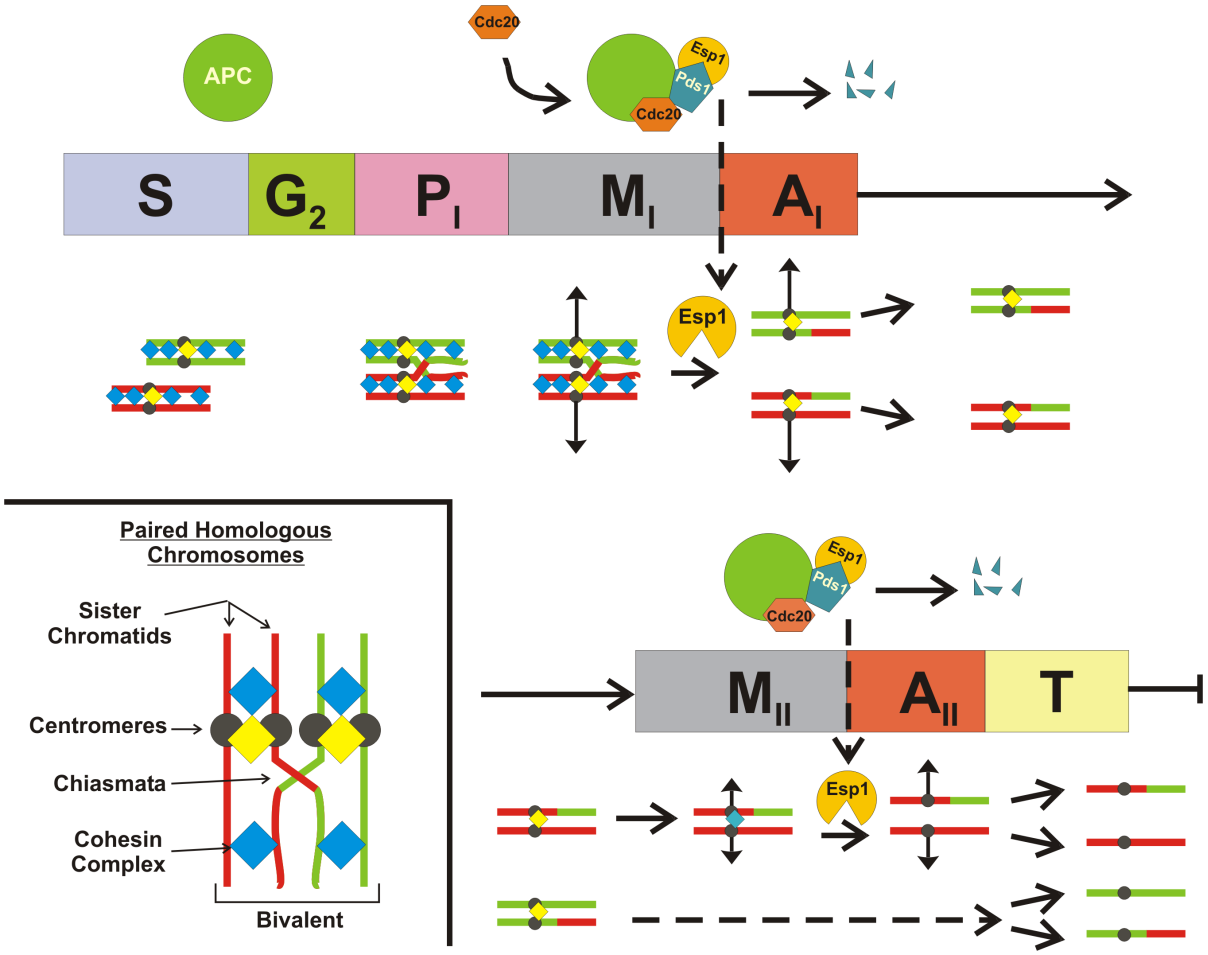

Figure 1.5. The APC is required for meiotic cell cycle transitions. During meiosis, one round of DNA synthesis is followed by two successive rounds of nuclear division. Prior to nuclear division, meiotic nuclei undergo an elongated prophase I, during which chromatids from homologous chromosomes must recombine by crossover recombination. The first meiotic nuclear division is specific to meiosis because homologous chromosomes, rather than sister chromatids (see inset figure), are aligned and separated in anaphase I. Therefore, only non-centromeric cohesion is destroyed by Esp1, which targets the meiosis specific cohesin subunit, Rec8, which has been substituted for Scc1 during DNA synthesis. In the second nuclear division, which is the mitosis-like division, centromeric cohesin is deprotected (possibly through an APC-dependent pathway), and Pds1 is again targeted for ubiquitin mediated proteolysis, leading to separation of sister chromatids into four haploid progeny cells.

ubiquitin ligase with many different subunits, some of which were modified post-translationally by phosphorylation. However, our knowledge of the function of individual subunits and the importance of specific phosphorylation sites was poorly understood. Furthermore, nothing was known about the role of APC phosphorylation during the meiotic cell cycle and very little was known about APC-mediated ubiquitination in this process. At the same time, protein mass spectrometry (MS) was beginning to flourish as a powerful tool for characterizing protein sequence and modification; and the laboratory of Dr. Christoph Borchers was well equipped to apply these tools for analysis of the APC in budding yeast. *In this thesis, I have used protein mass spectrometry to investigate the subunit composition and phosphorylation modifications of the APC for the purpose of improving our understanding of APC-mediated cell cycle regulation.* The results have led to the discovery of two previously unknown subunits and also the first demonstration that APC phosphorylation is necessary for meiotic cell cycle transitions.

The remainder of this thesis is divided into four chapters. In *Chapter II*: *"Protein characterization by mass spectrometry"*, I describe the fundamentals, instrumentation, and classical approaches used in the mass spectrometric analysis of proteins. I also describe a novel technique that I developed for the MS analysis of phosphorylated proteins, aspects of which I later used to study APC phosphorylation. In *Chapter III: "Mnd2 and Swm1 are stoichiometric components of the Saccharomyces cerevisiae anaphase-promoting complex"*, I describe how I and others in Dr. Borchers lab used mass spectrometry to identify two new APC subunits in budding yeast. I demonstrate that each subunit is present on the complex throughout the cell cycle at stoichiometric levels, and that neither subunit is required for mitotic viability but critical for meiotic viability. In *Chapter IV: "Phosphorylation of the*

APC inhibitory subunit, Mnd2, is necessary for efficient progression through meiosis I", I used mass spectrometry to identify specific phosphorylation sites on the subunit, Mnd2, which are critical for meiotic progression in budding yeast. Finally, in *Chapter V: "Conclusions and general discussion"*, I draw overall conclusions from my research, discuss the implications of my results, and propose new hypotheses that could provide an avenue for future research.

CHAPTER II

PROTEIN CHARACTERIZATION BY MASS SPECTROMETRY

Summary

In recent years, the application of mass spectrometry for protein characterization has made significant advancements and is now established as the most effective tool for the analysis of protein with regards to protein sequencing, protein-protein interactions, protein post-translational modification (PTM), and protein quantitation. The advantage of using mass spectrometry (MS) as a bio-analytical tool is that it allows one to measure the mass of any given bio-molecule with a high degree of accuracy, resolution, sensitivity, speed, and reproducibility. Accurate mass determination of peptides or proteins by MS can provide valuable information about protein sequence and therefore protein identity, as well as protein modification and quantity. Comparatively, traditional methods of protein sequence analysis (e.g. Edman degradation), require greater sample and reagent quantities as well as longer analysis times relative to routine MS strategies (Biemann and Scoble, 1987; Wilm et al., 1996). Moreover, the ability to perform accurate mass determination on full length proteins using MS is unsurpassed by any other methodology. In this chapter, I describe the fundamentals of mass spectrometry and their application to the analysis of proteins in what are commonly referred to as the *bottom-up* and *top-down* MS strategies. I further present a novel bottom-up MS method that I developed for the detection of multiply-phosphorylated peptides, called phosphatase-directed phosphorylation site determination (PPD), in which I use a cell cycle regulated protein to demonstrate proof-of-principle. Aspects of this method were later applied to the analysis of APC subunit phosphorylation that is described in chapter IV.

Fundamentals and instrumentation

Mass spectrometry is an analytical method of measuring the mass of ionized molecules in the gas phase. The method relies entirely upon instrumentation, the mass spectrometer, which consists of three fundamental components: the ion source, which generates gas phase molecular ions; the mass analyzer, which separates the molecular ions based on their mass-to-charge (*m/z*) ratio; and the detector, which registers the number of molecular ions at each *m/z* value. Following are general descriptions of ion sources and mass analyzers and their relevance to protein MS experiments. For more detailed information on any one particular subject, please see the references contained therein and (Gross, 2004).

The ion source

The two most common ion sources used to generate gas phase molecular ions (especially of biological molecules) are matrix-assisted laser desorption ionization (MALDI) and electrospray ionization (ESI) (Figure 2.1). MALDI is a derivative of an older ionization technique called laser desorption ionization (LDI), in which pure analytes are ionized directly by bombardment with pulsed laser energy. At that time, LDI was functional for analyzing small molecules (1 – 2 kDa) that were easily ionized and vaporized by direct laser energy, but was insufficiently capable of desorption/ionization of larger molecules such as proteins or peptides (Dreisewerd, 2003). A significant improvement in LDI was achieved by embedding the sample analyte within a crystalline matrix that was conducive to generating gas phase ions of large molecules (e.g. peptides and proteins) upon excitation with an ultraviolet or infrared laser beam (Karas and Hillenkamp, 1988). In the MALDI technique, excitation and rapid heating of the chemical matrix induced by short laser pulses results in proton transfer

from the matrix to the analyte and spontaneous sublimation of the ionized molecule into the gas phase (Dreisewerd, 2003; Hillenkamp and Karas, 1990) (Figure 2.1). Many different methods for MALDI sample preparation exist; however, the most common is the dried droplet method in which an equivalent volume of sample analyte and concentrated matrix solution is crystallized on the surface of a steel target plate (Karas and Hillenkamp, 1988). Different chemical matrices can be used, each of which exhibits characteristics optimal for different sample analytes (Bornsen, 2000; Gonnet et al., 2003; Laugesen and Roepstorff, 2003; Schiller et al., 2006; Shahgholi et al., 2001). In addition to its simplicity and ease of use, MALDI MS exhibits two main advantages. First, a single dried droplet has a long 'shelf life' and can be repetitively analyzed many times over, which is particularly useful when working with complex sample mixtures. Second, in general, MALDI generates mostly single (as opposed to multiple) charge state ions, which can reduce mass spectrum complexity and improve ion assignment. The concentration of ion signals within a single charge state can theoretically increase spectrum intensity and provide more favorable ion statistics (due to higher ion count) for any given ion. The major disadvantage of MALDI is that it requires samples to be dehydrated before analysis, and is therefore incompatible with on-line chromatographic separation techniques.

The advent of ESI MS for the analysis of large biomolecules occurred at around the same time as MALDI MS, when Fenn et al. discovered that ESI was able to form multiply charged molecular ions (Fenn et al., 1989; Whitehouse and Cleland, 1985) that consequently expanded the range of a mass analyzer from a few kilodaltons to almost 1 million daltons (Rostom and Robinson, 1999). In contrast to MALDI, ESI MS is conducted with samples in the liquid phase. In this case, sample analyte is loaded into a metal or metal-coated capillary

needle which is electrically charged with respect to a cylindrical electrode at the entrance chamber of a mass analyzer. The potential difference between the needle and the chamber generates an electric field at the needle's tip that charges the surface of the emerging liquid and disperses it into a mist of charged droplets, some of which contain the sample analyte. As the charged droplets migrate along the electric field toward the entrance to the mass analyzer, the solvent rapidly evaporates until the charge density reaches a threshold that causes the sample analyte to desorb into the gas phase as a molecular ion (Fenn et al., 1989; Whitehouse and Cleland, 1985) (Figure 2.1). In comparison to MALDI, ESI MS is considered a "softer" ionization technique that may preserve the sample analyte without causing fragmentation of covalent and even non-covalent bonds. Indeed, ESI MS can be used to determine the mass of protein-small molecule (Bligh et al., 2003; Borchers et al., 2004) as well as protein-protein non-covalent complexes (Loo et al., 2005; Veenstra, 2006). There are two major advantages to using ESI MS for protein analysis. First, ESI MS is easily coupled with liquid phase chromatography (LC) techniques such as reverse phase HPLC or reverse-phase HPLC coupled with strong ion exchange chromatography (Han et al., 2001; Link et al., 1999; Washburn et al., 2001; Wolters et al., 2001; Yates et al., 1999). Indeed, separation of sample mixtures by liquid chromatography prior to MS analysis dramatically expands the number of different molecular ions observed in a single sample by reducing ion suppression effects commonly observed in MS analyses of complex mixtures. Second, the mass accuracy of ESI MS on proteins larger than ~4 kDa is much greater than what can be achieved using MALDI MS. By generating multiple charge states for a single protein of given mass, the mass measurement is based on an average of many ion signals across the *m/z* scale. In addition, the *m/z* scale for mass spectra generated by ESI MS is generally

maintained below m/z 3000, at which the accuracy of the mass analyzer is optimal. The major disadvantage of ESI MS is that the generation of multiple charge states for each analyte can significantly increase spectrum complexity. In addition, the ionization efficiency of any given analyte can vary widely due to solvent characteristics, the presence of impurities, and the analyte itself (Garcia, 2005; Garcia et al., 2002; Shou and Naidong, 2005).

The characteristic differences between MALDI MS and ESI MS make the two ionization mechanisms complementary. For instance, when using both techniques for the detection of complex peptide mixtures the number of different peptides detected within a single sample is generally greater than the number detected by either technique alone (Stapels and Barofsky, 2004; Stapels et al., 2004). In addition, two less common ion sources have become popular for applications not well suited for MALDI or ESI MS: atmospheric pressure chemical ionization (APCI) (Byrdwell, 2001), and atmospheric pressure photoionization (APPI) (Raffaelli and Saba, 2003).

The mass analyzer

The mass analyzer combined with the detector is the measuring component, and therefore the 'heart' of a mass spectrometer. There are five types of mass analyzer: time-of-flight (TOF), quadrupole (Q), ion trap (Trap), Fourier transform ion cyclotron resonance (FTICR) (reviewed in Aebersold, 2003), and Orbitrap (Hu et al., 2005). In this section I describe each mass analyzer, although most of the data generated for this thesis was conducted on TOF and quadrupole mass spectrometers (Figure 2.1).

In a TOF mass analyzer, ion masses are determined by measuring the time-of-flight for an

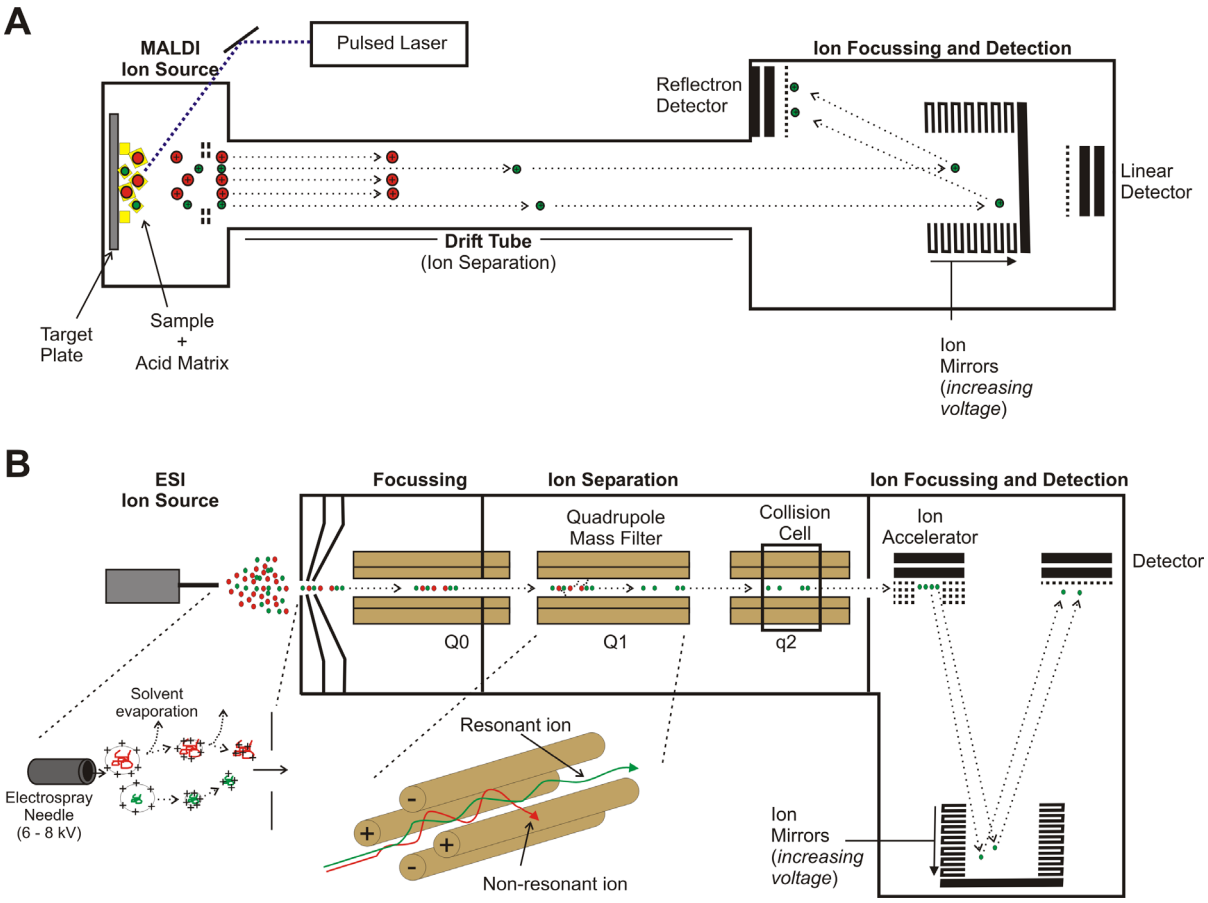

Figure 2.1. Schematic diagrams of MALDI-TOF and ESI-QqTOF MS instrumentation. (A) MALDI-TOF instrument diagram. Sample analytes are co-crystallized with an acid matrix on a steel target plate. Firing a pulsed laser at the crystal matrix induces rapid sublimation and ionization of the sample into the gas phase as an ion packet. After normalizing the kinetic energy of an ion packet, the ions are separated in a time-of-flight tube as they drift from the entrance to the exit. Ions with higher *m/z* will travel slower than ions with lower *m/z*. The ions are then detected in a linear or reflectron path by the respective detectors. The resolution of the ions separated in the drift tube is drastically improved in the reflectron mode, in which case ions "reflect" off of an ion mirror that functions to normalize the kinetic energy of like ions before they reach the detector. (B) ESI-QqTOF hybrid instrument diagram. Sample analytes are emitted as an electrospray from an electrified needle, resulting in droplets that carry multiple proton charges. Solvent rapidly evaporates until a threshold of surface charge density is reached in a "coloumbic explosion" that forms the quasi-molecular sample ion (Fenn et al., 1989). The ions are focused in Q0 and then filtered by a quadrupole mass analyzer (Q1), which uses ratio of dc and rf voltages to selectively filter ions of a specific *m/z*. Non-selected ions display an unstable trajectory that leads them to crash into the rods of the quadrupole (zoomed figure). Ions that pass through Q1 enter q2, which can be used as a collision cell in tandem MS experiments. In the QqTOF instrument, the filtered ions pass through a time-of-flight analyzer before reaching the detector. (Figure adapted from instrument diagram for the Applied Biosystems Sciex Q-Star Pulsar instrument).

ion traveling from the ion source, through a drift or TOF tube, and to the detector (Stults, 1995). In order to distinguish between ions generated at different times by the source, ions are measured in 'packets' that are generated through pulsed ion extraction by the ion source. Ions within a packet are focused into a beam, and accelerated in a voltage gradient that serves to normalize the kinetic energy of each ion before it enters the TOF analyzer. Once the ion packet is released into the TOF tube, each ion drifts in parallel towards the end of the tube without the input of additional energy. The rate of drift is directly proportional to an ion's mass-to-charge ratio (*m/z*), where ions of higher mass or less net charge travel slower than ions of lower mass or greater net charge. Once ions within a packet contact the detector, the signal is sent to a digitizer that calculates the drift time with respect to the ion pulse frequency and TOF tube length, and displays the summed data for multiple ion packets as a mass spectrum. TOF analyzers are often combined with MALDI ion sources, in which ion extraction can be controlled by the laser pulse frequency. TOF analyzers exhibit the highest mass range of any analyzer and also a high degree of ion transmission, which improves detection sensitivity. However, TOF analyzers are not very good at ion selectability, and are therefore poor mass filters.

Quadrupole mass analyzers work by generating an electric field between four axial metal rods through which ions pass en route to the detector. The voltages applied to the four rods consist of both direct current (dc) as well as radio frequency (rf) potentials that combine to create a quadrupolar field, which can be altered to permit transmission of only ions within a given *m/z* range. Ions outside the *m/z* range set by the quadrupolar field display unstable trajectories that result in their collision with the quadrupole rods and failure to reach the detector (Figure 2.1). To generate a mass spectrum, the quadrupole is used to scan across a

range of *m/z* values by altering the dc and rf potentials of each rod. Quadrupole mass analyzers are multi-functional, acting as mass filters or collision cells (March et al., 1989), making them ideal for tandem mass spectrometric experiments (Jonscher and Yates, 1997; Yost and Boyd, 1990).

In an ion trap mass analyzer, ions are stored or 'trapped' before they are selectively released to the detector by scanning the dc and rf potentials of the trap across a desired *m/z* range (Brancia, 2006; Jonscher and Yates, 1997; McLuckey et al., 1994). Using an ion trap, one can trap and release ions with a specific *m/z*, and also excite the ions by altering the rf potentials of the trap. Ion trap configurations are typically either three-dimensional or two-dimensional (also called linear ion traps). In a three-dimensional ion trap, ions are stored in a point in space at the center of the trap. Three-dimensional ion traps exhibit relatively low mass resolution due to space charge effects that occur as the trap reaches its maximum ion capacity. However, linear ion traps have reduced this problem by utilizing a quadrupole as a cylindrical trap, thereby increasing the ion capacity and reducing the space charge effect. Linear ion traps (LIT) exhibit better sensitivity, mass resolution, and mass accuracy compared to traditional three-dimensional ion traps (Aebersold and Mann, 2003). In comparison with other mass analyzers, ion traps are typically more sensitive and they also allow multi-stage MS experiments (discussed below). However, their susceptibility to space charge effects can compromise their mass resolution and accuracy.

The FTICR mass analyzer is an ion trap that provides the greatest mass resolution available of any mass spectrometer. Mass determination by FTICR MS relies on the principle that ions move in a circular orbit in a magnetic field, and the frequency of cycling or *cyclotron frequency* is proportional to the *m/z* of the ion. In FTICR MS, incoming ions are

trapped in this circular path by superconducting magnets. As ions enter the magnetic field, they are energized with an excitation pulse that sweeps across a frequency range. When the cyclotron frequency of an ion is in resonance with the excitation frequency, the ion absorbs the energy, which subsequently increases the ion's circular orbit. The ions whose orbits becomes expanded (i.e. ions of the same *m/z* value) are detected as an image current by a 'receiver plate' inside the trap. The image current is proportional to the number of ions and their distance from the receiver plate. The mass spectrum is generated by applying a Fourier transform to the digitized image current (Bogdanov and Smith, 2005; Marshall et al., 1998). Similar to traditional ion traps, ions with a particular *m/z* can be trapped, released, or excited, in the ICR cell. In addition, multi-stage MS can also be performed. However, FTICR MS allows far greater mass accuracy and resolution than what can be achieved by three-dimensional or linear ion traps. The performance of FTICR MS, most notably the resolving power, increases with increasing magnetic field (Marshall et al., 1998).

The fifth and most recent type of mass analyzer, called an orbitrap, provides mass resolution close to FTICR, but without the need for large superconducting magnets (Hu et al., 2005; Scigelova and Makarov, 2006). Similar to FTICR, molecular ions are trapped non-destructively in circular orbits that can be selectively expanded to create image currents that are detected and converted to mass spectra via Fourier transformation. However, in the orbitrap, ions are trapped about a central spindle electrode that is co-axial with an outer barrel-like electrode. The mass-to-charge of an ion is proportional to, and measured from the frequency of its harmonic oscillations controlled by the electric field of the orbitrap. Like the FTICR, the orbitrap is used in hybrid mass spectrometers that also contain quadrupole and linear ion trap mass analyzers.

Tandem mass spectrometry

The manipulation of molecular ions using multiple mass analyzers arranged in sequence is called tandem mass spectrometry (MS/MS). MS/MS was first described as a method for detecting and analyzing trace elements out of complex mixtures (McLafferty, 1981a; McLafferty, 1981b), and was later shown to be useful for determining the amino acid sequences of proteins (Hunt et al., 1981; Hunt et al., 1986). In the experiments by Hunt et. al, proteins were cleaved by enzyme proteolysis to produce peptides that were analyzed using a mass spectrometer in which three quadrupole mass analyzers were joined in tandem. In this *triple quadrupole* (QqQ) mass spectrometer the first and third quadrupoles (Q_1 and Q_3) were used as mass filters, while the second quadrupole (q_2) was employed as a collision cell. Q_1 was used to select a narrow *m/z* range that allowed transmission of only one peptide species to q_2. In q_2, the peptide collides with a neutral gas (N_2 or Ar) and becomes fragmented in a process termed collision-induced dissociation (CID) (sometimes called collision-activated dissociation, CAD). The fragments generated by CID in q_2 were then separated in Q_3 before reaching the detector to create the tandem mass spectrum. CID often results in fragmentation at the peptide bond between amino acid residues (Hunt et al., 1986). In the simplest case, one fragmentation event creates two possible peptide ions: an N-terminal ion, or *b-ion*; and a C-terminal ion, or *y-ion* (Johnson et al., 1987; Roepstorff and Fohlman, 1984). During CID, fragmentation commonly occurs at multiple peptide bonds within the peptide, resulting in the formation of multiple b and y fragment ions whose masses differ by the mass of one or more of the 20 known amino acids. Since the amino acid mass differences produced by CID are known (Hunt et al., 1986), the tandem mass spectrum can be used to determine the amino acid sequence of the entire peptide (Figure 2.2).

In variations of the triple quadrupole instrument, such as the QqLIT, the Q_3 quadrupole has been replaced by a linear ion trap. The incorporation of an ion trap allows one to perform multi-stage mass spectrometric experiments (called MS^n), the most common of which is the MS^3 experiment. In a typical QqLIT MS^3 experiment, Q_1 allows transmission of a selected ion, which is then fragmented by CID in q_2 (MS/MS). The fragments from q_2 can be stored in the LIT followed by ion ejection of all but one specific fragment ion. The remaining fragment ion can be activated by altering the rf potentials of the LIT, which induces fragmentation or MS/MS/MS. The resulting fragment ions can then be selectively scanned to the detector as an MS^3 spectrum. Similar experiments have also been demonstrated with mass spectrometers lacking an ion trapping mass analyzer such as the Qq-TOF, whereby samples undergo in-source fragmentation (MS/MS) followed by ion selection in Q_1, secondary fragmentation in q2, and fragment analysis in the TOF tube (Konishi and Tominaga, 2006) (Figure 2.1). The MS^3 experiment has been shown to be very useful for analysis of peptide PTMs, like phosphorylation, which can be lost or difficult to sequence in typical MS/MS experiments (Chang et al., 2004).

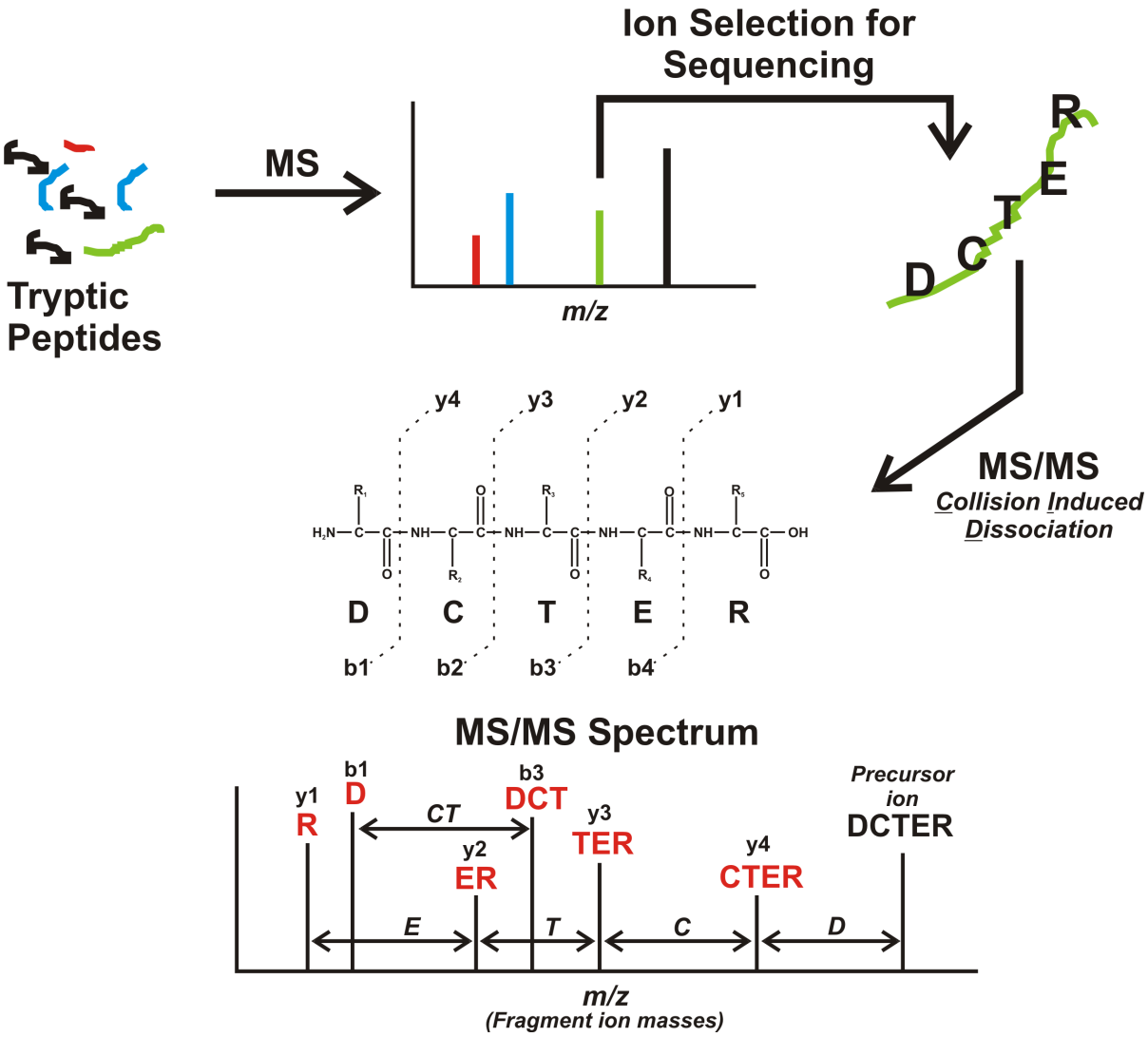

Figure 2.2. Tandem mass spectrometry of peptides. Using a hybrid mass spectrometer such as the QqTOF (described in Figure 2.1), a collection of peptides, generated by tryptic digestion of a sample protein, are first analyzed by MS, in which case the mass spectrum displays the m/z for each peptide in the mixture. The ion of interested is then selected for tandem MS (MS/MS) sequencing (for example, by quadrupole mass analyzer). The selected ion passes through a collision cell containing neutral gas molecules that collide with the peptide, thereby inducing dissociation of the peptide into fragments. Collision induced dissociation occurs predominantly at the peptide bond between amino acid residues. The resulting fragments are analyzed by a second mass analyzer (for example, by time-of-flight), which separates the fragment ions by *m/z* before they reach the detector. Since the mass of every amino acid is known, the resulting MS/MS spectrum can be used to determine the sequence of the parent peptide.

Mass spectrometry of proteins: *bottom-up* and *top-down* approaches

Mass spectrometry has become the most effective tool for characterizing proteins since the inventions of the MALDI and ESI ionization techniques, which drastically improved the sensitivity of mass spectrometers for large molecular ions. MS is now commonly used to analyze proteins that are expressed endogenously at biologically relevant levels. However, before the existence of MALDI and ESI, most MS techniques were limited to the analysis of small molecules or short peptides capable of being ionized by ionization sources available at the time. Thus, proteins were digested enzymatically or otherwise hydrolyzed chemically prior to MS analysis (Herlihy et al., 1980; Nau and Riordan, 1975), which resulted in much smaller MS-compatible peptide fragments. Once the masses were determined for each peptide fragment, they could be compared to the theoretical peptide masses predicted for a particular protein based on the translated DNA gene sequence. Using this technique, amino acids prone to chemical modification (e.g. enzyme active sites, or surface exposed residues) could be determined by comparing peptide masses before and after protein modification and looking for which peptide fragments underwent mass shifts corresponding to the addition of the chemical modifier (Nau and Riordan, 1975). This type of mass-matching analysis was further improved by using tandem MS to provide amino acid sequence information on individual peptides (Hunt et al., 1981; Hunt et al., 1986). *The concept of breaking down a protein into smaller peptides that can be analyzed individually by MS and/or tandem MS has come to be known as the* ***bottom-up*** *approach* (Figure 2.3 A).

Concomitant with the advent of bottom-up mass spectrometry was the creation of whole genome sequence databases that could be used in combination with bottom-up mass spectra as a tool for identifying unknown proteins in a method called peptide mass fingerprinting. In

the simplest form of this method, a protein is digested (usually with trypsin protease) and the peptides are subsequently detected by MS. Tryptic digestion of a protein occurs exclusively C-terminal to arginine or lysine residues (Olsen et al., 2004), which results in a particular combination of peptides, each with a distinct mass that, as a whole, can serve as a unique identifier for the digested protein, also called a peptide mass fingerprint. Using mass matching computer algorithms, the peptide mass fingerprint is used to query a genome-wide peptide mass database of translated sequences that have been theoretically digested (*in silico*) with the same enzyme. Successful identification of a protein is achieved when a statistically significant number of masses from the peptide mass fingerprint accurately match the theoretical mass fingerprint for a particular protein in the database (Aebersold and Mann, 2003; Phizicky et al., 2003; Tyers and Mann, 2003; Zhu et al., 2003). Whole genome sequence databases can also be searched with peptide sequence, in which case the fragment ions from an MS/MS experiment are used. This generally improves the statistical confidence of protein identification and also reduces the total number of matching peptides needed for success. Importantly, database searching algorithms can also be used to evaluate the presence of PTMs (e.g. phosphorylation, acetylation, methylation, oxidation, etc.) that alter the mass of an unmodified peptide by discrete values, although MS/MS is often required to confirm the result. The bottom-up approach to MS protein characterization is now the primary tool used in proteomics research, which seeks to quantify the expression, post-translational modification, and protein-protein interactions of every protein in a living cell (Aebersold and Mann, 2003; Phizicky et al., 2003; Tyers and Mann, 2003; Zhu et al., 2003).

Bottom-up proteomics relies heavily on protein and peptide chromatography, since the ion detection capacity of mass spectrometers is limited, particularly for complex peptide or

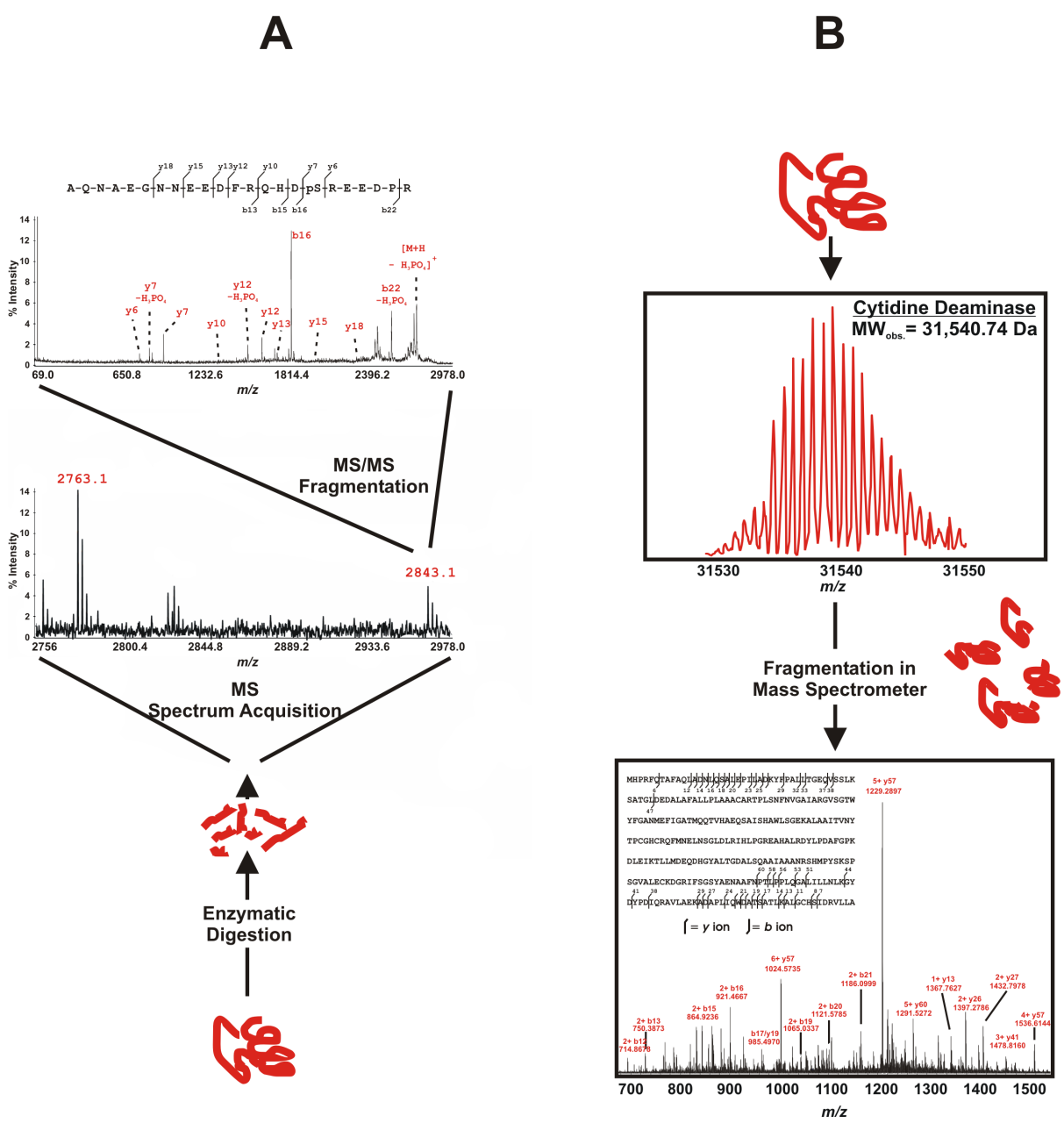

Figure 2.3. Bottom-up and top-down protein mass spectrometry. (A) The bottom-up approach. Full-length proteins are first broken down into peptides by enzymatic digestion, and the peptides are analyzed by MS and MS/MS. (B) The top-down approach. Full-length proteins are analyzed by MS and MS/MS without enzymatic digestion. Here, top-down FTICR-MS analysis of cytidine deaminase from *E. coli* is shown. MS analysis reveals the accurate molecular weight of the protein (the deconvoluted ESI mass spectrum of cytidine deaminase is shown, in which each peak represents a different isotope number). Subsequent MS/MS analysis by collision induced dissociation results in fragment ions that can be used to determine the sequence of the full-length protein.

protein mixtures (Annesley, 2003). The type of chromatographic separation used prior to MS analysis depends on the goals unique to a particular experiment but often includes one or more of the following techniques: 1D or 2D SDS-PAGE, reverse-phase liquid chromatography, strong cation/anion exchange, and capillary or free-flow electrophoresis. Proteomics experiments have been widely used to identify protein-protein interactions (Blagoev et al., 2003; Gavin and Superti-Furga, 2003; Ho et al., 2002; Ranish et al., 2003), protein post-translational modifications (Ficarro et al., 2002; Gruhler et al., 2005; Nousiainen et al., 2006; Olsen et al., 2006), and to quantitate cellular protein levels (Gygi et al., 1999; Mann et al., 2002; Oda et al., 1999; Ong et al., 2003; Sechi and Chait, 1998).

Although bottom-up proteomics is a powerful technology for protein identification and characterization, the method does have limitations. First, in many cases, not all of the peptides generated by proteolytic digestion of the whole protein are detected, due to a variety of factors such as ion suppression (Annesley, 2003). Second, peptide ionization/detection efficiency can be drastically lowered by the presence of PTMs, such as phosphorylation, which increases the electronegativity of the peptide (Craig et al., 1994; Janek et al., 2001; Steen et al., 2006). Third, the stoichiometry of PTMs cannot be easily quantified without the use of peptide standards, due to differences in ionization/detection efficiency of the modified and unmodified peptides (Bonenfant et al., 2003; Ibarrola et al., 2003; Steen et al., 2005).

*The **top-down** approach to protein mass spectrometry, in which protein sequence information is obtained from analysis of the intact protein as opposed to peptides, is an alternative technique that circumvents some limitations of the bottom-up approach.* Top-down mass spectrometry was originally conceived in the late 80's and early 90's, when it was discovered that tandem mass spectrometry could be used to interrogate the multiply-

charged ions found in ESI mass spectra of large proteins (Henry et al., 1989; Loo et al., 1990; Loo et al., 1992). In this case, the accurate molecular weight of an intact protein is determined by ESI MS, which produces a distribution of multiply-charged ions that are detected and then displayed in the MS spectrum (Figure 2.3 B). The determined mass can then be compared to the predicted amino acid sequence of the whole protein. Deviations in the calculated and measured mass provide an immediate indication that the protein is altered in some way by changes in amino acid composition or post-translational modification. Next, any one of the multiply-charged states (e.g. the 15+ charge state) detectable in the MS spectrum can be interrogated by MS/MS, yielding fragment ions that provide sequence and PTM information for the protein. Thus, in the top-down approach, proteins are fragmented within the mass spectrometer as opposed to the bottom-up approach, in which a protein is reduced to peptide fragments by enzymatic proteolysis.

The MS analysis of proteins exhibits several advantages over the analysis of peptides. First, determining the mass of the intact protein provides comprehensive information on the global protein state. Second, the ionization/detection efficiency of intact proteins is generally not as affected by the presence of PTMs such as phosphorylation. Third, differences in the ionization/detection efficiencies of post-translationally modified and unmodified protein isoforms is often minimal, so semi-quantitative information on isoform stoichiometry can be obtained by comparison of the peak areas in the MS spectrum. Fourth, top-down MS analyses do not depend on enzymatic cleavage, so proteins that lack sufficient enzyme cleavage sites can be interrogated. The main disadvantages of the top-down approach include: one, MS analyses of proteins are generally less sensitive than MS analyses of peptides; two, successful protein ionization (particularly by ESI) can often depend heavily on

the amino acid sequence and is therefore different for each protein; three, protein ionization depends heavily on the properties of the solvent and may differ from protein to protein. Since the strengths and limitations of the bottom-up and top-down approach are complementary, many have used both methods to achieve complete characterization of a protein (Borchers et al., 2006; Chait, 2006; Chalmers et al., 2005; Millea et al., 2006; Nemeth-Cawley et al., 2003; Strader et al., 2004).

Mass spectrometry of phosphoproteins: challenges and novel solutions

This section includes modified portions from: Torres, M.P., Thapar, R., Marzluff, W.M., Borchers, C.H., (2005) *J. Prot. Res.* **4**(5): 1628-35.

Summary

Mass spectrometry is currently the method of choice for characterizing protein phosphorylation because of its high sensitivity, accuracy, and sequencing capability. However, protein phosphorylation often exists in low stoichiometry and can drastically hinder the MS ionization/detection efficiency of peptides and sometimes proteins (Mann et al., 2002). Here a combination of top-down and bottom-up MS approaches were used to characterize the cell cycle regulated protein, *Drosophila* stem loop binding protein (dSLBP). Accurate molecular weight determination of dSLBP by FTICR MS and FTICR MS/MS top-down experiments showed that there was removal of the initiator methionine, acetylation of the N-terminus, and five occupied phosphorylation sites (Borchers et al., 2006). The location of four of the five phosphorylation sites could not be determined by top-down MS, nor could they be located by traditional bottom-up MS methods. To address this problem, I developed

a technique called phosphatase-directed phosphorylation site determination (PPD), which combines on-target phosphatase reactions, MALDI MS/MS of IMAC beads on target, and hypothesis-driven MS (HD-MS). PPD was used successfully to localize the remaining four phosphorylation sites within the last four serine residues of dSLBP. Aspects of this method were later applied to the analysis of APC phosphorylation (Chapter IV).

Introduction

Reversible phosphorylation is one of the most common post-translational protein modifications used to regulate protein activity in all multicellular organisms (Johnson et al., 1987; Mann et al., 2002). Thus, mapping phosphorylation sites within phosphoproteins is an essential step towards understanding the effects of phosphorylation on protein biochemistry. Mass spectrometry is currently the method of choice for identifying phosphorylation sites because of its high sensitivity, accuracy and sequencing capability. However, suppression effects and low sensitivity for phosphopeptides in the MS mode are still challenges to MS-based phosphorylation site mapping (Kratzer et al., 1998; Liu et al., 2003). In addition, the fragmentation spectra of phosphopeptides in the MS/MS mode are often less interpretable and informative than those of the unphosphorylated peptide (Ho et al., 2002). In many cases the MS/MS spectra of phosphopeptides show fewer sequence specific fragmentation ions while the loss of phosphate (H_3PO_4, 98 Da) is the most abundant ion signal. This makes identification of the phosphopeptide difficult if not impossible without *a priori* protein sequence information.

Reducing the complexity of peptide mixtures by separating peptides and enriching phosphopeptides can overcome the suppression effect. Coupling liquid chromatography

directly to mass spectrometers (LC-MS) employed in electrospray mode (ESI) is one common method to separate and analyze peptides (Edwards and thomas-Oates, 2005). Another common method is to employ MALDI instead of ESI as the ionization mode in LC-MS, in which case the chromatography is uncoupled from the mass spectrometer but allows the re-analysis of peptides after interpretation of the MS spectra (Bodnar et al., 2003; Zheng et al., 2003). The advantage of using LC-MALDI-MS is that it permits the analysis of peptides, like phosphopeptides, which exhibit lower ion abundances that are typically not selected for sequencing in data-dependent online LC-MS/MS experiments. Immobilized metal affinity chromatography (IMAC) is another commonly used method to specifically enrich phosphopeptides from complex peptide mixtures (Andersson and Porath, 1986; Posewitz and Tempst, 1999; Raska et al., 2002; Stensballe et al., 2001; Xhou et al., 2000). A particularly elegant derivation of this approach is the direct MALDI-MS and MALDI-MS/MS analysis of phosphopeptides bound to IMAC beads that are spotted directly on a MALDI target plate (Raska et al., 2002). In this approach, elution with buffers incompatible with MS is avoided and therefore clean-up steps that can lead to sample loss are not required. However, the inherent low sensitivity of phosphopeptides in the MS mode is still a problem, even after IMAC enrichment.

Several methods have been developed to address the low detection sensitivity for phosphopeptides in the MS mode, which make use of prior knowledge regarding the peptide to be analyzed and employ MS/MS experiments in absence of a detectable peptide in the MS mode. One of these methods is called hypothesis-driven multiple-stage mass spectrometry (HMS-MS) as described by Chang, *et al.* (Chang et al., 2004). This technique relies on the high sensitivity of the mass spectrometer to ions generated by the neutral loss of phosphate

from phosphopeptides in the MS/MS mode. In this case, one postulates that any or all potential phosphorylation sites within a given protein may be phosphorylated and constructs a list of *m/z* values corresponding to the singly-charged phosphopeptide ions that could be produced by the enzyme used for digestion. Each potential molecular ion is then tested by MS/MS, and those that show a neutral loss of phosphate are further analyzed by MS^3 of the $(M+H-98)^+$ peak to confirm or reject the hypothesis that the expected phosphopeptide is present. In the case where the protein has numerous potential phosphorylation sites, this method can not only be time-consuming but also sample consuming, which may limit its application. Furthermore, this method requires knowledge about the proteins to be studied, and therefore, is not applicable for general proteomic experiments.

Another method of overcoming the low detection sensitivity for phosphopeptides in the MS mode is to treat a fraction of the sample with phosphatase, which enzymatically removes phosphoryl groups and thereby improves the ionization efficiency of the peptide in the positive ion mode (Hirschberg et al., 2004; Liu et al., 2003; Reimann et al., 2001a; Stensballe et al., 2001; Xhou et al., 2000). In this case, dephosphorylated peptides (original MWs – (n x 80 Da) appear as new and/or more abundant peaks in the MS spectrum, compared to the spectrum of the untreated sample. Furthermore, in general, the MS/MS analysis of the dephosphorylated peptide compared to the phosphorylated peptide shows improved sequence coverage resulting in unambiguous identification. Recently, Ficarro *et al.* (Ficarro et al., 2002) demonstrated the value of using phosphatase treatment for improved detection of phosphopeptides which were enriched by IMAC and analyzed by LC-ESI-MS. In that study, more then 28% of all phosphopeptides discovered in a phosphoproteome screen of *Saccharomyces cerevisiae* were detected only after dephosphorylation with alkaline

phosphatase. With MALDI-MS, the phosphatase treatment can be performed directly on the MALDI-target (Loughrey Chen et al., 2002), which is advantageous since fewer steps are involved that increase the potential for sample loss. Furthermore, in comparison to HD-MS, phosphatase treatment followed by MS analysis does not require any information about the proteins to be studied *a priori*. The major disadvantage of using phosphatase treatment, however, is that the resulting MS/MS spectra lack information on the specific sites of phosphorylation within the peptide.

In this study, we investigated phosphorylation on the cell cycle regulated *Drosophila* stem loop binding protein (dSLBP) using a combination of top-down and bottom-up mass spectrometry. SLBP is a phosphoprotein, and phosphorylation is required for its degradation at the end of S-phase in mammalian cells (Zheng et al., 2003). Phosphorylation within the C-terminal RNA processing domain (RPD) is necessary for efficient histone pre-mRNA processing (Dominski et al., 2002), and plays a role in stabilizing the structure of dSLBP (Thapar et al., 2004). Top-down FTICR-MS analysis revealed the presence of four occupied phosphorylation sites within the last 19 amino acids of the dSLBP-RPD C-terminus, which contains 6 phosphorylatable residues. Using traditional bottom-up MS strategies to identify the occupied sites failed, and the location of the four phosphorylation sites remained a mystery. To solve this problem, we developed and applied a new method that combines the advantages of IMAC, on-target phosphatase reactions, and hypothesis-driven MS (HD-MS). Here, directed MS/MS experiments are used for every possible phosphorylated state of each peptide initially observed by MALDI-MS analysis of the IMAC bound peptides after dephosphorylation. Through a combination of these individual techniques, this method, which we call "Phosphatase-directed Phosphorylation-site Determination" (PPD), overcomes

the problem of low sensitivity for phosphopeptides in the MS mode. In addition, the method employs a strategy that minimizes off-line chromatographic steps, thereby reducing the potential for sample loss. Finally, the method eliminates the need for *a priori* information on the protein, making it suitable for unbiased proteomic studies. In this study, we demonstrate the feasibility of PPD for the detection of phosphopeptides in proteolytic digests, and show that the technique is particularly useful for the detection of phosphopeptides that exhibit low ionization efficiency such as the multiply-phosphorylated dSLBP-RPD C-terminal peptide.

Experimental procedures

Phosphopeptides and proteins. Synthetic phosphopeptides KDIR4 (TRDIYETDYpYRK, m = 1702.7 Da) and PKA-I (GRTGRRNpSIHDIL, m = 1574.7 Da) were purchased from Anaspec (San Jose, CA) and dissolved in HPLC-grade water to give a 4μM solution. Beta-casein (Sigma Aldrich Co., St. Louis, MO) was dissolved in 25mM ammonium bicarbonate (ABC) to give a 10μM solution, and was digested with 1μg sequencing-grade trypsin (Promega, Madison, WI) at 37°C overnight. Approximately 10 pmoles of the digested β-casein was acidified with 100mM acetic acid for use in the PPD assay.

The His-tagged C-terminal half of histone mRNA Stem-Loop Binding Protein from *Drosophila melanogaster* (dSLBP) was expressed in a baculovirus expression system (Dominski et al., 2002), purified over a Ni-nitrilotriacetic acid (NTA) resin column (Qiagen, Chatsworth, CA), and eluted with a solution containing 20mM Tris-HCl, pH 8.5, 100mM KCl, 100mM imidazole, 10mM 2-mercaptoethanol, and 10% glycerol. The final concentration was 1μg/μL. A 10μL aliquot of the protein was purified on a C4 Zip-Tip (Millipore), and eluted with 20μL 80% acetonitrile, 0.1% trifluoroacetic acid. A 7μL aliquot

of the eluate was then digested with either porcine trypsin (Promega) or lysyl-endopeptidase (Lys-C) (Wako Chemicals USA, Richmond, VA) at a 1:20 and 1:7 enzyme-to-substrate ratio (respectively) in 100µL 50mM ABC at 37°C for 16 hours. Digests were purified over a C18 Zip-Tip (Millipore, Billerica, MA), and eluted with 10µL 50% acetonitrile, 0.1% trifluoroacetic acid. A 5µL aliquot (~100 pmoles) of the eluate was used in the PPD assay.

Immobilized Metal Affinity Chromatography. The general IMAC method used was based on that of Posewitz and Tempst (Dominski et al., 2002; Posewitz and Tempst, 1999). Briefly, 0.5µL - 2.5µL metal-free NTA beaded agarose (Sigma) (~425 beads/µL) was dispensed into compact reaction columns (CRCs) with 35 µm frits (USB Corp., Cleveland, OH), and washed with 30µL HPLC water. The beads were then charged by washing with 3 x 30µL of 50mM $Fe(NO_3)_3$ dissolved in 12mM HCl. The charged beads were rinsed with 30µL of HPLC-grade water, and then 30µL of 0.1% acetic acid. Peptide samples were prepared for IMAC by diluting to 40µL and 50mM acetic acid, after which the entire volume was added to the IMAC-containing CRCs and incubated at 25°C overnight with shaking at 600 rpm. The IMAC beads were washed with 30µL 0.1% acetic acid, 30µL 30% acetonitrile/0.1% trifluoroacetic acid, and 30µL 0.1% acetic acid. The final volume was reduced to 5-10µL, and between 0.25 – 0.4µL of settled bead-slurry (corresponding to between 20 – 70 individual beads or 5% – 10% of total bead slurry) was used for MALDI-TOF MS analysis.

On-target dephosphorylation assay. On-target dephosphorylation was accomplished by spotting 0.25 – 0.4µL of a peptide solution, or peptides bound to IMAC beads, on a MALDI target plate immediately followed by the same volume of alkaline phosphatase (PPase) (New England Biolabs, Beverly, MA) diluted to various concentrations in 100mM ABC. The

phosphatase reaction was allowed to progress at room temperature for various time periods, after which 0.5 – 0.8μL saturated α-cyano-4-hydroxycinnamic acid (CHCA) (in 50% acetonitrile/0.1% TFA) was added to the phosphatase-containing spot, and the solution was allowed to crystallize at room temperature. Alternatively, CHCA in 50% acetonitrile/ 0.1 - 1% phosphoric acid was used as the matrix solution.

Mass Spectrometry. Phosphatase optimization experiments were conducted using a Reflex III MALDI-TOF mass spectrometer (Bruker Daltonics) with pulsed ion extraction, using an AnchorChip target plate (Bruker Daltonics, Billerica, MA). All other MS experiments were performed on an ABI 4700 MALDI-TOF/TOF mass spectrometer (Applied Biosystems, Foster City, CA), using a standard 4700 target plate.

Results

Analytical scheme for PPD**.** The analytical strategy for PPD is shown (Figure 2.4). In brief, proteolyzed proteins are incubated in batch mode with IMAC beads in a compact reaction column (Figure 2.4 A). Unbound peptides are removed by washing, and a fraction of the phosphopeptide-containing beads are spotted directly on the MALDI target surface (Figure 2.4 B). IMAC-bound peptides are dephosphorylated by on-target addition of alkaline phosphatase to the beads (Figure 2.4 C). CHCA matrix is added to the de-phosphorylated beads, which are then analyzed by MALDI-TOF MS (Figure 2.4 D). The peptides detected in the MS mode are analyzed by MS/MS, which reveals the peptide sequence and the total number of Ser, Thr, and Tyr residues ($i = \Sigma(S, T, Y)$) that could potentially be phosphorylated (Figure 2.4 E). Finally, HD-MS/MS experiments are conducted at *m/z* values corresponding to each potential phosphorylation state (e.g. *m/z* + 1 HPO_3, + 2 HPO_3….i

HPO_3) of the given peptide on a separate aliquot of the IMAC beads that have been spotted but not dephosphorylated (Figure 2.4 F).

Optimizing on-target dephosphorylation. Current methods of peptide dephosphorylation call for enzyme incubations from 0.75 – 1 hour at 37°C with 1 unit of alkaline phosphatase, after which the dephosphorylated peptides are purified over POROS R3 reverse-phase chromatographic resin, followed by MS analysis (Stensballe et al., 2001; Xhou et al., 2000). We were interested in developing a similar phosphatase assay that would be amenable to direct analysis on MALDI target plates. For on-target analysis, the on-target reaction times would need to be reduced (because of sample evaporation), the enzyme quantities would need to be reduced (because of suppression effects), and the purification steps would also have to be eliminated to avoid sample loss.

Different dilutions of PPase (1:10, 1:100, and 1:500 in ABC) were prepared, and each solution was mixed on-target with an equal volume of the model phosphopeptide, PKA-I. The PPase was allowed to react at room temperature for 5 minutes, after which MALDI matrix solution was added and allowed to crystallize. The addition of matrix stops the phosphatase reaction, which was confirmed by adding the phosphatase after adding the matrix, in which case the dephosphorylated peptide was not observed in the MS spectrum (data not shown). The images taken from the MALDI-spots corresponding to different phosphatase dilutions demonstrate the effect of the phosphatase storage buffer on spot integrity (Figure 2.5 A, right). While incubation with PPase diluted 1:10 leads to heterogeneous crystallization typical of high salt solutions, the reaction with 1:100 PPase had a negligible effect on the crystallization process. Each spot was subsequently analyzed on a Reflex III MALDI-TOF mass spectrometer using identical conditions (Figure 2.5 A, left).

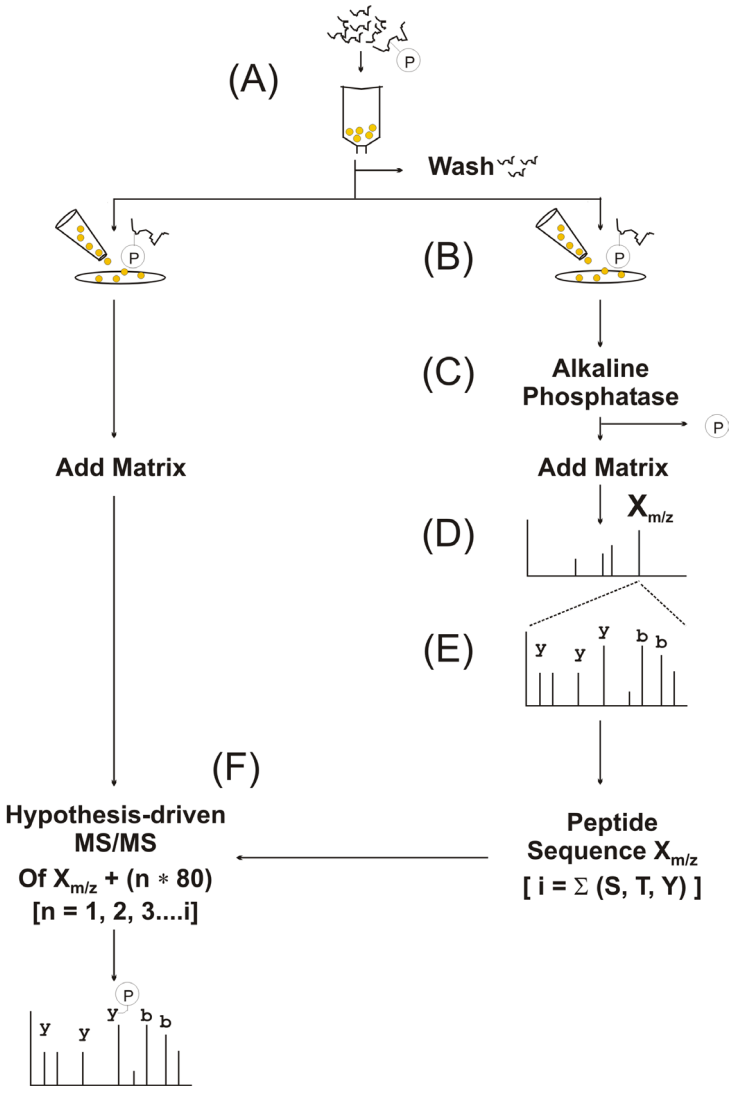

Figure 2.4. Analytical approach for phosphatase-directed phosphorylation site determination (PPD). Phosphopeptides from a protein digest are bound to IMAC beads and washed to eliminate non-binding peptides (A). The beads are split and dispensed directly onto a MALDI target plate (B) where they are immediately crystallized with matrix or reacted with alkaline phosphatase (C). Peaks that appear in the MALDI-MS spectrum of the phosphatase-treated sample (D) are sequenced by MALDI-MS/MS (E). Based on the mass of the dephosphorylated peptide ($X_{m/z}$), and the sequence (which provides the number of potential phosphorylation sites [i]), a series of hypothesis-driven MS/MS experiments are conducted on the untreated IMAC sample at m/z values corresponding to the predicted phosphorylated forms of the peptide [Xm/z + (n • 80)], where (n = 1, 2, 3….i) (F).

Apparent complete dephosphorylation was achieved at PPase dilutions 1:10 and 1:100, which are equivalent to 0.25 and 0.025 units of enzyme on the target, respectively. However, ion signals from the 1:10 dilution spot were much weaker than those observed for the 1:100 dilution spot, likely due to the presence various salts in the 10% phosphatase storage buffer. The PPase reaction was incomplete in spots treated with phosphatase diluted 1:500 indicating that the level of PPase activity was below that which is necessary for complete dephosphorylation within 5 minutes. Based on these results, the optimal PPase concentration for on-target peptide dephosphorylation and crystallization efficiency was found at a 1:100 dilution of the original PPase solution and was therefore used for all following experiments.

When conducting on-target enzyme reactions, careful considerations must be made to ensure that the reaction is complete before the spot droplet (~0.6μL) has evaporated, which typically occurs within 5 to 6 minutes. Thus, in order to minimize the time required for on-target dephosphorylation, the kinetics of the on-target PPase assay were measured using PKA-I. An aliquot of phosphatase (0.25μl of 1:100 dilution) was spotted on top of PKA-I solution (0.25μl), and allowed to incubate for various times at room temperature. Mass spectra generated from each spot are displayed in Figure 2.5 B (left). The percent dephosphorylation was estimated from the ratio of phosphorylated and dephosphorylated monoisotopic peak intensities in each spectrum and plotted versus time (Figure 2.5 B right). Approximately 90% of PKA-I was dephosphorylated within 2 minutes of phosphatase addition, and apparent complete dephosphorylation was achieved in 5 minutes. Based on these data, the rate of on-target peptide dephosphorylation was calculated to be approximately 500 fmoles min^{-1}, which is more than adequate for typical phosphopeptide

concentrations in MS experiments. Furthermore, these data show that the PPase reaction can be completed within a time frame such that the spotted sample does not evaporate at room temperature, and thus, does not require the use of a humidified reaction chamber.

Next, the on-target dephosphorylation assay was evaluated with phosphopeptides (KDIR-4) affinity-bound through their phosphate moieties to the immobilized Fe(III) on the IMAC beads. As a control for the specificity of the phosphate/metal interaction, we ran a parallel experiment in which KDIR-4 was incubated with un-charged IMAC beads (*i.e.*, lacking the immobilized metal). After incubation and washing, an aliquot of both charged and un-charged beads (between 20 to 70 beads per spot) were subjected to on-target dephosphorylation and analyzed by MALDI-MS. KDIR-4 phosphopeptide was detected only on the charged IMAC beads, and was completely dephosphorylated after treatment with phosphatase (Figure 2.5 C). These results indicate that phosphopeptides bound to IMAC beads in a metal-dependent fashion can be dephosphorylated directly on the MALDI target plate within 5 minutes at room temperature, without adverse effects on subsequent MS analysis.

When analyzing the phosphorylated KDIR-4 sample, ion signals were evident only when the laser was aimed directly at the beads. This is in contrast to our previous experiments using a MALDI-QTOF instrument that showed that the matrix leads directly to elution of affinity-bound phosphopeptides (Raska et al., 2002). However, in the previous studies, DHB instead of CHCA was used as the MALDI matrix because we found that DHB was the optimal matrix for our MALDI-QTOF experiments in contrast to our MALDI-TOF/TOF used in this study. When analyzing the de-phosphorylated sample, the ion signals were strongest when aiming the laser at the edges around the clusters of beads, suggesting that

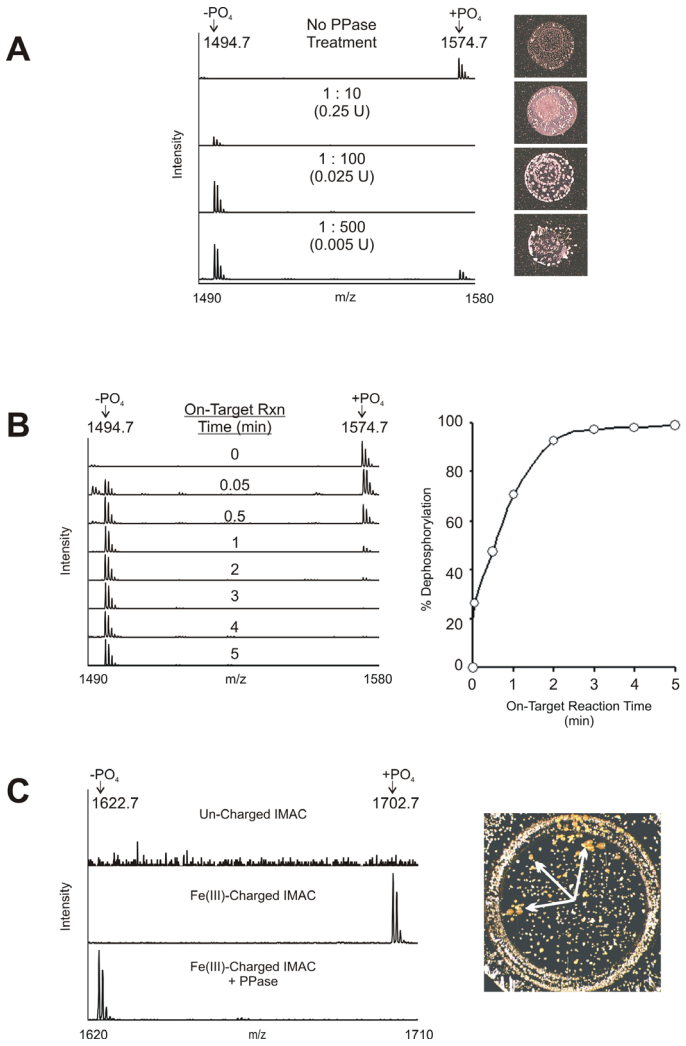

Figure 2.5. Optimizing on-MALDI-target dephosphorylation of phosphopeptides. (A) MS spectra of 1 pmole PKA-I phosphopeptide after alkaline phosphatase treatment on MALDI target plates. The dilution of phosphatase in 100mM ABC and the corresponding total units (U) of enzyme are indicated above each respective spectrum (left). All spectra were collected under identical conditions and are in the same intensity scale. Images to the right of each spectrum demonstrate the MALDI spot integrity at each dilution. (B) On-target dephosphorylation kinetics. MS spectra of 1 pmole PKA-I phosphopeptide exposed to alkaline phosphatase on a MALDI target for the indicated time duration at room temperature (left). Scatter plot of percent dephosphorylation versus time (right). (C) On-target dephosphorylation of KDIR-4 phosphopeptide specifically bound to Fe(III)-charged IMAC beads. MS spectra from uncharged (Top) or Fe(III)-charged IMAC beads after incubation with KDIR-4 phosphopeptide followed with (Bottom) or without (Middle) on-target phosphatase treatment (left). Photograph of phosphopeptide-bound IMAC beads (>50 count) after treatment with alkaline phosphatase (right). The beads, (yellowish in color) tend to cluster into groups on the MALDI target plate as indicated by white arrows.

either the phosphatase reaction or the ABC buffer was eluting the peptide from the Fe(III)-chelated NTA groups on the IMAC beads. To evaluate the ability of ABC buffer to elute phosphopeptides from the Fe(III)-charged IMAC beads, we conducted a series of elution experiments using IMAC beads that were incubated with KDIR-4 phosphopeptide as described for Figure 2.5. In each experiment an aliquot of the beads was spotted onto the target plate with CHCA matrix (in 50% MeCN / 0.1%TFA) and analyzed by MALDI-MS. MALDI-MS analysis of the beads without any additional treatment revealed the KDIR-4 phosphopeptide at *m/z* 1702.7 (Figure 2.6 A). The ion signal was no longer detected after sequentially spotting the beads followed by ABC without phosphatase (Figure 2.6 B). However, when the ABC buffer contained the phosphatase, the dephosphorylated form of KDIR-4 was detected (Figure 2.6 C). Next, the remaining IMAC beads left in the compact reaction column were washed with ABC buffer. The wash solution was devoid of peptide as determined by collecting and desalting the solution with a C18 Zip-tip followed by MALDI-MS analysis (Figure 2.6 D). Importantly, we confirmed that KDIR-4 phosphopeptide could be purified using the C18 Zip-Tip by purifying a test sample diluted in the same ABC buffer (data not shown). No ion signals could be detected directly from the IMAC beads after the ABC wash, or after re-equilibration of the IMAC beads with 0.1% acetic acid (Figure 2.6 E and F). Taken together, this suggests that ABC treatment of phosphopeptides bound to Fe(III)-charged IMAC beads results in the strong immobilization of the phosphopeptide in such a way that 1) is irreversible by re-equilibration with acetic acid, 2) that precludes ionization directly from the beads, and 3) which can be overcome if phosphatase actively removes the phosphoryl group from the peptide. These data also suggested to us that the phosphatase must be reacting directly with the bound form of the phosphopeptide while the

phosphoryl group is still attached to the immobilized Fe(III) atom. This possibility is not altogether unlikely considering that crystallized alkaline phosphatase enzymes display a notably shallow binding pocket, which is believed to play a part in their enzymatic non-specificity (Hollfelder and Herschlag, 1995; Kim and Wyckoff, 1991; O'Brien and Herschlag, 1999), and which could potentially allow access to a phosphate moiety that is immobilized by the Fe(III)-chelated NTA molecule at the surface of an agarose bead.

Evaluation of PPD for Analyzing the Phosphorylation sites of β-casein**.** Bovine β-casein has been extensively used as a model phosphoprotein for MS assay development because it is easy to purify and contains five residues that are stoichiometrically phosphorylated (Greenberg et al., 1984). PPD was used to analyze tryptic digests of bovine β-casein, which contains 2 major phosphopeptides: a monophosphopeptide (containing phosphoserine 50) and a tetraphosphopeptide (containing phosphoserines 30, 32, 33, 34). A 10 pmole aliquot of a β-casein tryptic digest was incubated overnight with Fe(III)-charged IMAC beads and approximately forty-five beads (5-6% of the total bead count corresponding to less than 500 fmol β-casein) were spotted onto two separate spots on the target and analyzed by PPD. In this experiment, all MS and MS/MS data were generated on an ABI 4700 TOF/TOF mass spectrometer. A single abundant peak was detected in the PPase-untreated sample at *m/z* 2061.8, corresponding to the monophosphorylated β-casein phosphopeptide $_{p}$β(48–63) (Figure 2.7 A). In the PPase-treated sample, we detected 5 peaks corresponding to the dephosphorylated forms of both β-casein phosphopeptides: the dephosphorylated form of the monophosphopeptide, β(48–63) (*m/z* 1981.8), and 4 different peaks corresponding to non-tryptic forms (β(23–40) *m/z* 1918.9, and β(22–40) *m/z* 2033.0), and tryptic forms (β(17–40) *m/z* 2646.3, and β(16–40) *m/z* 2802.4) of the β_1 phosphopeptide (Figure 2.7 B).

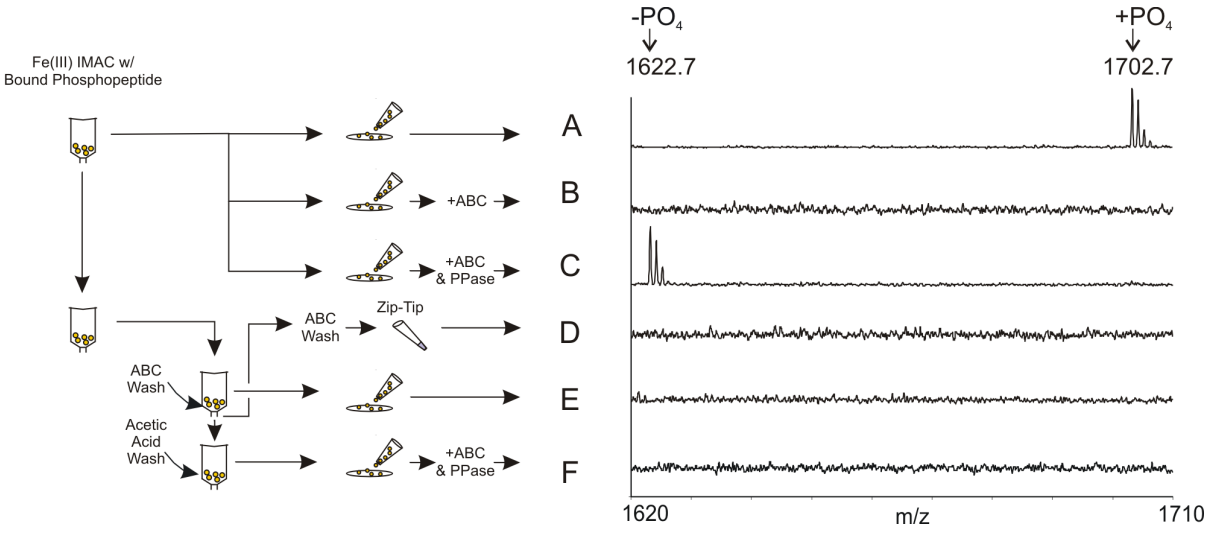

Figure 2.6. Effect of ammonium bicarbonate on the on-target dephosphorylation and MS detection of KDIR4 phosphopeptide. One pmole of KDIR-4 phosphopeptide was bound to Fe(III)-charged IMAC beads and analyzed by MALDI-TOF MS as indicated by the flow chart on the left. The resulting MS spectra from each experiment is indicated on the right. A fraction of the phosphopeptide-bound IMAC beads (3% – 5 % of the total bead count used in the binding reaction) were analyzed directly (A), after on-target treatment with 50mM ABC (B), or after on-target treatment with 50mM ABC containing 0.025U alkaline phosphatase (C). The remaining beads (~85% of the total original bead count used in the binding reaction) were washed with an excess volume of 50mM ABC. A fraction of the ABC-washed beads (3% - 5%) were analyzed directly (D), and the entire ABC wash solution was also analyzed after C18 Zip-Tip purification (E). Finally, the remaining beads were re-equilibrated with an excess volume of 0.1% acetic acid and a fraction of the beads was analyzed directly (F).

An MS/MS spectrum from the β(16–40) ion at *m/z* 2802.4 is shown (Figure 2.7 C). We also detected 3 peaks which did not match β-casein phosphopeptides (*m/z* 2299.0, 2427.1, and 2688.1), and were later assigned to different tryptic regions from α-S2 casein after MS/MS sequencing (α(16–35), α(16–36), and α(61–85), which are known to be phosphorylated.(Chang et al., 2004) Alpha-S2 casein is a phosphoprotein commonly found at low levels in β-casein preparations (Stewart et al., 1987).

HD-MS/MS was performed on the *m/z* value corresponding to the β-casein tetraphosphopeptide (β(16–40) at *m/z* 3122.4 (= 2802.4 Da + (4 x 80 Da)), even though no ion at this mass was detectable in the MS spectrum for the phosphorylated sample. It would be preferable to conduct all HD-MS/MS experiments directly on the IMAC beads without prior elution, thereby simplifying the assay and reducing chances for sample loss. However, when the HD-MS/MS experiment on the phosphorylated beads was attempted, no fragment ions from the β-casein tetraphosphopeptide were detected. Since phosphoric acid has recently been reported to improve phosphopeptide ion signals in MALDI and ESI-MS, (Stensballe and Jensen, 2004) we tried spotting 12% – 17% of the phosphorylated IMAC beads with CHCA dissolved in 50% MeCN and 1%, 0.5%, or 0.1% H_3PO_4. In this case, HD-MS/MS of *m/z* 3122.4 revealed multiple fragment ions from the β-casein tetraphosphopeptide, including neutral loss fragments $(M+H - H_3PO_4)^+$, y ions, and b ions (Figure 2.7 D). Although the same general fragmentation pattern was observed when using any of the three phosphoric acid solutions, the 0.5% H_3PO_4 solution gave the best ion signal. Thus, we conclude that PPD can be conducted on IMAC beads that are deposited onto MALDI target plates, that the method is useful for detecting phosphopeptides that exhibit low ionization efficiency (e.g., multiply-phosphorylated peptides), and that substitution of

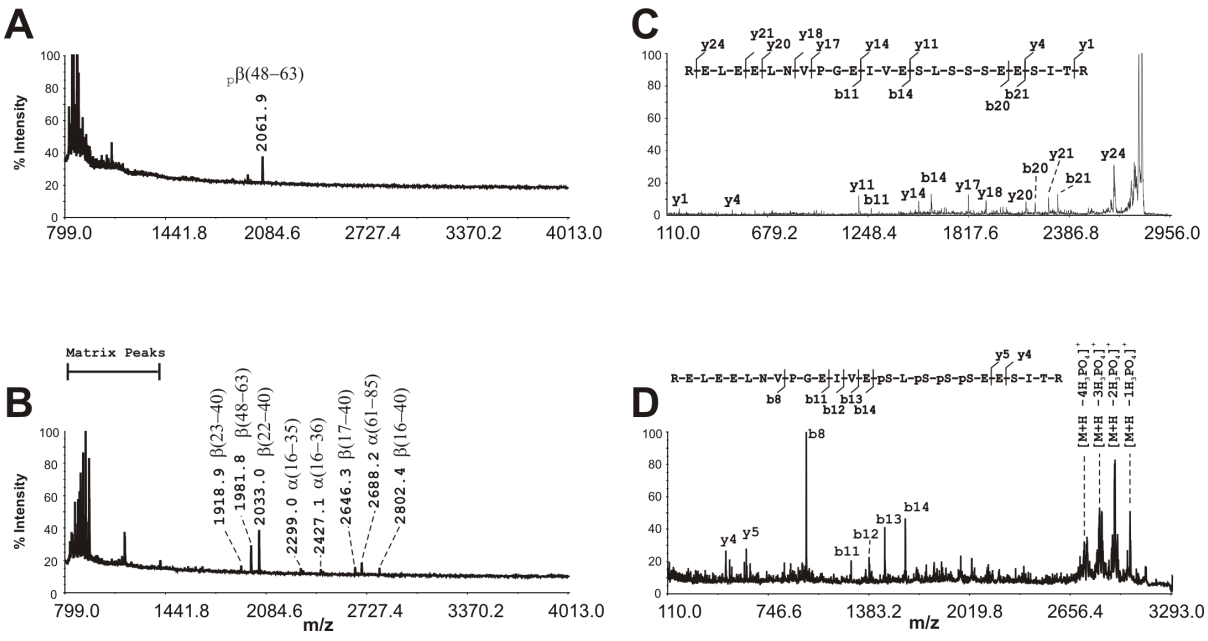

Figure 2.7. PPD of β-casein phosphopeptides immobilized on IMAC beads. (A) MS spectrum from Fe(III)-charged IMAC beads after incubation with a β-casein tryptic digest. (B) Same as in (A), but treated with alkaline phosphatase. Peptides are annotated as follows: β-casein, (β); $\tilde{\alpha}$S2 casein, (α); each peptide's position within the primary sequence of the protein are given in parentheses. (C) MS/MS spectrum from the β(16–40) peak at *m/z* 2802.4, seen in (B). (D) HD-MS/MS spectrum from the β–casein tetraphosphopeptide at *m/z* 3122.4 directly bound to IMAC beads.

0.5% phosphoric acid for 0.1% TFA in the matrix buffer improves HD-MS/MS on the phosphorylated IMAC beads.

Application of PPD for analyzing dSLBP *in vivo* phosphorylation**.** In order to demonstrate the practical value of PPD in analyzing biological samples, this technique was used to analyze phosphorylation sites within the C-terminus of the metazoan histone mRNA regulator, dSLBP. Accurate molecular weight determinations and "top-down" MS/MS experiments conducted on *Drosophila* SLBP (dSLBP) by FTICR-MS revealed the existence of four phosphorylation sites near the C-terminus of the protein (Borchers et al., 2006). However, multiple attempts to map the phosphorylation sites within the C-terminus using "bottom-up" strategies – including LC-MS and traditional IMAC methods, in which peptides were pre-enriched on and eluted from IMAC beads with sodium phosphate or ammoniated water were not successful. Thus, the exact phosphorylation sites near the C-terminus of dSLBP remained unknown.

The PPD method was applied to phosphorylation site mapping of the dSLBP C-terminus because it does not rely on the detection of phosphopeptides in the MS mode and also does not require elution from the IMAC beads. A Lys-C digest composed of approximately 100 pmoles dSLBP was enriched in phosphopeptides using IMAC, and ~10% of the beads were analyzed (10% per spot) directly without elution. No peptides were detected in the MS spectrum from the phosphorylated sample (Figure 2.8 A). However, after on-target treatment of the beads with PPase, a single peak at *m/z* 2735.2 was evident (Figure 2.8 B). MS/MS sequencing of peak 2735.2 revealed a 25-residue peptide, L8-9, (K)SLHIYDPPTQARDTAKDSNSDSDSD(-), which contained a single missed cleavage and included 8 potential phosphorylation sites within the C-terminus of dSLBP (Figure 2.8 C).

To determine the degree and location of phosphorylation within the L8-9 peptide, HD-MS/MS was conducted at m/z values corresponding to every potential phosphorylation state of the peptide in the IMAC sample not treated with PPase. The most intense HD-MS/MS signal was observed for the quadruply-phosphorylated state of L8-9 at *m/z* 3055.1 (Figure 2.8 D). The HD-MS/MS spectrum from *m/z* 3055.1 showed four distinct neutral loss ions, corresponding to a loss of one, two, three, or four phosphates (-98, H_3PO_4) from the tetraphosphorylated peptide. Sufficient number of sequence-specific fragment ions were also evident, which allowed us to positively confirm the peptide as dSLBP L8-9. Most importantly, the appearance of the b17 ion indicates that only the last 4 serine residues are phosphorylated. An HD-MS/MS spectrum was also obtained for a triply-phosphorylated form of L8-9 (*m/z* 2975.1), although at much lower intensity than that of the tetraphosphopeptide. A sufficient number of fragment ions confirmed the identity of the peptide as L8-9, and the presence of the b17 fragment ion indicates that the 3 phosphorylation sites are localized within the last 4 serine residues. However, the exact location of the 3 phosphorylation sites could not be determined from the HD-MS/MS spectrum, which is likely due to the negative charge on the smaller y-ions of this peptide. The relative intensities of the quadruply- and triply-phosphorylated HD-MS/MS spectra were consistent with data obtained from mass measurements of the intact full-length protein by nano electrospray ionization mass spectrometry, FT-ICR MS (data not shown), and previously reported results (Dominski et al., 2002). The phosphorylated form of Lys-C peptide L9 could not be detected by HD-MS/MS. This peptide might not be present in the enzymatic digest or may not be detectable since this peptide is even more negatively charged than L8-9. In conclusion, while previous bottom-up and top-down proteomic methods failed

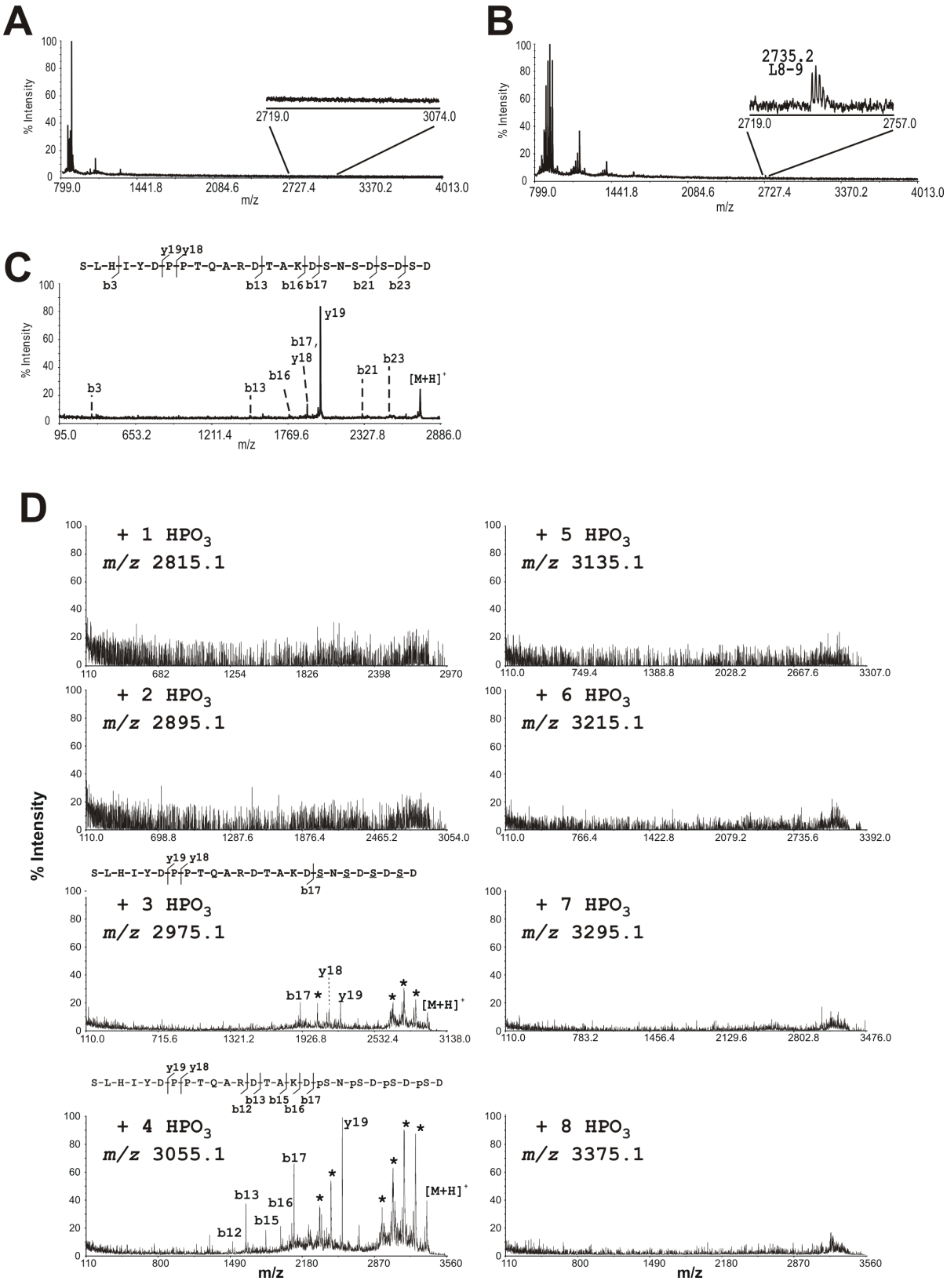
A
% Intensity
2719.0
3074.0
m/z
B
2735.2
L8-9
2719.0
2757.0
C
S-L-H-I-Y-D-P-P-T-Q-A-R-D-T-A-K-D-S-N-S-D-S-D-S-D
y19 y18
b3
b13 b16 b17
b21 b23
y19
b17,
y18
b16
b23
b21
[M+H]+
b3
b13
D
+ 1 HPO3
m/z 2815.1
+ 5 HPO3
m/z 3135.1
+ 2 HPO3
m/z 2895.1
+ 6 HPO3
m/z 3215.1
% Intensity
S-L-H-I-Y-D-P-P-T-Q-A-R-D-T-A-K-D-S-N-S-D-S-D-S-D
b17
+ 3 HPO3
m/z 2975.1
+ 7 HPO3
m/z 3295.1
S-L-H-I-Y-D-P-P-T-Q-A-R-D-T-A-K-D-pS-N-pS-D-pS-D-pS-D
b12 b13 b15 b16 b17
+ 4 HPO3
m/z 3055.1
+ 8 HPO3
m/z 3375.1
m/z

Figure 2.8. PPD analysis of dSLBP after *in vivo* phosphorylation. (A) MS spectrum of IMAC beads after incubation with dSLBP Lys-C peptides. (B) Same as in (A) but treated with alkaline phosphatase. (A and B insets) Expanded region of the MS spectra for comparison between (A) and (B). (C) MS/MS spectrum of the ion at m/z 2735.2 from the phosphatase treated spectrum, identified as the C-terminal dSLBP peptide L8-9. (D) HD-MS/MS spectra at m/z values corresponding to each of 8 potential phosphorylation states of the L8-9 dSLBP peptide acquired directly from the PPase-untreated IMAC beads. Neutral loss ions (-98 Da, H3PO4) are indicated by an asterisk. Phosphorylation sites that have been positively localized by HD-MS/MS are indicated with a lower case "p" next to the phosphorylated residue (e.g. pS). Phosphorylation sites implicated but not positively localized by HD-MS/MS are underlined.

to determine the exact location of the C-terminal phosphorylation sites in dSLBP, the PPD experiments successfully identified the phosphorylation sites as S269, S271, S273, and S275.

Discussion

The method described here, called PPD, combines IMAC phosphopeptide enrichment, on-target phosphatase treatment of IMAC-bound peptides, and hypothesis-driven MALDI-MS/MS of IMAC-bound peptides. Here, we have demonstrated proof-of-principle experiments that show feasibility of PPD by detecting and sequencing a tetra-phosphopeptide from β-casein, as well as phosphopeptides in α-S2 casein that occur as low abundance impurities in β-casein preparations. We have further shown the competence of this method for analysis of *in-vivo* phosphorylated protein. In this particular case, PPD identified, for the first time, four C-terminal *in-vivo* phosphorylation sites in dSLBP, which were not detectable by top-down or traditional bottom-up approaches.

A current limitation of the PPD method is in the ability to manually handle small volumes with a minimal number of IMAC beads, which necessarily affects the sample requirements, and sensitivity of the approach. Efforts to improve sensitivity by using fewer beads per binding reaction, thereby increasing the number of bound phosphopeptides per bead, have made little improvement in the sample requirements as it becomes even more difficult to maintain a high percentage of the total bead count used in the binding reaction in these cases. Despite these limitations, robotic liquid handling systems have been used successfully to improve similar limitations for direct MALDI-MS of individual antibody beads, and are currently being improved (C. Borchers, personal communication).

In some respects, the PPD and HMS-MS methods may be considered complementary.

Whereas the PPD method requires that the phosphopeptides within the sample are successfully isolated by the IMAC procedure, the HMS-MS method requires prior knowledge of the sample's protein content and sequence. However, depending on the size and number of different proteins to be analyzed within a sample, the use of PPD may offer a distinct advantage over the HMS-MS method. To demonstrate this concept, the number of MS/MS analyses that would be theoretically required to map the four C-terminal phosphorylation sites in dSLBP using HMS-MS or PPD was compared. A total of 15 independent HMS-MS analyses would be required to cover all potential phosphopeptides in the sample if there were no missed cleavages. As many as 44, 78, or 82 independent HMS-MS analyses would be required if one assumed the existence of phosphopeptides with up to 1, 2, or 3 missed cleavages, respectively. In contrast, PPD analysis revealed the existence of a single C-terminal peptide containing 8 potential phosphorylation sites. Therefore, when using PPD, only 8 HD-MS/MS experiments were required to localize the 4 C-terminal phosphorylation sites. Thus, PPD can significantly reduce instrument time and MALDI spot consumption compared to HMS-MS, an advantage that increases with the complexity of the sample and the size of the proteins to be analyzed. Moreover, using the PPD method over HMS-MS would be preferable when analyzing samples where the protein content and sequence is not known *a priori*, such as in complex protein mixtures.

By utilizing a combination of IMAC, on-target dephosphorylation, and MALDI-MS, PPD permits the analysis of phosphopeptides, which exhibit lower ion abundances and thus are typically not selected for sequencing in data-dependent online LC-MS/MS experiments. The use of on-target reactions can minimize losses due to unnecessary sample handling. Furthermore, using MALDI-MS rather than online LC-MS also allows multiple repetitive

MS and MS/MS analyses, which can increase the amount of information acquired from a single sample.

PPD can be used to map phosphorylation sites in mixtures of unknown proteins because the strategy employs IMAC for unbiased enrichment of phosphopeptides. Thus, it extends the range of the HMS-MS method because PPD does not rely on *a priori* knowledge of the sample protein or the particular phosphorylated peptide, and phosphopeptides containing missed cleavages can be easily detected. Furthermore, using PPD, the number of MS/MS analyses required to screen potential phosphopeptides is greatly reduced.

The PPD method is also designed to overcome two major obstacles to MS detection of phosphopeptides: the suppression of phosphopeptide ions in complex sample mixtures and the inherent low sensitivity of phosphopeptide detection in the MS mode. The combined approach inherent in PPD has proven to be a useful technique for identifying peptides that are phosphorylated at multiple sites, and has been successful for determining phosphorylation sites in multiply-phosphorylated peptides where other approaches have failed.

CHAPTER III

MND2 AND SWM1 ARE STOICHIOMETRIC COMPONENTS OF THE *SACCHAROMYCES CEREVISIAE* ANAPHASE PROMOTING COMPLEX

(Including modified portions from: Hall, M.C., Torres, M.P., Schroeder, G.K., Borchers, C.H., (2003) *J. Biol. Chem.* **278** (19), 16698-16705.)

Summary

Eleven subunits have been previously identified in the APC from budding yeast. In this study, two additional subunits, Mnd2 and Swm1, have been identified by mass spectrometry. Both Mnd2 and Swm1 were found specifically associated with a highly purified preparation of the APC from haploid yeast whole cell extract. Moreover, the APC co-purified with epitope- tagged Mnd2 and Swm1. Both proteins were present in APC preparations from haploid cells arrested in G1, S, and M phases, indicating that they are constitutive components of the complex throughout the yeast cell cycle. The stoichiometry of Mnd2 and Swm1 relative to other APC subunits was similar as determined by reverse-phase HPLC and UV detection as well as ^{35}S-labelling *in vivo* and SDS-PAGE. Previous studies described meiotic defects for mutations in *MND2* and *SWM1*. Here, it is shown that *mnd2Δ* and *swm1Δ* haploid strains exhibit accumulation of G2/M cells comparable with that seen in *apc9Δ* or *apc10Δ* strains and consistent with an APC defect. Taken together, these results demonstrate that *Swm1* and *Mnd2* are functional components of the yeast APC.

Introduction

The eukaryotic cell division cycle involves the replication of chromosomal DNA and its equal distribution to daughter cells in a highly regulated series of events. As one of the essential regulatory components of chromosome segregation in eukaryotes the APC targets numerous substrate proteins involved in mitosis, meiosis, and other cellular processes for degradation by the proteosome by catalyzing their polyubiquitination, and is regulated by checkpoint signaling pathways that monitor DNA and chromosome integrity (Musacchio and Hardwick, 2002) (reviewed in chapter I).

Eleven constitutive core subunits of the APC have been identified in the budding yeast, *Saccharomyces cerevisiae* (Hwang and Murray, 1997; Zachariae et al., 1998b; Zachariae et al., 1996), and in vertebrates (Gmachl et al., 2000; Grossberger et al., 1999; Peters et al., 1996). Homologs of most of the subunits have been found in other model systems as well, including *Schizosaccharomyces pombe*, *Caenorhabditis elegans*, and *Drosophila melanogaster* (Harper et al., 2002). Ten of the 11 known APC subunits of budding yeast have human homologs, with yeast Apc9 being the only exception. The extensive homology between APCs of organisms as diverse as humans and yeasts points to an ancient evolutionary origin and reflects the importance of the APC in controlling some of the most fundamental cell cycle events in eukaryotes.

The presence of so many subunits makes the APC and unusual E3 enzyme in terms of its size and complexity. The actual catalytic reaction involving transfer of ubiquitin from an E2 enzyme to a substrate proteins is intrinsic to a single small RING finger subunit, Apc11 (Gmachl et al., 2000; Leverson et al., 2000) (reviewed in chapter I). Another subunit, Apc2, containing a highly conserved cullin domain present in other E3 ubiquitin ligases interacts

with Apc11, and is important for catalyzing ubiquitin transfer. The specific functions of the remaining subunits are diverse and complex, and may involve substrate recruitment and specificity, cellular localization, or interaction with and response to regulatory proteins such as cyclin-dependent kinases and spindle assembly checkpoint proteins. Some subunits function in a purely structural manner by forming a scaffold that allows proper complex assembly (reviewed in chapter I).

While purifying the APC from budding yeast extracts, two previously unidentified proteins were consistently observed under high salt conditions with the core complex. In this chapter, I provide evidence that these two proteins, Mnd2 and Swm1, are in fact constitutive components of the core APC. Both proteins exist in stoichiometric amounts relative to other APC subunits and both are found associated with the complex during G1, S, and M phases. Swm1 is believed to be identical to Apc13, a small protein observed previously in APC preparations that was never identified (Zachariae et al., 1998b). In addition, yeast strains lacking either protein display some accumulation in G2/M phase, consistent with an APC defect. The importance of these identifications is discussed with regard to what is now known about the meiotic phenotypes of each protein.

Experimental procedures

Yeast methods and strain construction

Yeast strains expressing Cdc27, Swm1, and Mnd2 (Table 3.1) containing carboxyl-terminal 3xFLAG epitopes were constructed by integration of PCR products amplified from the template p3FLAG-KanMX (gift from Dr. Toshio Tsukiyama; Fred Hutchinson Cancer Center) at the desired location as described (Gelbart et al., 2001). Integrants were selected on

Table 3.1
S. cerevisiae strains used in this study

Strain	Relevant Genotype	Source
W1588-4c[a]	*MAT*a *ade2-1 can1-100 his3-11,15 leu2-3,112 trp1-1 ura3-1*	R. Rothstein
YKA151[a]	*CDC27-3FLAG:KanMX4*	M.T.
YKA152[a]	*MND2-3FLAG:KanMX4*	M.T.
YKA153[a]	*SWM1-3FLAG:KanMX4*	M.T.
YKA155[a]	*CDC27-3FLAG:KanMX4 bar1Δ::URA3*	Hall MC
BY4741	*MAT*a*His3D1 leu2D0 met15D0 ura3D0*	SGDP[b]
2713[c]	*apc9Δ::KanMX4*	SGDP[b]
4607[c]	*apc10Δ::KanMX4*	SGDP[b]
5960[c]	*mnd2Δ::KanMX4*	SGDP[b]
3619[c]	*swm1Δ::KanMX4*	SGDP[b]

[a]Derived from W1588-4c, which is a derivative of W303 in which the weak *rad5* mutation has been repaired (Hall et al., 2003).
[b]SGDP, *Saccharomyces* Genome Deletion Project.
[c]Derived from BY474, and the values correspond to the SGDP record number.

YPD agar containing 500 μg/mL G418, and correct integration of the cassette was confirmed by PCR and DNA sequencing. Deletion of the *BAR1* gene from W1588-4c was achieved by integration of a *URA3* cassette amplified by PCR from pRS406 at the *BAR1* locus. Replacement of *BAR1* with *URA3* was confirmed by PCR. Strains from which the *APC9*, *APC10*, *SWM1*, or *MND2* genes had been deleted (Table 3.1) as well as their parent strain, BY4741, were from the *Saccharomyces* Genome Deletion Project, available through ResGen. The presence of the correct deletion was confirmed in each of these strains by PCR using primers flanking the appropriate open reading frame.

Cell cycle arrests were performed in mid-log phase cultures of strain YKA155 as follows. For G1 arrest, α-factor peptide (University of North Carolina peptide synthesis facility) was added from a 5 mg/mL stock in ethanol to a final concentration of 50 μg/L. For S phase arrest, hydroxyurea (Sigma) powder was added directly to cultures at a final concentration of 10 mg/mL. For M arrest, nocodazole (Sigma) was added from a 1.5 mg/mL stock in dimethyl sulfoxide to a final concentration of 15 μg/mL. Cell cycle arrests were monitored by phase-contrast micrsocopy until >90% of the cells had achieved the desired morphology (unbudded for G1 and large budded for S and M).

Purification of the APC

Approximately 10^{11} cells from late log phase cultures were washed with water and resuspended in 200 mL of cold (4°C) APC buffer (25 mM HEPES-NaOH, pH 7.5, 400 mM NaCl, 10% glycerol, 0.1% Triton X-100, 0.5 mM dithiothreitol, 25 mM NaF, 25 mM β-glycerophosphate, and 1 mM activated sodium orthovanadate) containing freshly added complete protease inhibitor tablets (Roche Applied Science) and 0.5 mM

phenylmethylsulfonyl fluoride. All subsequent steps were performed at 4°C or on ice. Cells were disrupted six times for 1.5 min with 0.5-mm glass beads in a bead beater (Biospec Products), allowing 5 min between pulses for cooling. Extract (~200 mL) was pre-cleared by centrifugation for 30 min at 35,000 x g and cleared a second time for 1 hour at 92,000 x g. The soluble extract (5 – 15 mg/mL protein) was incubated with 100 µL of pre-equilibrated EZview anti-FLAG M2 antibody-coupled agarose resin (Sigma) for 2 hours. The affinity resin was collected by centrifugation, washed four times for 10 min with 25 mL of APC buffer, transferred to a microcentrifuge tube, and washed an additional three times with 1 mL of APC buffer. APC was eluted by two sequential 30 min incubations at 30°C with 200 µL of APC buffer containing 500 µg/mL 3xFLAG peptide (Sigma). Elutions were pooled, and APC was precipitated with 6 volumes of cold acetone. For the peptide block control, an extract from YKA151 was split into two equal volumes. From one half, APC was purified as described above. From the other half, APC was purified by using an identical volume of anti-FLAG resin that had been pre-blocked with 3xFLAG peptide (as used in the elution) in APC buffer for 1 hour before addition to the extract. Otherwise, the two preparations were performed identically.

Identification of SDS-PAGE gel bands by mass spectrometry

Proteins eluted from the anti-FLAG affinity resin were separated by SDS-PAGE on 4-12% Bis-Tris NuPAGE gels (Invitrogen) and stained with Coomassie Brilliant Blue R-250 (Bio-Rad). Individual gel bands were carefully excised with a razor and subjected to trypsin proteolysis using a ProGest automated digester (Genomic Solutions). Extracted tryptic peptides were analyzed on a Reflex III MALDI-TOF mass spectrometer (Bruker Daltonics).

Data were internally calibrated with trypsin autoproteolysis peaks and submitted to the MASCOT database search engine (Matrix Science) for protein identification by peptide mass fingerprinting. All identifications in this study represent statistically significant matches from the database of *S. cerevisiae* proteins. When a statistically significant match was not obtained by peptide mass fingerprinting, individual peptides from the spectrum were subjected to nano-electrospray tandem MS on a QStar QqTOF mass spectrometer (Applied Biosystems) to confirm the protein identity.

Determination of APC subunit Stoichiometry

Estimating APC subunit stoichiometry by reverse-phase HPLC and UV detection was accomplished by washing the APC affinity preparation before FLAG peptide elution with 4 x 25 mL volumes of 25 mM $NaPO_4$ wash buffer (pH 7.5) containing 400 mM NaCl and 10% glycerol. The APC was then eluted with 3xFLAG peptide as described above; however, 25 mM $NaPO_4$ buffer was used in place of APC buffer to eliminate the presence of detergent. The entire eluate was loaded onto an Agilent 1100 series HPLC coupled to a C4 Mass Spec reverse phase column (Vydac), and an 1100 series UV spectrophotometer (Agilent), and a Foxy 200 fraction collector (ISCO Inc). Conditions for HPLC separation were as follows: buffer A, 5% acetonitrile (ACN)/0.1% trifluoroacetic acid (TFA); buffer B, 95% ACN/0.09% TFA; gradient, 5% B for 5 minutes, 5% to 65% B in 65 minutes, 65% to 95% B in 10 minutes. Fractions were collected every minute, frozen at –80°C, and lyophilized. The protein identity of each peak in the HPLC chromatogram was determined by digestion with porcine trypsin in 50 mM ammonium bicarbonate (1:20 enzyme-to-substrate ratio) followed by LC-MS/MS analysis of each digest using a Qq-TOF instrument (Waters-Micromass)

connected to a capillary HPLC coupled with a C18 reverse phase column (LC Packings). Identifications were determined using the Mascot search engine using both MS and MS/MS data. The C4 chromatographic peak areas at A_{210} were normalized by the number of amino acids in the corresponding subunit identified by LC-MS/MS. Stoichiometries are reported relative to the catalytic RING subunit, Apc11.

To estimate the stoichiometries of Apc1 and Apc5, the APC was labeled metabolically with ^{35}S-cysteine and ^{35}S-methionine. Briefly, a saturated 5 mL culture was diluted to OD_{600} = 0.2 in 50 mL YPD and allowed to grow to OD_{600} = 0.7. Cells were harvested by centrifugation, washed once with sterile water, and resuspended in 35 mL synthetic complete media lacking cysteine and methionine and containing 1 mCi each of L-^{35}S-cysteine and L-^{35}S-methionine (ICN Inc.). After labeling for 1 hour at 30°C, cells were collected by centrifugation, washed once with water, transferred to a 2 mL screwcap tube, and frozen at –80°C. Radioactive APC was purified, eluted, and precipitated as described above except lysis was achieved by vortexing in a microfuge tube containing glass beads. The purified APC was separated by SDS-PAGE as described above, and the gel was dried and vacuum-pressed onto Whatman filter paper (Millipore). The dried gel was exposed to a storage phosphor screen and scanned using a STORM phosphorimager (Molecular Dynamics). Image densitometry was conducted using Scion Image software and band intensity values were normalized by total cysteine/methionine content for each subunit (Scion Corp.).

Flow cytometry

For flow cytometry, cells from 0.5 mL of culture were washed with 1 mL of water and fixed overnight in 1 mL of 70% ethanol at 4°C. Cells were rinsed twice with 1 mL of 50 mM

Tris-HCl, pH 8.0, and incubated for 2-3 hours at 50°C with 2 µg/mL RNase A and 1 mg/mL proteinase K in 50 mM Tris-HCl. After washing with 1 mL of FC buffer (200 mM Tris-HCl, pH 8.0, 200 mM NaCl, 78 mM MgCl), cells were resuspended in 500 µL of FC buffer containing 5 µM Sytox Green (Molecular Probes, Inc.). DNA content was measured on a FACScan instrument. Percentages of G1, S, and G2/M cells were calculated using ModFit LT software (Verity Software House, Inc.).

Results

The majority of the results contained within this chapter have been generated by me. However, Figures 1A, and Table 3 were generated by Schroeder GK and Hall MC, respectively. Additional data describing Mnd2 and Swm1 as core APC subunits is described in a paper for which I am the second author (Hall, M.C., Torres, M.P., Schroeder, G.K., Borchers, C.H., 2003).

Identification of Mnd2 and Swm1 in APC purifications

I constructed a yeast strain, YKA151, which produces the Cdc27 protein with a C-terminal 3xFLAG epitope tag from its natural chromosomal locus for immunoaffinity purification of the APC. In preparations of APC from YKA151, each of the 11 known subunits as well as two other bands that had not been previously described as APC subunits was positively identified by MS analysis (Figure 3.1 A, third lane). It should be noted that the conditions used for the affinity purification of APC include a high salt concentration (425 mM Na^+) at all steps, demonstrating the high salt stability of the APC. A control purification in which the anti-FLAG affinity beads were pre-blocked with the antigenic 3xFLAG peptide was

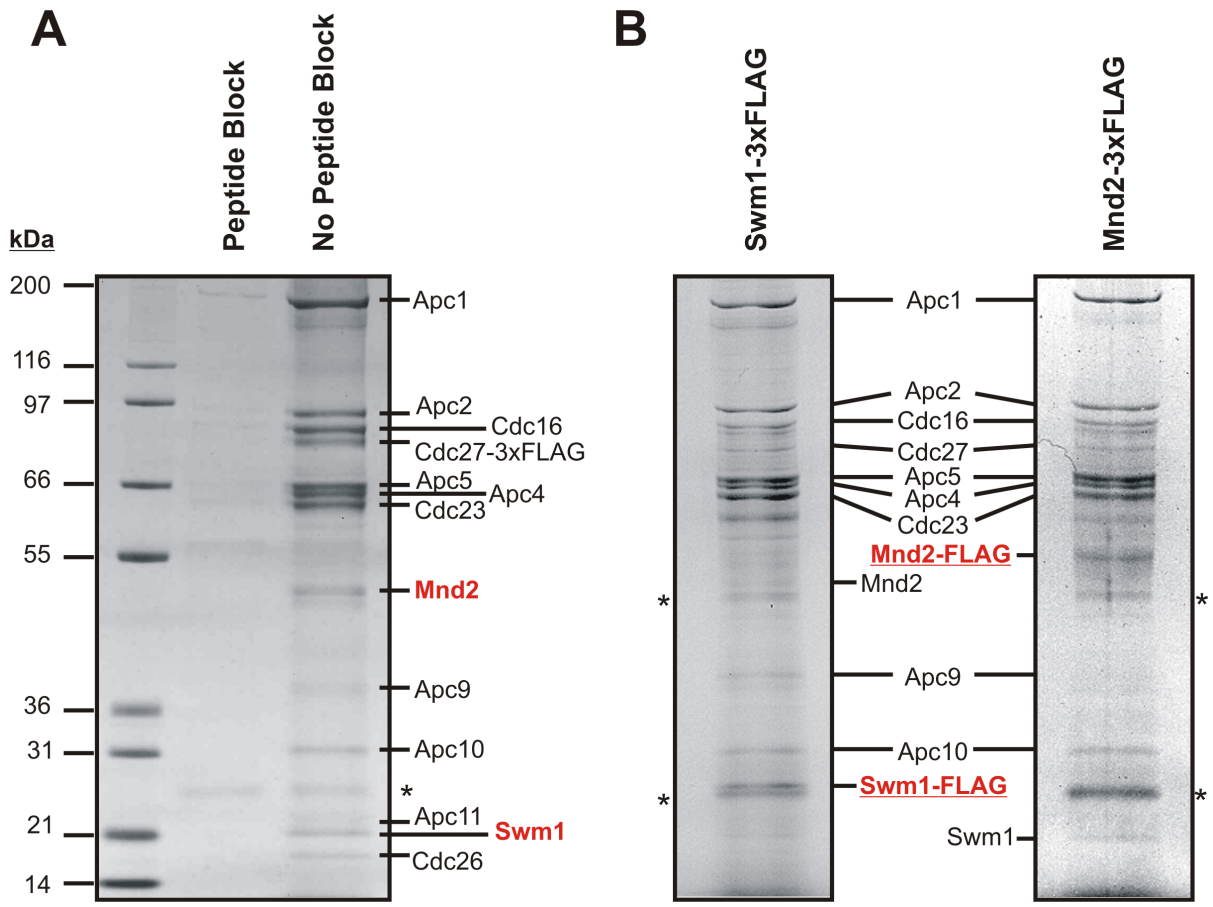

Figure 3.1. Mnd2 and Swm1 co-purify with yeast APC. Immunoaffinity purifications of the APC from yeast whole cell extracts were separated by SDS-PAGE as described under "Experimental Procedures" and stained with Coomassie Blue. Each lane represents the material obtained from ~10^{11} cells. Individual bands were excised and digested with trypsin, and the proteins were identified by mass spectrometry. All labeled proteins represent statistically significant scores obtained by the MASCOT search engine. (A) (*produced by G. Schroeder*) APC was prepared from strain YKA151, which produces 3xFLAG epitope-tagged Cdc27. The samples in both lanes were treated identically except that the anti-FLAG beads in the first sample were pre-blocked with 3xFLAG peptide before incubation with the cell extract. (B) APC was purified from strain YKA152, which produces 3xFLAG epitope-tagged Mnd2, and strain YKA153, which produces epitope-tagged Swm1. Bands labeled with an asterisk in each preparation were identified as mouse IgG. Most of the visible but faint unlabeled bands on these gels were identified as proteolytic fragments of APC subunits.

conducted to determine whether these proteins were specifically associated with APC as opposed to non-specifically associated with the affinity resin (Figure 3.1 A, second lane). Both protein were effectively competed away by the blocking peptide, suggesting that their presence was due to direct interaction with the APC. The two proteins, Mnd2 and Swm1, have both been implicated in meiosis, but at different stages (Rabitsch et al., 2001; Ufano et al., 1999). Little else was known about these two proteins at the time of publication.

Known APC subunits co-purify with FLAG epitope-tagged Mnd2 and Swm1

To provide more convincing evidence that Mnd2 and Swm1 are true subunits of the APC, I constructed yeast strains producing 3xFLAG-tagged versions of Mnd2 and Swm1 (YKA152 and YKA153, respectively). Next, I subjected whole cell extracts from these strains to the same stringent immunoaffinity purification protocol used with YKA151. Proteins in these preparations were identified from Coomassie-stained SDS-PAGE gels by peptide mass fingerprinting. In both cases, I identified 9 of the 11 known APC subunits co-purifying with the epitope-tagged protein (Figure 3.1 B). Apc11 and Cdc26 were not identified; however, these two small subunits generally required tandem MS for identifications due to the low number of tryptic peptides generated. Regardless, these results conclusively demonstrate that Mnd2 and Swm1 are stably associated with the core APC in haploid yeast cells.

Mnd2 and Swm1 are constitutive components of the APC during the cell cycle

Although its activity fluctuates, the APC is a stable complex that is present throughout the cell cycle (Peters JM 1996, Grossberer R 1999). To determine if Mnd2 and Swm1 are also

associated with the APC during different cell cycle stages, the APC was affinity-purified from cell cultures arrested in G1, S, and M phases (Figure 3.2 A-C). Mnd2 and Swm1 were identified by mass spectrometry and were present in approximately equivalent abundance at all three cell cycle stages with respect to the other APC subunits, as judged by the intensity of the Coomassie-stained SDS-PAGE gel.

Mnd2 and Swm1 are stoichiometric components of the APC

To estimate the stoichiometry of Mnd2 and Swm1 relative to other APC subunits, I used reverse-phase HPLC (RP-HPLC) coupled with UV detection. RP-HPLC resulted in near-baseline separation of most APC subunits, which were analyzed by LC-MS/MS and subsequently identified with statistical significance by searching the Mascot database of *S. cerevisiae* proteins (Figure 3.3 A). Apc1 and Apc5 were not identified by RP-HPLC analysis even though they were detected in the input material by SDS-PAGE and Coomassie staining (data not shown). Apc1 and Apc5 are the two most hydrophobic proteins in the APC, and may not efficiently elute from the reverse-phase column. The area underneath the A_{210} peaks for each subunit was normalized by the number of amino acids in the appropriate subunit. To estimate stoichiometry, the resulting values were compared to the value obtained for the peak containing the catalytic RING subunit, Apc11. This experiment was repeated five different times with five different APC preparations, and the data were averaged to provide the final stoichiometry estimate (Table 3.2). The stoichiometry of Mnd2 relative to Apc11 appears to be 1-to-1, which was similar to the stoichiometries determined for most other APC subunits. The stoichiometry of Swm1 relative to Apc11 was found to be 2-to-1. Thus, Mnd2 and Swm1 are stoichiometric components of the APC.

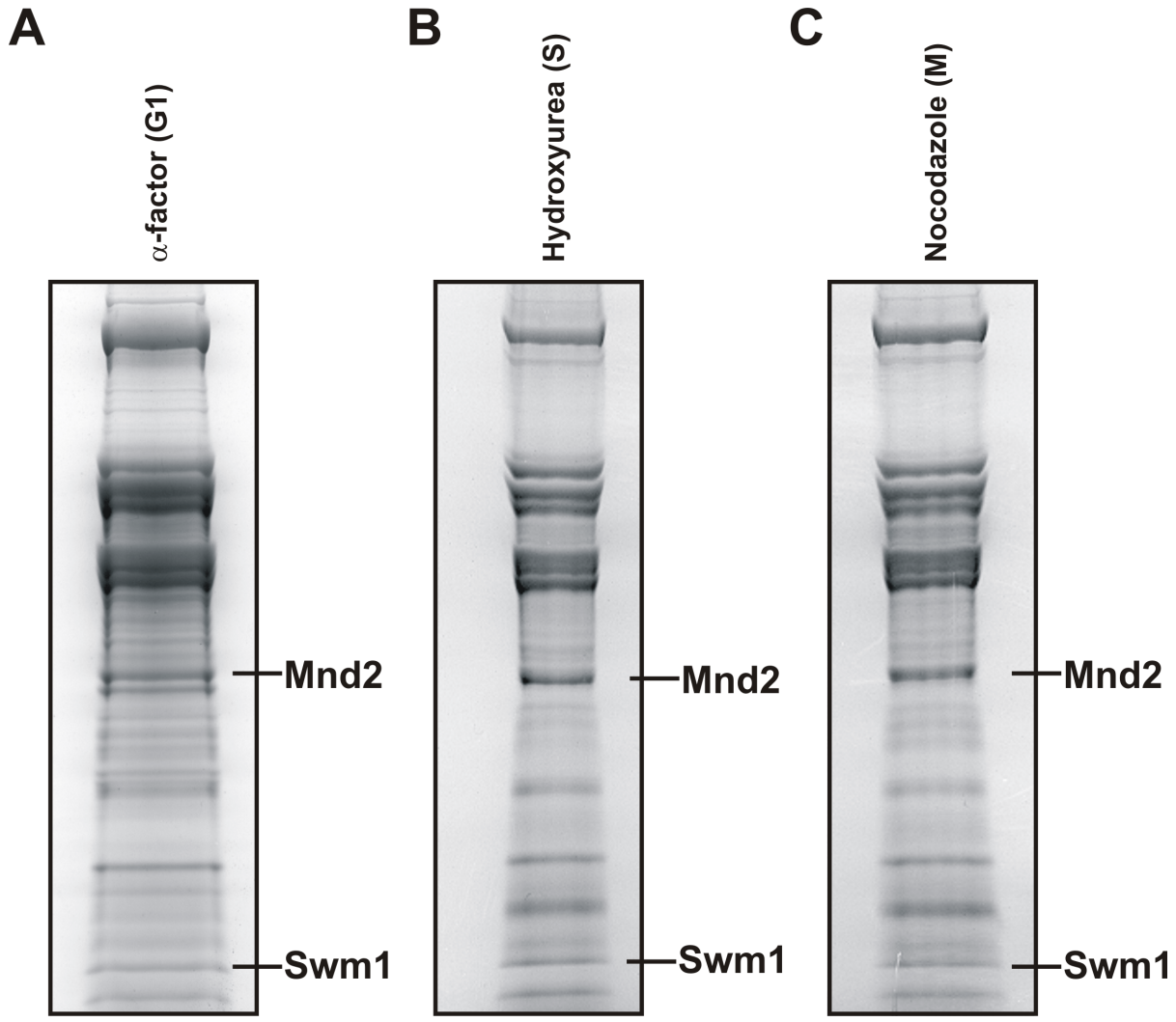

Figure 3.2. Mnd2 and Swm1 are constitutive components of yeast APC. APC was immunoaffinity purified as described under "Experimental Procedures" from haploid yeast cell cultures arrested in G1 phase with α-factor peptide (A), S phase with hydroxyurea (B), or M phase with nocodazole (C). The purified APC in each case was separated by SDS-PAGE, and proteins were visualized by staining with Coomassie Blue. The presence of Mnd2 and Swm1 in each of the three preparations was confirmed by mass spectrometry. A small sample of cells from each of the haploid cultures was analyzed by flow cytometry to confirm the cell cycle arrest (data not shown).

To evaluate the stoichiometry of Apc1 and Apc5, I purified APC from yeast grown in the presence of ^{35}S-cysteine and ^{35}S-methionine (Figure 3.2 B). In order to relate the stoichiometric ratios between the gel and RP-HPLC, I compared both subunits to the band corresponding to Cdc16, which was well resolved from all other bands. Using this method, the stoichiometry of Apc1 relative to Cdc16 was found to be 1-to-2, while the stoichiometry of Apc5 relative to Cdc16 was found to be 1-to-1 (Table 3.2). Like Cdc16 and Apc5, the stoichiometry of other APC subunits relative to Apc1 also appeared to be greater than 1-to-1. I was unable to reliably quantify the stoichiometry of any subunit below Cdc23 by ^{35}S-labeling due to excessive background. Based on the stoichiometries determined by both SDS-PAGE and HPLC methods, the total mass of the APC is estimated to be ~1.65 megadaltons (Table 3.3). This value was found to correspond well with other experimental estimates of APC mass, between 1.64 and 1.71 megadaltons (Passmore et al., 2005).

Deletion of MND2 or SWM1 results in accumulation of G2/M cells

Defects in APC function generally result in a cell cycle arrest at metaphase or a delay in progression of the cell cycle through mitosis. To determine if cells lacking *MND2* or *SWM1* exhibit a moderate cell cycle arrest associated with an APC defect, the DNA content of *mnd2Δ* and *swm1Δ* haploid cells growing at 37°C in log phase cell culture was determined by flow cytometry. For controls, the results from the same experiment with wild-type, *apc9Δ*, and *apc10Δ* were compared. The *apc9Δ* strain exhibited a slight but noticeable and statistically significant accumulation of G2/M cells compared with the wild-type strain (Table 3.4), consistent with the delayed anaphase entry reported previously for *apc9Δ* (Zachariae et al., 1998b). The *mnd2Δ* strain exhibited an accumulation of G2/M cells that

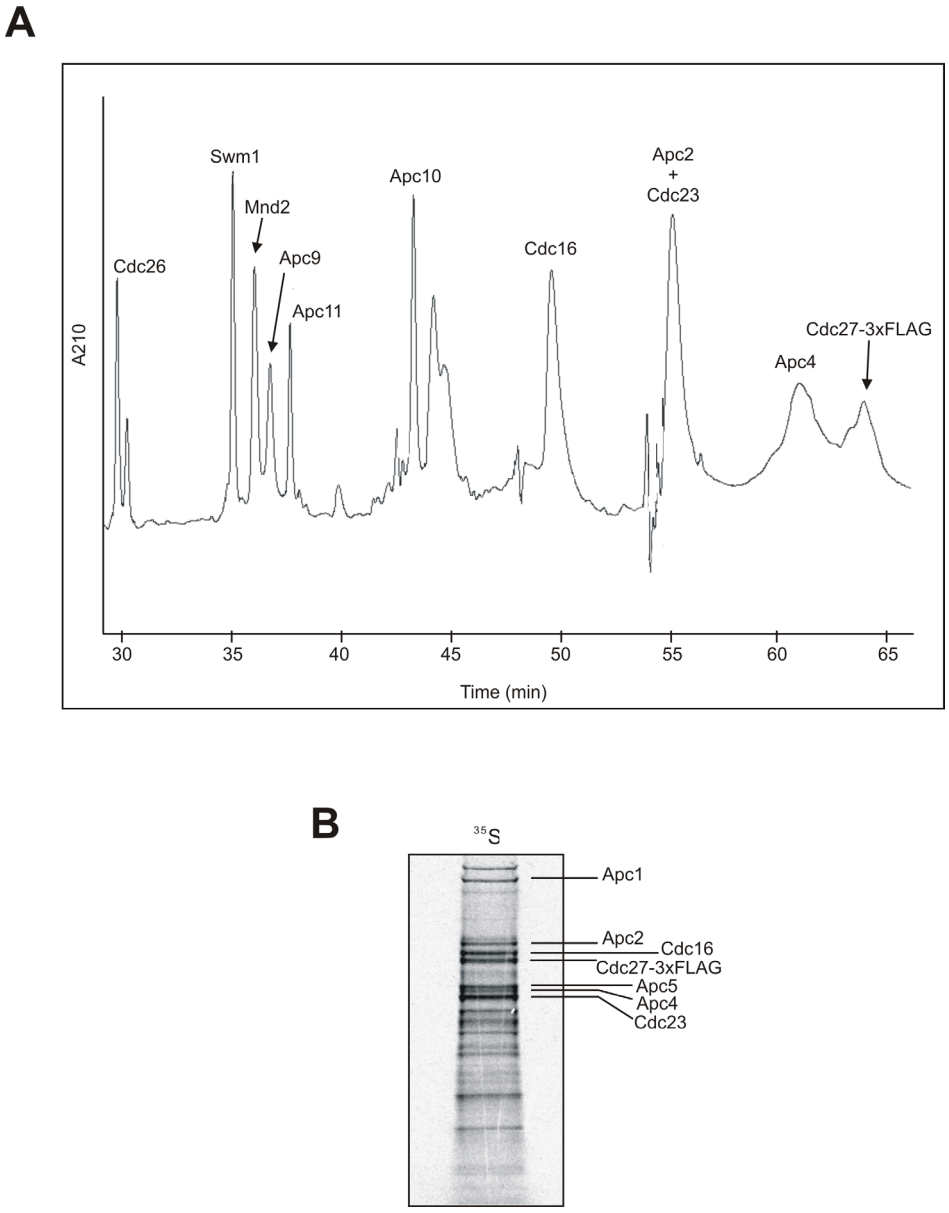

Figure 3.3. Determination of APC subunit stoichiometries. (A) APC was immunoaffinity purified and separated by reverse-phase HPLC as described under "Experimental Procedures" from haploid yeast cell cultures. The subunit identity of each chromatographic peak was determined to be statistically significant by LC-MS/MS protein identification. The peak area at A_{210} was compared to the amino acid length of the respective subunit to determine stoichiometries. The chromatograph shown is representative of the five individual experiments used to determine stoichiometry. (B) To determine the stoichiometries of Apc1 and Apc5, APC was immunoaffinity purified as described under "Experimental Procedures" from haploid yeast cell cultures grown in the presence of ^{35}S-cysteine and ^{35}S-methionine. The labeled bands shown were determined by alignment with other APC preparations that were stained with Coomassie Blue (not shown here). Stoichiometries are shown in Table 3.2.

Table 3.2
APC subunit stoichiometries

APC subunit stoichiometries were determined by 5 independent reverse-phase HPLC analyses and one ^{35}S-labeling experiment. For HPLC analysis, the peak area at A_{210} was ratioed to the number of amino acids in each subunit and then compared to the catalytic RING subunit, Apc11. HPLC data represents an average of all 5 independent experiments. The stoichiometries of Apc1 and Apc5 were determined by ^{35}S-labelling, in which case the band intensity was determined by image densitometry. The band intensity was ratioed to the total number of cysteine and methione residues in the protein, and then compared to Apc1. Cdc16 was included to allow comparison between the two methods.

	HPLC Replicate[a]							
	A	**B**	**C**	**D**	**E**	**Avg.**	**SD**	**Stoichiometry**
Apc1								
Apc2	1.58	1.10	0.79	0.91	0.57	0.99	0.38	1
Cdc16	1.71	1.54	0.34	0.82	0.61	1.01	0.6	1[b]
Cdc27	0.62	1.01	0.36	0.57		0.51	0.37	1[c]
Apc5								
Apc4	1.95	1.26	0.72	0.52	0.93	1.08	0.56	1
Cdc23	1.58	1.1	0.79	0.91	0.57	0.99	0.38	1[b]
Mnd2	0.31	1.06	0.81	0.69	0.88	0.75	0.28	1
Apc10	1.66	2.30	1.16	1.62	1.24	1.59	0.45	2
Apc9	0.77	1.22	0.8	0.85	1.10	0.95	0.2	1
Swm1	3.00	2.41	1.99	2.32	1.77	2.30	0.47	2
Apc11	1.00	1.00	1.00	1.00	1.00	1.00	0.00	1
Cdc26			1.94			1.94		2

Stoichiometry of Apc1 and Apc5 based on ^{35}S-labeling and comparison to Cdc16[d]

	No. Cys + Met	**^{35}S Signal**	**Ratio**	**Rel. To Apc1**	**Stoichiometry Relative to Apc1**
Apc1	55	781	14.2	1.00	1
Cdc16	38	1277	33.6	2.37	2
Apc5	30	739	24.6	1.73	2

[a] Stoichiometries determined by dividing the HPLC peak area at A_{210} by the number of amino acids in the protein and comparing this to Apc11.
[b] Since Apc2 and Cdc23 co-elute, the peak area was divided by the sum total amino acid content of both proteins, which necessitates the assumption of equivalent stoichiometry.
[c] I've found that Cdc27-3xFLAG is prone to rapid degradation after affinity purification, making it difficult to determine its stoichiometry very accurately.
[d] Stoichiometries determined by dividing the 35S signal by the total number of cysteine and methionine residues in the protein and comparing the value to the value obtained for Apc1.

Table 3.3
Determination of total APC mass

Stoichiometries of each yeast APC subunit based on reverse-phase HPLC and ^{35}S-labeling experiments. The mass of each APC subunit is multiplied by the stoichiometry value to give a total mass for each subunit. The total masses of all subunits are summed to give the total mass of the APC based on these stoichiometries.

	M.W. (Da)	**Stoichiometry**	**Total Mass (Da)**
Apc1	196,144	1	196,144
Apc2	99,978	2	199,956
Cdc16	94,992	2	189,984
Cdc27	85,437	2	170,873
Apc5	79,275	2	158,550
Apc4	75,256	2	150,512
Cdc23	73,114	2	146,228
Mnd2	42,826	2	85,651
Apc10	28,776	4	115,104
Apc9	30,856	2	61,713
Swm1	19,356	4	77,424
Apc11	18,865	2	37,730
Cdc26	14,081	4	56,323
TOTAL			**1,646,192**

was comparable in magnitude with the *apc9Δ* strain, suggesting that it too has a similar delay in mitotic progression. The accumulation of G2/M cell in the *apc10Δ* strain was more pronounced than that of *apc9Δ* or *mnd2Δ*, although perhaps not as much as would be expected given its severely retarded growth (data not shown). Finally, the *swm1Δ* strain exhibited a dramatic increase in the percentage of G2/M cells compared with the wild-type parent strain (63% versus 29%; Table 3.4). Considering the convincing evidence that Swm1 is a component of the APC, it is reasonable to conclude that *swm1Δ* cells have a substantial delay in progression through mitosis resulting from an APC defect that is reflected in their dramatic accumulation of G2/M cells. Although it cannot be ruled out that Mnd2 and/or Swm1 have APC-independent cellular functions that affect progression through G2 and M phase, our results are consistent with the conclusion that Mnd2 and Swm1 are constitutive components of the yeast APC that contribute to normal APC activity during mitosis.

Discussion

In this report, strong evidence is provided that Mnd2 and Swm1 are constitutive core subunits of the budding yeast APC during the mitotic cell cycle. Both subunits were also found associated with the APC purified from meiotic cells (Bonenfant et al., 2003). Swm1 is likely equivalent to a 19 kDa protein labeled Apc13 that was previously observed in an APC affinity purification (Zachariae et al., 1998b), but not identified at the time. These findings bring the total number of confirmed subunits in budding yeast to 13. The ability to identify two previously unidentified subunits of the APC emphasizes the power of mass spectrometry as a sensitive and accurate analytical tool for biological research and the utility of the 3xFLAG epitope for immunoaffinity purification of protein complexes. Another group

Table 3.4

Quantitative analysis of G2/M content from wild-type and deletion strains

All strains are isogenic with the exception of the noted gene deletions. Percentages represent averages and S.D. values from three cultures grown at 37°C that are depicted in Fig. 4,B and C. Data values were generated by ModFit LT flow cytometry analysis software. (This data was generated by Mark C. Hall for inclusion in the paper Hall MC, Torres MP, et al., 2003).

Strain	**G_2/M %**
Wild-type	29.2 $\pm$ 0.7
apc9Δ	40.0 $\pm$ 0.6
apc10Δ	46.2 $\pm$ 3.4
mnd2Δ	36.2 $\pm$ 0.9
swm1Δ	63.0 $\pm$ 0.8

recently achieved the same identification of Mnd2 and Swm1 by coupling mass spectrometry and the tandem affinity purification (TAP) method (Yoon et al., 2002).

As would be expected for a core component of the APC, the association of Mnd2 and Swm1 appears to be stoichiometric with other APC subunits as determined by RP-HPLC. Interestingly, Swm1 appears to exist at 2-to-1 relative to other APC subunits, similar to what was found for Apc10. Apc10 has been shown to be necessary for APC processivity, which may explain the need for multiple copies in the complex that could facilitate rapid exchange of substrates subsequent to each polyubiquitination reaction. The need for multiple copies of Swm1, which is not required for vegetative growth, was not originally clear at the time these data were collected. However, Swm1 has since been found to be critical for structural integrity of the APC by stabilizing association of Cdc16 and Cdc27 (Schwickart et al., 2004); and, when missing, negatively affects APC substrate turnover during mitosis (when Cdc20 is the co-activator) and G1 phase (when Cdh1 is the co-activator) (Page et al., 2005).

I also determined the stoichiometry of Apc1 and Apc5, which could not be determined by RP-HPLC. While Apc5 exists at a similar stoichiometry to the other APC subunits, Apc1 is 1-to-2 relative to most other subunits. Since it is unlikely that Apc1 is sub-stoichiometric in the APC, there must be multiple copies of each other subunit in the complex. Indeed, recent evidence has shown that Apc1 could exist as a scaffold upon which multiple subcomplexes assemble (Thornton et al., 2006). Moreover, later studies on the stoichiometry of budding yeast APC subunits have shown similar results, and go further to suggest the existence of multiple active sites in the complex (Passmore et al., 2005).

The report by Passmore et. al (2005), which used radioactive labeling to quantify subunit stoichiometry did not provide data for Swm1, Cdc26, or Apc11. Thus, my observation that

Swm1 exists in multiple copies may hint at a unique biophysical role for Swm1 that is specific to the meiotic APC. Indeed, Swm1 has been shown to be necessary for spore wall assembly near the end of the meiotic cell cycle (Ufano et al., 1999). The role of Swm1 in these meiotic events may be mediated through its function as an APC subunit.

The role of Mnd2 in APC function during mitosis appears to be minimal, since cells lacking *MND2* can grow normally (Bonenfant et al., 2003), and display very little accumulation of G2/M cells even at elevated temperature. Similar results were reported by an independent laboratory, and also showed that co-deletion of *MND2* with other subunits did not have a significant effect on vegetative growth (Page et al., 2005). However, *mnd2Δ* cells are completely incapable of progressing beyond the first nuclear division of meiosis, arresting in prophase I with uncondensed chromatin (Rabitsch et al., 2001). Since we reported it as a core component of the APC (Bonenfant et al., 2003), a meiosis-specific function for Mnd2 has been described (Oelschlaegel et al., 2005; Penkner et al., 2005). Specifically, both groups showed that Mnd2 acts as an inhibitor of the meiotic APC co-activator, Ama1, in prophase I of meiosis. In cells lacking *MND2*, Ama1 activates the APC early in prophase I, and promotes polyubiquitination and subsequent degradation of the anaphase-inhibitor, Pds1, which results in premature separation of sister chromatids and meiotic arrest.

A specific function for Mnd2 and Swm1 during meiosis raises a question about the nature of their nonessential role in mitosis. The E3 ligase activity of budding yeast APC has clearly evolved with Swm1 functioning to stabilize the structure of the complex (Schwickart et al., 2004; Thornton et al., 2006). However, Mnd2 is not required in the same way as Swm1, and therefore, must be needed during the vegetative cell cycle for another purpose. One

possibility is that *MND2* must be expressed in vegetative cells before the initiation of meiosis to ensure that it is present and able to inhibit premature sister chromatid separation well before Ama1 is expressed, which appears to begin as soon as cells "decide" to enter meiosis before pre-meiotic S phase (Oelschlaegel et al., 2005). This possibility seems likely in yeast, since the environmental signal to enter meiosis (low carbon and nitrogen availability) is mediated through protein signaling cascades that alter gene transcription (Schneper et al., 2004). Perhaps waiting to express *MND2* such that it appears at the same time as Ama1 would not be sufficient to inhibit the APC in time. To date, no experiments have been conducted to explain why Mnd2 exists during vegetative growth in yeast.

At the time this work was originally reported, no obvious mammalian homologs of Mnd2 or Swm1 had been described (Ufano et al., 1999). This is still true for Mnd2, however, recent evidence suggests that Swm1 has distant homologs in many other organisms including humans (Schwickart et al., 2004). Indeed, the authors show that the human homolog of Swm1 is capable of complementing a *SWM1* deletion in budding yeast. The involvement of APC subunits in meiosis-specific functions that may be shared in humans is no doubt an exciting new avenue of APC research that could have important implications in the biochemical understanding of mammalian gametogenesis.

CHAPTER IV

PHOSPHORYLATION OF THE APC INHIBITORY SUBUNIT, MND2, IS NECESSARY FOR EFFICIENT PROGRESSION THROUGH MEIOSIS I

(Including modified portions from: Torres, M.P. and Borchers, C.H., (submitted to *J. Biol. Chem.*)

Summary

The yeast APC subunit, Mnd2, is necessary for maintaining sister chromatid cohesion in prophase I by inhibiting premature ubiquitination and subsequent degradation of substrates by the APC^{Ama1} ubiquitin ligase. In late meiosis Mnd2 is de-activated to allow APC^{Ama1} activity that is necessary later in the meiotic program. The mechanism of regulating Mnd2 function during meiosis is unknown, but has been suggested to be phosphorylation dependent. In a proteomics screen for post-translational modifications on the APC, we discovered that Mnd2 is phosphorylated during mitosis in a cell cycle dependent manner. We have identified the sites of mitotic phosphorylation and characterized their abundance during the cell cycle. Collective mutation of the phosphorylation sites to either alanine or aspartic acid has no effect on vegetative growth rates. However, the ability of the alanine mutant to progress through meiosis is severely compromised, resulting in sporulation levels that are approximately 10% - 15% of the wild type strain. In contrast, sporulation of the aspartic acid mutant is partially recovered to approximately 50% of the wild type strain. Similar to the *MND2* deletion strain, alanine or aspartic acid mutants that did not form spores arrested after pre-meiotic S-phase with a single undivided nucleus. In comparison to the wild type and aspartic acid mutant strains, the alanine mutant displayed low levels of the APC^{Ama1} meiotic substrate, Clb5. Taken together, these data suggest that Mnd2 phosphorylation is necessary for APC-mediated progression beyond the first meiotic nuclear division.

Introduction

Proper progression through the eukaryotic cell cycle is achieved in large part through coordinated regulation of protein degradation mediated by E3 ubiquitin ligases (reviewed in (Hershko, 2005; King et al., 1996; Peters, 1998; Tyers and Jorgensen, 2000)). During mitosis and meiosis, targeted protein degradation is tightly associated with the organization of chromosomes and their equivalent distribution into two separate progeny cells during anaphase, and is controlled by a multi-subunit ubiquitin ligase called the anaphase-promoting complex (APC) (Harper et al., 2002; Murray, 2004; Peters, 2006). As an E3 ligase, the APC transfers ubiquitin onto lysine residues of substrate proteins in an iterative manner that forms poly-ubiquitin chains on the surface of a substrate protein (King et al., 1995; Sudakin et al., 1995). The poly-ubiquitinated substrate is then recognized by the 26S-proteosome and degraded, while the ubiquitin is recycled. The APC is itself regulated, which ensures that the timing of substrate degradation is tied to the completion of other cellular processes. Indeed, mis-regulation of the APC can lead to disastrous results including cell cycle arrest or improper chromosome segregation and cell death (Bashir and Pagano, 2003; Schiller et al., 2006; Yamasaki and Pagano, 2004).

Regulation of the APC during mitosis is accomplished by several mechanisms, including the association of co-activator proteins and through phosphorylation of individual subunits within the complex. Two co-activator proteins, Cdc20 and Cdh1, facilitate the association of substrate proteins with the APC at different stages of the mitotic cell cycle (Pfleger et al., 2001; Reimann et al., 2001a; Song and Lim, 2004; Song et al., 2004; Visintin et al., 1997). Each co-activator is regulated through mechanisms involving both phosphorylation and protein-protein interactions (Reimann et al., 2001a; Song and Lim, 2004; Song et al., 2004)

(Loo et al., 1992; Sudakin et al., 2001) (Han et al., 2001; Zachariae et al., 1998a). Additionally, specific subunits of the APC are phosphorylated in a cell cycle dependent manner, which has been shown to enhance binding and activation by Cdc20 (Kramer et al., 2000; Lahav-Baratz et al., 1995; Shteinberg et al., 1999). APC subunit phosphorylation is controlled in large part by mitotic cyclin-dependent kinase (CDK) activated by the Clb2 cyclin which is later targeted for destruction by the APC upon exit from mitosis (Rudner et al., 2000; Rudner and Murray, 2000). As a result, the APC exists in a hyper-phosphorylated state during mitosis and a hypo-phosphorylated state during G1 phase. Mutation of the CDK consensus sites in the APC subunits Cdc16, Cdc27, and Cdc23, results in reduced APC^{Cdc20} activity towards Clb2 *in-vivo*, as well as a delay in the onset of anaphase (Rudner et al., 2000; Rudner and Murray, 2000). Currently, there is no evidence to suggest whether or not mutation of known mitotic APC phosphorylation sites will have detrimental effects on meiotic cell cycle transitions.

In budding yeast the APC is regulated during meiosis not only by Cdc20 and Cdh1 co-activators, but also by a meiosis-specific co-activator called Ama1 (Blanco et al., 2001; Janek et al., 2001), which is necessary for spore wall assembly and expression of late meiotic genes (Cooper et al., 2000). *AMA1* gene transcription and splicing occurs only in meiotic cells (Cooper et al., 2000), and begins during pre-meiotic S phase (Oelschlaegel et al., 2005). However, the co-activator is selectively inhibited early in meiosis by the APC subunit Mnd2 (Oelschlaegel et al., 2005; Penkner et al., 2005).

Mnd2 is found in complex with the APC during both the mitotic and meiotic cell cycles (Bonenfant et al., 2003; Passmore et al., 2003; Yoon et al., 2002). Yeast lacking Mnd2 proceed normally through the mitotic cell cycle but are unable to complete sporulation,

arresting before the first meiotic nuclear division with uncondensed chromatin (Rabitsch et al., 2001). Recent evidence has shown that Mnd2 specifically inhibits APC activation by Ama1 during prophase I. In cells lacking Mnd2, uninhibited APC^{Ama1} prematurely targets securin (Pds1) for degradation, which results in the premature separation of sister chromatids due to unrestrained separase (Esp1) activity (Oelschlaegel et al., 2005), followed by cell cycle arrest. Uninhibited APC^{Ama1} was also found to control the degradation of Clb5 during meiosis. Although inhibited early in meiosis, APC^{Ama1} becomes active during anaphase I despite the presence of Mnd2, suggesting that the inhibitory function of Mnd2 is regulated post-translationally during meiosis. It has been further suggested that regulation of Mnd2 might be linked to its phosphorylation status (Oelschlaegel et al., 2005).

In a screen for cell cycle-dependent post-translational modifications that occur on the APC during mitosis, we discovered that Mnd2 is one of 5 major phosphorylated subunits in the complex. Here we show the identity of Mnd2 phosphorylation sites and their relative changes during the cell cycle using mass spectrometry. To determine the functional significance of Mnd2 phosphorylation, we used site-directed mutagenesis to generate yeast strains harboring Mnd2 phosphorylation site mutants and then tested these mutants for their ability to progress through mitosis or meiosis. Vegetative growth of *mnd2* phosphorylation site mutants is unperturbed. However, sporulation of a *mnd2-(S/T-A)* strain is severely compromised, while reciprocal mutation to aspartic acid partially recovers sporulation efficiency. The defects in sporulation of the alanine mutant are consistent with those of the deletion strain, including arrest before the first meiotic nuclear division and reduced ability to accumulate Clb5. Taken together, these data support a role for phosphorylation in the regulation of Mnd2 as an APC^{Ama1} inhibitor in early meiosis.

Experimental procedures

Plasmid and strain construction

Standard methods for the growth, maintenance, and transformation of yeast and bacteria and for the manipulation of DNA were used. All constructed plasmids were verified by DNA sequencing. Yeast strains used in this study are listed in Table 4.1. Strain, W1588-4c is a derivative of W303 in which the weak rad5 mutation has been repaired (Zhao et al., 1998). Strains expressing Cdc27 and Mnd2 with C-terminal 3xFLAG epitopes were constructed by integrating PCR amplicons amplified from p3FLAG-KanMX plasmid (a gift from Dr. Toshio Ysukiyama; Fred Hutchinson Cancer Center) into the yeast genome as previously described (Gelbart et al., 2001). The Apc1-TAP strain was generated by integration of PCR amplicons from pBS1539 as previously described (Puig et al., 2001). Construction of phosphorylation site mutations in MND2 was accomplished using the QuikChange multi-site-directed mutagenesis kit (Stratagene) according to the manufacturer's specifications (oligonucleotide sequences available upon request). Mutations were made and sequenced in pIVEX-FLAG-MND2, in which the MND2 ORF was originally cloned into the NotI/SalI sites (Bonenfant et al., 2003). After mutagenesis, the XhoI fragment from pIVEX-FLAG-MND2 or pIVEX-FLAG-mnd2 phosphorylation site mutant (containing all 14 mutations within the last 702 base pairs of the ORF) was subcloned into the XhoI site of pMT004, a pRS404 vector containing the first 405 base pairs of the MND2 ORF (up to the naturally existing XhoI site) and 500 base pairs of the upstream promoter region. The resulting wild type, S/T-A mutant, and S/T-D mutant plasmids were linearized with HindIII and integrated into the trp locus of YKA311, in which the open reading frame for MND2 in the high efficiency sporulating yeast strain, RSY333, was replaced with KanMX4 by PCR-

Table 4.1
S. cerevisiae strains used in this study

Strain	Relevant Genotype	Source
W1588-4c[a]	*MAT*a *ade2-1 can1-100 his3-11,15 leu2-3,112 trp1-1 ura3-1*	R. Rothstein
DLY3033	*MAT*a *cdc15-2 bar1Δ::URA3*	J. Pringle
RSY333	*MAT*a *cyh2 ho::LYS2 leu2::hisG lys2 trp1::hisG ura3-1*	R. Strich
RSY335	MAT*a*/a cyh2 ho::LYS2 leu2::hisG lys2 trp1::hisG ura3-1	R. Strich
YKA152[a]	*MND2-3FLAG:KanMX4*	M.T.
YKA155[a]	*CDC27-3FLAG:KanMX4 bar1Δ::URA3*	Hall MC
YKA156[b]	*CDC27-3FLAG:KanMX4*	M.T.
YKA181[a]	*APC1-TAP:URA3 CDC27-3FLAG:KanMX4*	M.T.
YKA191[a]	*APC2-TAP:URA3 CDC27-3FLAG:KanMX4*	M.T.
YKA311[c]	*mnd2Δ::KanMX4*	M.T.
YKA312[c]	*mnd2Δ::KanMX4 trp1::pRS404-mnd2(S/T-A)-TRP1*	M.T.
YKA313[c]	*mnd2Δ::KanMX4 trp1::pRS404-MND2-TRP1*	M.T.
YKA314[c]	*mnd2Δ::KanMX4 trp1::pRS404-mnd2(S/T-D)-TRP1*	M.T.
YKA315[c]	*mnd2Δ::KanMX4 Ycp50::HO*	M.T.
YKA316[c]	*mnd2Δ::KanMX4 trp1::pRS404-mnd2(S/T-A)-TRP1 Ycp50::HO*	M.T.
YKA317[c]	*mnd2Δ::KanMX4 trp1::pRS404-MND2-TRP1 Ycp50::HO*	M.T.
YKA318[c]	*mnd2Δ::KanMX4 trp1::pRS404-mnd2(S/T-D)-TRP1 Ycp50::HO*	M.T.

[a]Derived from W1588-4c, which is a derivative of W303 in which the weak *rad5* mutation has been repaired (Hall et al., 2003).
[b]Derived from DLY3033.
[c]Derived from RSY333.

mediated transformation (Cooper et al., 2000). Diploid strains were created by transformation with YCp50::HO expressing wild type HO endonuclease, and selecting for transformants on SD-URA. Successful conversion to diploid was confirmed by flow cytometry.

Cell cycle arrests

To arrest cells in G1 phase, cultures were first grown for two generations in YPD media as measured by optical density 600 nm (corresponding to growth from OD_{600} = 0.2 to 0.8), followed by addition of synthetic alpha-factor peptide (University of North Carolina peptide synthesis facility) to a final concentration of 50 μg/L. For M phase arrests in the temperature sensitive strain YKA156, cells were grown for two generations at the permissive temperature (27°C) and arrested by shifting the temperature to 37°C, which results in late M phase arrest (Bardin et al., 2003; Jaspersen et al., 1998; Jaspersen and Morgan, 2000). The degree of cell cycle arrest was monitored by phase contrast microscopy and cells were harvested by centrifugation after >90% of the culture reached the desired morphology (un-budded for G1 arrest and equivalently budded for M arrest). Harvested cells were washed once with deionized water, centrifuged once more, and frozen at –80°C overnight prior to protein purification.

Affinity purifications and phosphatase assays

Yeast cells were lysed at 4°C in pre-chilled lysis buffer containing 25 mM HEPES-NaOH pH 7.5 (Fisher), 400 mM NaCl (Sigma), 10% glycerol (Fisher), 0.5 mM DTT (Sigma), 0.1% Triton X-100 (Sigma), 50 mM NaF (Sigma), 1.3 mM activated sodium ortho-vanadate

(Sigma), 50mM β-glycerophosphate (Spectrum), 0.5 mM phenylmethylsulfonyl fluoride (Roche), and complete protease inhibitor tablets (Roche) as described in Chapter III (Hall 2003).

Phosphatase assays on full-length protein were conducted on the APC directly bound to the affinity matrix after washing with detergent free sodium phosphate buffer. The affinity matrix was first conditioned 4 x 7 minutes with 1 mL phosphatase buffer containing 50 mM Tris-HCl pH 7.5, 0.1 mM EDTA, 2 mM MnCl. Next, the matrix was split, and one half treated with 1000 units λ-phosphatase dissolved in 1 bead equivalent volume phosphatase buffer at 30°C for 30 minutes. Both halves were then washed 2 x 7 minutes with 1 mL detergent free sodium phosphate buffer and the APC was eluted as previously described. MALDI target phosphatase assays were conducted as previously described in Chapter II (Borchers et al., 2006).

GST fusion protein

MND2 wild type, S/T-A, or S/T-D genes were subcloned into pGEX-4T1 by PCR from the pRS404 vectors harboring each gene isoform. The resulting N-terminal GST-fusion constructs were over-expressed in BL21 pLysS cells according to the manufacturer's protocol (Stratagene). Cells were lysed by sonication in 1x PBS and cleared by centrifugation. GST fusion proteins were purified from the cell lysate by batch incubation with glutathione sepharose™ 4B (Amersham Biosciences). Each GST fusion protein was digested with trypsin to verify the amino acid sequence by MALDI-TOF MS.

Chromatography

Full-length APC subunits eluted from the affinity matrix were fractionated by reverse-phase HPLC as described in Chapter III. In-gel digestion with porcine trypsin was conducted as previously described (Borchers et al., 2004). Separation of tryptic peptides was accomplished by capillary HPLC using an Agilent 1100 series capillary-LC system with Pepmap C18 column (LC Packings) connected in-line with a Probot MALDI target micro-fraction collector (LC Packings).

Mass spectrometry

Lyophilized C4 HPLC fractions containing full-length Mnd2 were reconstituted in 5uL 85% ACN, 0.1% TFA and one-tenth of the sample was prepared for MALDI-TOF MS by the dried droplet method with a saturated solution of sinapic acid (Fluka) in 50% ACN/0.1% TFA. The reconstituted sample was then analyzed directly on a Reflex III matrix-assisted laser desorption ionization – time of flight (MALDI-TOF) mass spectrometer (Bruker Daltonics Inc.) operating in linear mode. Linear-mode MALDI-TOF mass spectra were obtained immediately after calibrating the mass spectrometer using a mixture of bovine serum albumin (Sigma) and cytochrome C (Sigma) that were spotted in close proximity to the sample.

LC micro-fractions were analyzed on an ABI 4700 MALDI-TOF/TOF mass spectrometer (Applied Biosystems Inc.), using a saturated solution of recrystallized α-cyano-4-hydroxycinnamic acid in 50% ACN/0.1% TFA as the matrix.

In vivo ^{32}P-labeling

Yeast strains were labeled with monosodium phosphate [^{32}P] in vivo as previously described (Rudner and Murray, 2000). Briefly, saturated overnight 5 mL cultures were diluted to OD_{600} = 0.2 in 50 mL YPD and allowed to grow to OD_{600} = 0.6 at which time DMSO was added to 1%. At OD_{600} = 0.8, each culture was arrested in M phase by addition of nocodazole to 15 μg/mL. After arresting for 3 hours, cells were harvested by centrifugation, washed once with sterile water, and resuspended in 35 mL synthetic complete media lacking phosphate and containing DMSO, nocodazole, and 1 mCi $NaH_2[^{32}P]O_4$ (ICN Inc.). After labeling for 1 hour at 30°C, cells were collected by centrifugation, washed once with water, transferred to a 2 mL screwcap tube, and frozen at –80°C.

Cells were lysed by adding cell-pellet equivalent volumes of lysis buffer and 0.5 mm glass beads to the pellet and vortexing 6 x 2 minutes at maximum power with 5 minute rest intervals on ice. All following steps were conducted at 4°C. The extract was cleared by centrifugation in a microcentrifuge at 16,100 x g for 20 minutes and the supernatant was transferred to a fresh 2 mL screwcap tube followed by affinity purification as previously described. The APC was eluted as described above and then precipitated to remove excess volume and salt by adding 10 volumes cold acetone and incubating at –20°C overnight. The precipitate was collected by centrifugation at 16,100 x g for 20 minutes, air dried at room temperature, and then resuspended in 1x LDS loading buffer (Invitrogen Inc.) containing 100 mM DTT. The sample was separated on a pre-cast 4-12% Bis-Tris acrylamide gel (Invitrogen Inc.), dried, and exposed to a storage phosphor screen for analysis by phosphorimager (STORM, Amersham Biosciences Inc.).

Growth curves, sporulation assays, and western blotting

To measure relative growth rates of strains harboring mnd2 phosphorylation site mutants or complete ORF deletions, saturated overnight cultures grown in YPD media were diluted 20-fold into 5 mL of fresh YPD media and grown for approximately 1 or 3 hours at 30°C or 37°C, respectively. Each culture was then diluted to OD_{660} = 0.025 (~3E5 cells/mL) in 3 separate tubes with 5 mL of fresh YPD media and grown at 30°C or 37°C for 8 to 9 hours. Growth was monitored every 2 hours by measuring the absorbance at 660nm with a SmartSpec 3000 spectrophotometer (Bio-Rad Inc.).

To induce sporulation, single colonies picked from YP-glycerol agar plates were spread over the entire surface of a fresh YPD agar plate and grown for 24 hours at 30°C, ensuring that overnight growth saturated the YPD plate. All following steps were conducted at 30°C. The YPD plates were replica plated to pre-sporulation (PSP) agar plates (1% potassium acetate, 1% yeast extract, 2% peptone) until >95% of the cell population were unbudded (23 – 24 hours) as counted using a hemacytometer, followed by replica plating to sporulation media (SPM) agar plates (1% potassium acetate, 0.1% yeast extract, 0.05% dextrose). The percentage of tetrads was monitored by light microscopy using a hemacytometer. Cells were collected by gently scraping a fraction of the cells followed by resuspension in water, centrifugation, snap-freezing the pellet in a dry-ice/ethanol bath, and storage at -80°C (for western blots). Additionally, an aliquot of the scraped cells was resuspended in 70% ethanol (for FACS or fluorescence microscopy).

Protein levels were analyzed by western blotting after breaking cells with glass beads in TCA lysis buffer, (10mM Tris-HCl pH 8.0, 25mM ammonium acetate, 1mM Na_2EDTA, 10% trichloroacetic acid). The TCA precipitated protein pellet was dissolved in resuspension

solution (3% SDS, 100mM Tris-HCl pH 11.0), and the total protein concentration of each sample was quantified by absorbance at 750 nm using a DC protein assay kit (BioRad). For normalized comparison, 40ug of total protein was loaded in each lane. Primary antibody to Clb5 (Santa Cruz sc-20170; 1:1000) was used in PBS-T (1x phosphate buffered saline, 0.1% Tween) with 5% non-fat dried milk. Detection of bound primary antibody was accomplished with an ECL-Plus chemiluminescent detection kit (Amersham) and horseradish peroxidase-conjugated goat-anti-rabbit secondary antibody (Chemicon International). Mnd2 was detected in western blots using a custom made and purified rabbit polyclonal antibody to the N-terminus of the protein (Sigma Genosys Inc.).

Fluorescence Microscopy and Flow Cytometry

Cells fixed in 70% ethanol were harvested by centrifugation, washed twice, and resuspended in 1x PBS at 25°C. Approximately 10 µL of the cell suspension was adsorbed onto a poly-L-lysine glass microscope slide for 5 minutes after which the excess suspension was removed and replaced with 10 µL of DAPI solution (2 µg/mL) for 5 minutes. After removal of the excess DAPI solution, each sample was washed twice for 2 minutes with 30 µL 1x PBS and allowed to dry at room temperature. Finally, 10 µL of mounting solution (90% glycerol, 1 mg/mL p-phenylenediamine, 20 ng/mL DAPI) was added to the top of each sample, covered with a coverslip, and compressed with weight for at least 1 hour. Cells were imaged by differential interference contrast (DIC) or by fluorescence detection of DAPI-stained nuclei. Measurements of cellular DNA content were collected on a FACScan flow cytometer as previously described (Bonenfant et al., 2003).

Results

Molecular weight determination of APC subunits by mass spectrometry

Recent mass spectrometric (MS) analyses have shown that at least 5 of 11 different human APC subunits are phosphorylated on a total of 43 different Ser or Thr residues, many of which are differentially phosphorylated in a cell cycle dependent manner (Kraft et al., 2003). In comparison, only 3 of 13 APC subunits in yeast have been shown to be phosphorylated *in vivo* (Rudner et al., 2000; Rudner and Murray, 2000), and although specific sites have been inferred from canonical CDK consensus sequences, there has not been a focused proteomics-scale analysis of APC subunits thus far. Therefore, to reveal the presence of previously unknown post-translational modifications on the APC (including phosphorylation), we measured the full-length molecular weights of individual APC subunits by MALDI-TOF MS and compared these measurements to the calculated masses of each subunit based on sequence information found in the Saccharomyces Genome Database (http://www.yeastgenome.org/). The analytical approach is described in (Figure 4.1). Since APC activation has been shown to be dependent on subunit phosphorylation that is maximal in M phase and minimal in G1 phase, we specifically compared the subunit molecular weights between these two phases. To prioritize downstream biochemical analyses, we categorized subunits into one of three groups in reference to their modification state between M and G1 phases: unmodified, constantly modified, and differentially modified. We were particularly interested in subunits that were differentially modified, because they fit the current model of APC activation and could potentially be involved in APC regulation.

RP-HPLC separation of the APC resulted in near-baseline resolution of each subunit except for Apc1 and Apc5 as previously described in Chapter III. MALDI-TOF MS

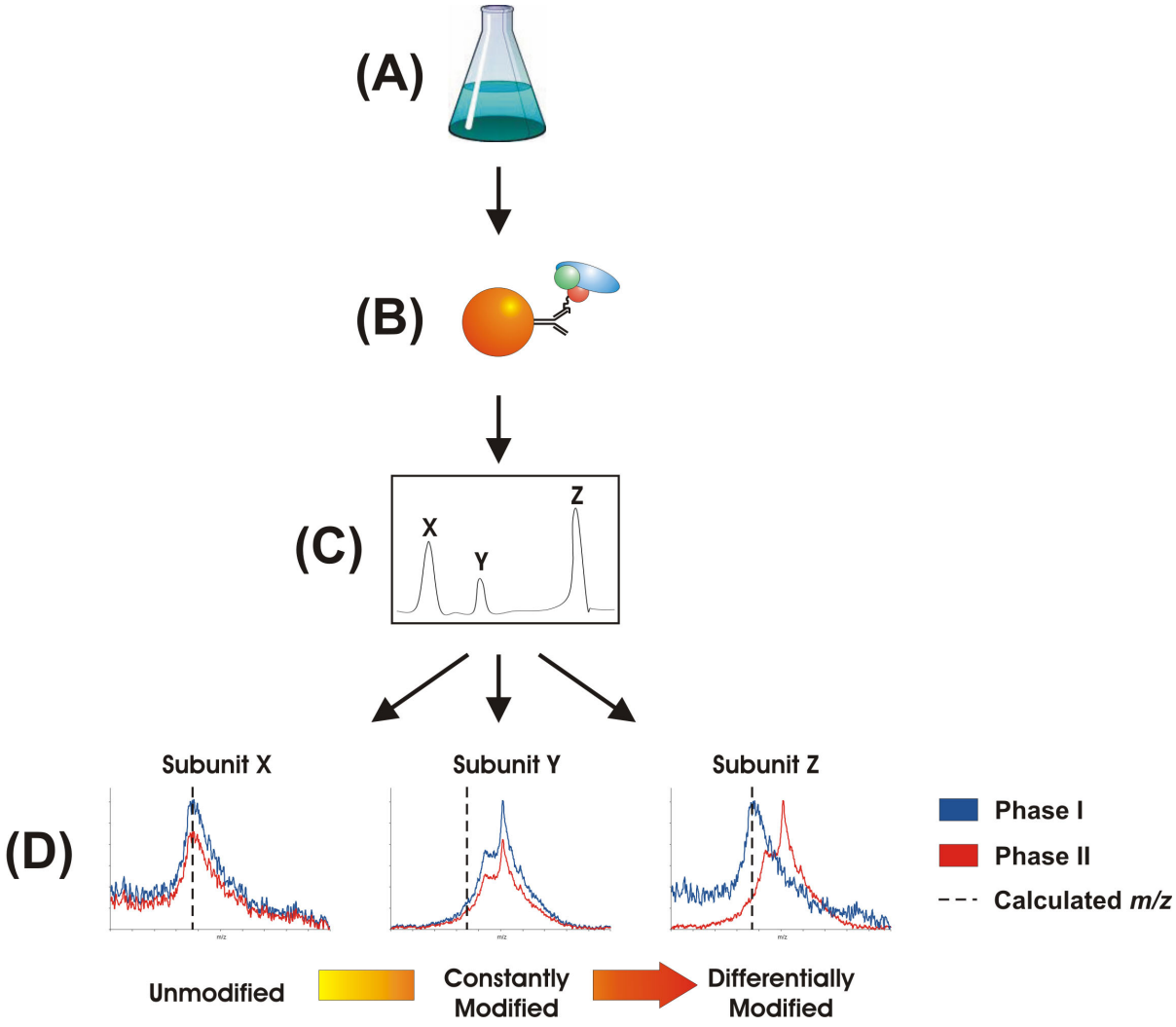

Figure 4.1. Analytical scheme for analyzing cell cycle regulated APC post-translational modifications. (A) Growth and arrest of yeast cell cultures. (B) APC immunoaffinity purification. (C) Reverse-phase HPLC separation of individual subunits. (D) MALDI-TOF MS analysis of individual subunits compared between phase 1 (G1), phase 2 (M), and the calculated molecular weight as determined by the primary structure of each subunit. Based on this analysis, each subunit was categorized into one of three groups depending on the results of the comparison: unmodified, constantly modified, or differentially modified.

molecular weight determinations for the remaining APC subunits are shown (Table 4.2). Eight out of the eleven RP-HPLC-separated subunits could be determined by this method. Two subunits, Apc9 and Apc10/Doc1, were unmodified in both M and G1 phase. Three subunits, Apc11, Cdc26 and Swm1, were constantly modified. Two subunits, Mnd2 and Cdc23, were the only subunits to display differential modification. Apc2 was the largest subunit for which we were able to determine a molecular weight, and appeared to be slightly degraded in M phase since we observed a molecular weight that was lower than that which was calculated based on genome sequencing. The difference in the measured and calculated masses of Cdc26 could be due to phosphorylation, since a recent report has identified a single mitotic phosphorylation site in the fission yeast homolog, Hcn1 (Yoon et al., 2006). The difference in the measured and calculated masses of Swm1 corresponds with the removal of the N-terminal methionine and acetylation of serine, which was confirmed by high-accuracy ESI-MS (data not shown). The differential modification of Cdc23 was also assumed to be due to phosphorylation, since it too has been shown to be differentially phosphorylated in metabolic labeling experiments with budding yeast (Rudner and Murray, 2000). We could not determine reasonable molecular weights for Apc4, Cdc16, and Cdc27-3xFLAG due to difficulties with MALDI of Apc4 and Cdc16, and due to significant protein degradation of Cdc27-3xFLAG.

The most interesting mass difference that we observed in our MS screen of molecular weights occurred in the subunit Mnd2, which we previously identified as a stoichiometric component of the APC whose deletion exhibits a strong meiotic phenotype (Rabitsch et al., 2001), but no mitotic phenotype (Chapter III). MALDI-TOF MS analysis of Mnd2 in M phase revealed a 392 Da positive shift (m/z 43,217) in its apex mass with respect to the

Table 4.2

Molecular weight determinations of APC subunits in G1 and M phase by MALDI-TOF MS

		α-Factor Arrest (G1)				Nocodazole Arrest (M)				
APC Subunit*	**m (Da)**	**m_1 (Da)**	**Δ_1**	**m_2 (Da)**	**Δ_2**	**m_1 (Da)**	**Δ_1**	**m_2 (Da)**	**Δ_2**	**Modification Category**
Cdc26	14081	14195	114			14226	145			*Constantly modified* – Likely due to phosphorylation **
Apc11	18865	18843	-22	19041	198	18829	-36	19012	183	*Constantly modified*
Swm1	19355	19252	-103	19412	160	19267	-88	19453	186	*Constantly modified* – ΔMW = -Met + Acetyl-Ser.***
Apc9	30856	30874	18			30867	11			*Unmodified*
Apc10	28776	28789	13			28786	10			*Unmodified*
Mnd2	42825	42919	94			43217	392			*Differentially modified*
Cdc23	73113	73238	125			73666	553			*Differentially modified* – Likely due to phosphorylation
Apc4	75256									Not determined accurately due to insufficient ionization
Cdc27	89318									Not reliably determined due to significant protein breakdown.
Cdc16	94992									Not determined accurately due to insufficient ionization.
Apc2	99977	99956	-21			99860	-117			*Unmodified*

KEY: **m** = calculated mass; **m_1** = measured mass; **m_2** = measured mass of modification peak; **Δ_1** = m_1-m; **Δ_2** = m_2-m_1.

* Apc1 and Apc5 do not elute from our C4 RP-HPLC column and could not be measured in this analysis.

** Cdc26 was found to contain a single occupied phosphorylation site, Ser-48, by another laboratory (Yoon et al., 2006).

*** Confirmed by nano-ESI-MS (data not shown).

calculated molecular weight ($m_{unmodified}$ = 42,825 Da), suggesting that Mnd2 was post-translationally modified in M phase. We repeated this experiment with cells arrested in G1 phase and found only a modest positive mass shift of 94 Da (m/z 42,919) relative to the calculated molecular weight (Fig. 4.2 A). The mass deviation of Mnd2 between G1 and M phases ($m/z_{G1} - m/z_M$ = 298 Da) was the largest of any subunit we measured (data not shown), and suggested that the modification was cell cycle dependent.

Mnd2 is hyper-phosphorylated in vivo during mitosis.

Suspecting that Mnd2 may be phosphorylated, we determined if Mnd2 could be metabolically labeled with $NaH_2[^{32}P]O_4$ in yeast arrested with nocodazole. A comparison of FLAG affinity purifications from metabolically labeled yeast with or without a C-terminal 3xFLAG tag on the APC subunit, Cdc27, is shown (Figure 4.2 B, left lanes). We observed 6 distinct bands unique to the tagged strain that did not appear in the purification from a strain lacking a 3xFLAG tag. Alignment of the phosphorimage with a Coomassie-stained large-scale purification of the APC from nocodazole-arrested cells revealed the identity of the known phosphorylated subunits, Cdc16, Cdc27, and Cdc23. In addition, we observed phosphoproteins that aligned with Apc1, Apc2, and Mnd2 (Figure 4.2 B, right lane). In order to verify the identity of these 3 phosphoproteins, we introduced epitope tags onto the C-termini of Apc1, Apc2 (Apc1/2-TAP in Cdc27-3xFLAG background), and Mnd2 (3xFLAG), which would create a gel mobility shift in the ^{32}P-labeled phosphoprotein band in question if the identity was assigned correctly. Each tagged strain was metabolically labeled in the presence of nocodazole and the resulting FLAG affinity purification compared to the original Cdc27-3xFLAG ^{32}P-labeled purification (Figure 4.2 C). We observed a shift in gel mobility

for the phosphoproteins assigned to Apc1 and Mnd2. However, no shift was observed for the band assigned to Apc2, suggesting that this phosphoprotein is not Apc2, but rather, another phosphoprotein that co-immunoprecipitates (co-IP) with the APC or possibly a fragment of phosphorylated Apc1.

In order to determine if the apex mass shift observed between the Mnd2 MALDI spectra was completely or partially due to phosphorylation and to estimate the number of phosphorylation sites involved, we compared the full-length molecular weights of Mnd2 in M phase by MALDI-TOF MS before and after treatment with lambda phosphatase. Nocodazole induces a mitotic checkpoint arrest by inhibiting microtubule polymerization, which may induce phosphorylation of proteins that would not normally be phosphorylated during an unperturbed mitotic progression. Therefore, in this experiment, we opted to use a strain that harbors a temperature sensitive mutation in the mitotic exit network kinase, Cdc15. We have used this strain successfully in the past to characterize phosphorylation of the APC co-activator Cdh1 (Hall et al., 2004). APC purifications from yeast arrested in G1 or M phase cells were split, and half of each purification was treated with lambda phosphatase. The apex mass of Mnd2 from M phase cells was 43,221 Da before phosphatase treatment, and shifted to a mass of 42,837 Da after phosphatase treatment, which is within 12 Da of the calculated mass of the unmodified protein and indicated that the entire mass shift observed in M phase is due to phosphorylation (Figure 4.2 D). In comparison, the apex mass of Mnd2 from G1 phase cells was 42,926 Da before phosphatase treatment, and was shifted to 42,825 Da after phosphatase treatment, indicating that Mnd2 is less phosphorylated during G1 phase. Dividing the average mass difference between the measurements made before and after phosphatase treatment ($\Delta m = m_p - m_{dp}$) by the mass of a single phosphorylation

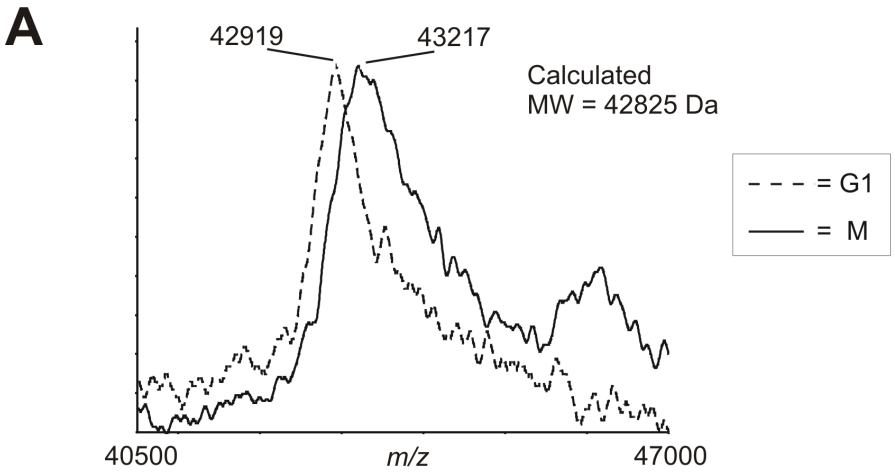
A
42919
43217
Calculated
MW = 42825 Da
- - - = G1
—— = M
40500
m/z
47000

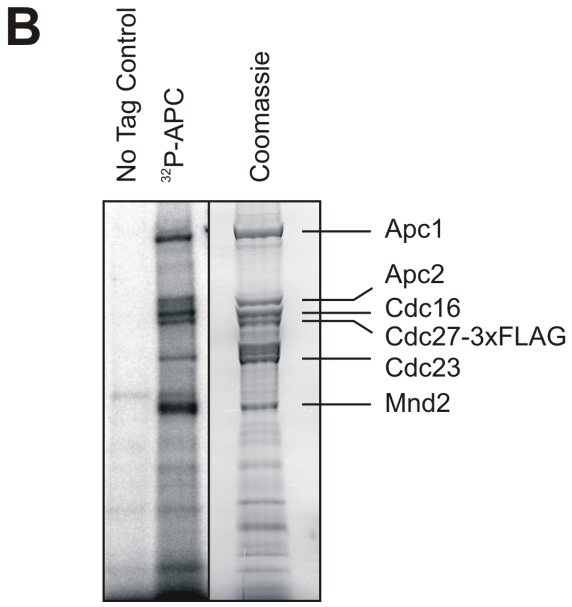
B
No Tag Control
32P-APC
Coomassie
Apc1
Apc2
Cdc16
Cdc27-3xFLAG
Cdc23
Mnd2

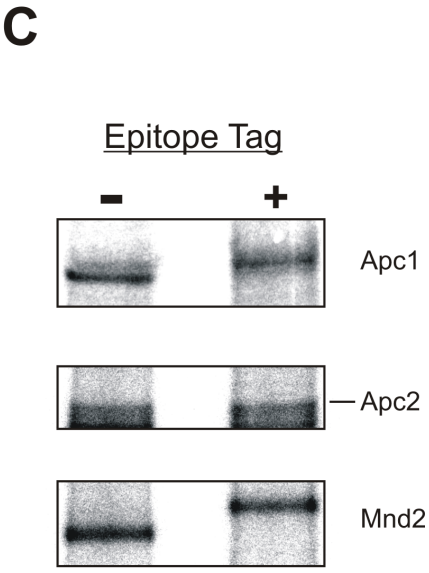
C
Epitope Tag
-
+
Apc1
Apc2
Mnd2

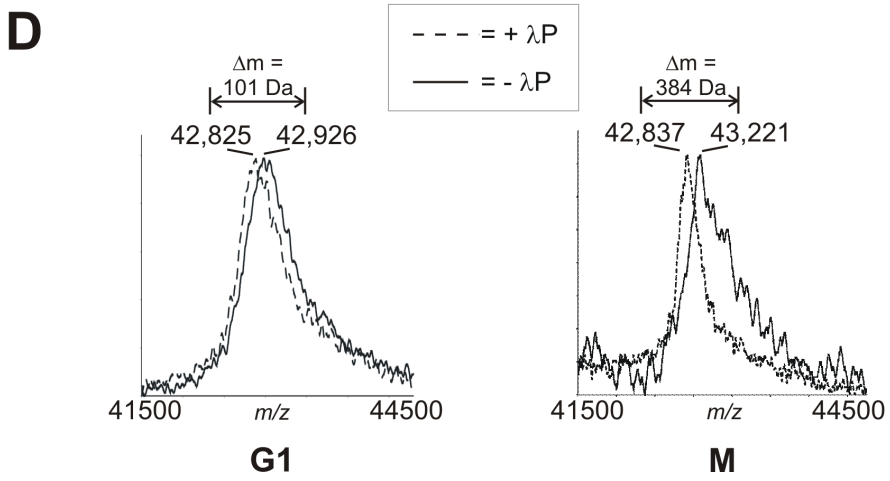
D
- - - = + λP
—— = - λP
Δm =
101 Da
42,825
42,926
41500
m/z
44500
G1
Δm =
384 Da
42,837
43,221
41500
m/z
44500
M

Figure 4.2. Mnd2 is a differentially phosphorylated component of the APC in mitotic cells**.** (A) Overlaid MALDI-TOF mass spectra of Mnd2 in G1 and M phases of the mitotic cell cycle. Mnd2 was co-purified with the APC from yeast harboring epitope-tagged Cdc27 and arrested in G1 phase with α-factor or M phase with nocodazole followed by HPLC separation and linear-mode MS analysis. (B) SDS-PAGE separation of APC purified from yeast arrested in M phase with nocodazole and labeled metabolically with $^{32}PO_4$ *in-vivo* (middle lane) or stained with Coomassie (right lane). The identity of relevant APC subunits in the Coomassie-stained gel is indicated. Cells lacking an epitope tag on Cdc27 were compared in parallel to allow discrimination of non-specific radiolabeled protein bands (left lane). (C) SDS-PAGE mobility comparison between three ^{32}P-labeled APC subunits with (+) and without (-) C-terminal epitope tags. In the (-) lane, APC was purified from YKA155, harboring a 3xFLAG epitope C-terminal to Cdc27. In the (+) lane, APC was purified by FLAG immunoprecipitation from doubly-tagged strains YKA181 (*CDC27-3xFLAG, APC1-TAP*), and YKA191 (*CDC27-3xFLAG APC2-TAP*); or the singly tagged strain YKA152 (*MND2-3xFLAG*). (D) Overlaid MALDI-TOF mass spectrum of Mnd2 in G1 and M phases of the mitotic cell cycle before and after treatment with lambda phosphatase (λP). Mnd2 was co-purified with the APC from the temperature-sensitive yeast strain YKA156 (*cdc15-2*) arrested in G1 phase with α-factor or M phase by temperature shift. While still bound to FLAG affinity matrix, the purifications were split, and half of the purification was treated with λP followed by HPLC separation and linear-mode MS analysis of both phosphorylated and de-phosphorylated proteins.

modification (HPO_3 = 80 Da) indicated that Mnd2 was phosphorylated on at least 4 to 5 different sites (384 Da ÷ 80 Da) during M phase, and only one site, on average, (101 Da ÷ 80 Da) during G1 phase. Furthermore, the 283 Da mass difference observed between the modified states of Mnd2 measured in the phosphatase assay corresponded very well with the measured mass difference of 298 Da determined with Mnd2 purified from nocodazole arrested cells. Though these data indicate a specific number of phosphate modifications on Mnd2, it has been our experience that these values are usually underestimates of the total number of phosphorylation sites of a protein possibly due to modification site heterogeneity and also due to the resolution of MALDI-TOF MS in the linear mode. Attempts to measure the intact protein mass by electrospray ionization MS were not successful. We conclude that Apc1 and Mnd2 are phosphorylated subunits of the budding yeast APC. We further conclude that Mnd2 phosphorylation is cell cycle-dependent.

Characterization of Mnd2 phosphorylation sites.

We used a combination of MS-based approaches to identify the phosphorylation sites in Mnd2 from M phase cells. Mnd2 peptides analyzed by MALDI-TOF/TOF MS surprisingly revealed only one ion at *m/z* 2823.1 that could be assigned to the tryptic Mnd2 monophosphopeptide, ^{140}AQNAEGNNEEDFRQHD$_p$SREEDPR^{162}, by tandem MS (Figure 4.3 A). The tandem mass spectrum contained a number of b and y fragment ions from the Mnd2 peptide including some in which there was a distinct neutral loss of phosphate (H_3PO_4) corresponding to a mass shift of 98 Da. We also assigned a second ion of very low intensity, *m/z* 1807.8, to the Mnd2 monophosphopeptide ^{258}IVPDDLLMRPTSLSR^{272} (Table 4.3). However, the low intensity of the fragment ions did not allow us to determine which of the

three possible phosphorylation sites was occupied (data not shown). Repeating this experiment and including a G1-arrested sample for comparison, we found that phosphorylation at Ser-156 occurred only during M phase (Figure 4.3 B). Similarly, no phosphorylation was observed during G1 phase for peptide Mnd2$^{258\text{-}272}$ (data not shown).

Based on our initial MS analysis, we could assign peptides to 70% of the Mnd2 sequence by mass fingerprinting and tandem MS, but found only 2 phosphorylation sites. The remaining 30% of uncovered sequence included two theoretical tryptic peptides: ^{170}VILPHILQENEEYDTGEGVTGLHSMPNDSMAILANNSANNSQNEEVSEEDEISYD-YDAEFDHVVDEDDNEEGEVPGEGVEGIEVQR^{255} (*m/z* 9525 Da), and ^{287}NPYDIDSD NDGEDSK^{301} (*m/z* 1683.6) that contained a total of 10 potential serine or threonine phosphorylation sites. We did not detect the peptide Mnd2$^{287\text{-}301}$ (including hypothetically post-translationally modified forms) in our initial MS analysis, even though its theoretical mass falls between the optimal range of detection for reflectron mode MALDI-TOF MS, which is between *m/z* 800 - 4000. We made this observation more than once during repeat experiments with Mnd2 from M phase cells (data not shown). We suspected that the difficulty in detecting peptides within these regions of Mnd2 could be due to their high D/E content, which can affect peptide ionization in the mass spectrometer, as well as phosphorylation, which can also affect peptide ionization and inhibit tryptic digestion at cleavage sites that neighbor a phosphorylated residue.

We used linear mode MALDI-TOF MS, which allows the detection of high mass protein species, to search for the large tryptic peptide Mnd2$^{170\text{-}255}$, as well as any miss-cleaved tryptic peptides that contained Mnd2$^{287\text{-}301}$. Using this approach, four major species of interest were detected at *m/z* 6618, *m/z* 6688, *m/z* 8393, and *m/z* 9838, none of which could be assigned to

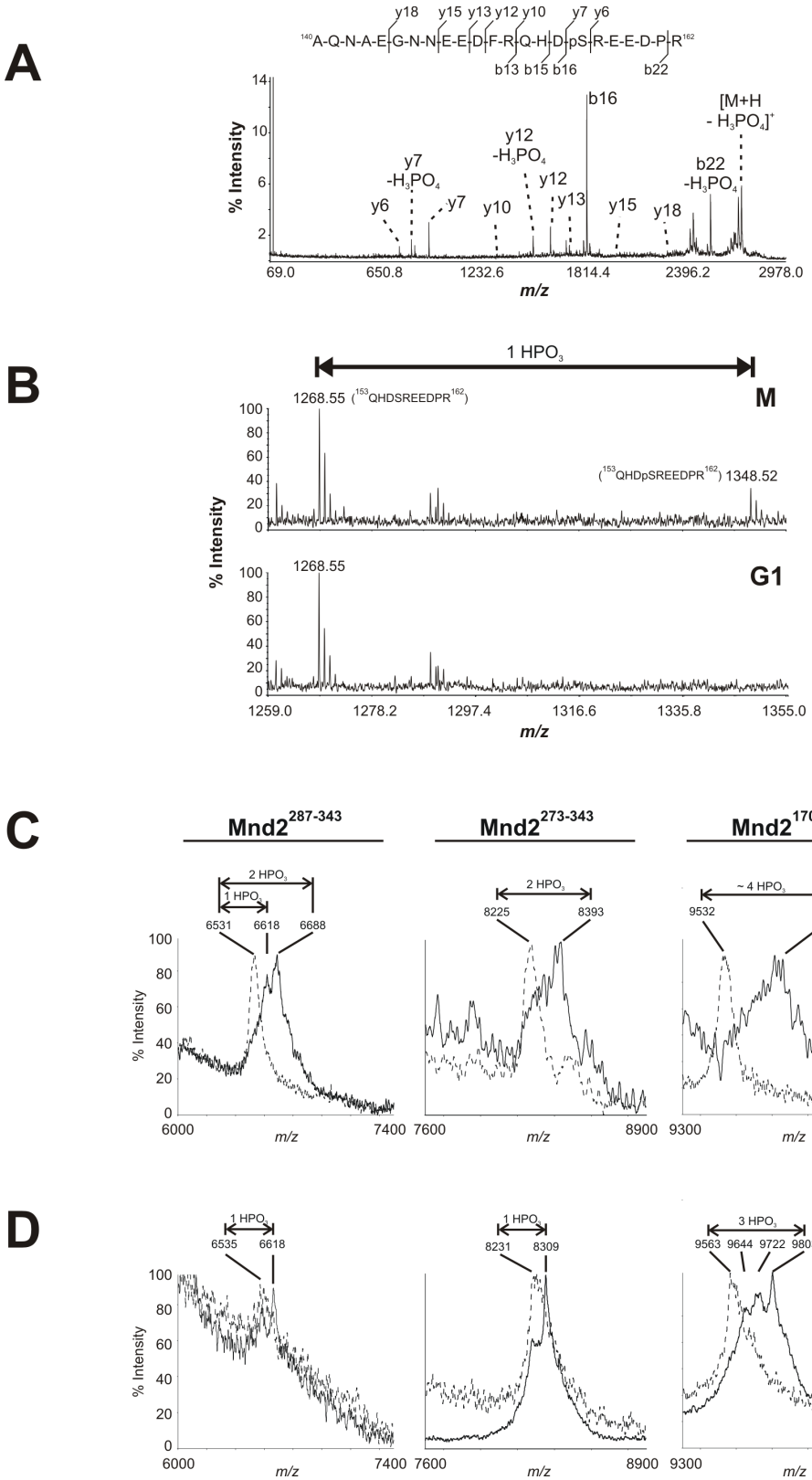
A
y18 y15 y13 y12 y10 y7 y6
140A-Q-N-A-E-G-N-N-E-E-D-F-R-Q-H-D-pS-R-E-E-D-P-R162
b13 b15 b16 b22
% Intensity
m/z
b16
[M+H - H3PO4]+
y12 -H3PO4
y7 -H3PO4
b22 -H3PO4
y6
y7
y10
y12
y13
y15
y18
B
1 HPO3
1268.55 (153QHDSREEDPR162)
M
(153QHDpSREEDPR162) 1348.52
G1
1268.55
C
Mnd2287-343
Mnd2273-343
Mnd2170-255
2 HPO3
1 HPO3
6531 6618 6688
8225 8393
~ 4 HPO3
9532 9838
M
D
1 HPO3
6535 6618
8231 8309
3 HPO3
9563 9644 9722 9803
G1

Figure 4.3. MS identification of Mnd2 phosphopeptides purified from M phase cells. (A) Tandem MS spectrum of *m/z* 2823.1 corresponding to the mono-phosphopeptide $Mnd2^{140-162}$. (B) Comparison of phosphorylation at Ser-156 in M phase (cells arrested with temperature shift), and G1 phase. In this experiment, *m/z* 2823.1 was not found, but rather a shorter form ($Mnd2^{153-162}$) containing only one missed cleavage, which was confirmed by tandem MS. (C) Overlaid linear mode MALDI-TOF mass spectra of high molecular weight tryptic Mnd2 phosphopeptides from M phase arrested cells before (solid line) and after (dashed line) treatment with alkaline phosphatase (AP). The average estimation of occupied phosphorylation sites is indicated by the shift after treatment with AP. Note that the AP-treated masses are all oxidized. (D) Same as (C), but from G1 phase arrested cells. Note that the AP-treated peptide $Mnd2^{170-255}$ contains two rather than one oxidized methionine residues, resulting in a slight shift in the mass spectra compared to (C).

the unmodified Mnd2 sequence. Comparison of the spectra with and without phosphatase treatment showed that each of the four species was phosphorylated, as indicated by negative shifts in the apex mass after phosphatase treatment (Figure 4.3 C). Using the apex mass of the ion species after phosphatase treatment, we were able to assign each peptide to Mnd2 as well as calculate the average number of occupied phosphorylation sites within each peptide (Table 4.3). Interestingly, the tryptic peptides assigned to *m/z* 6618, *m/z* 6688, and *m/z* 8393 each contained multiple missed cleavage sites, and included the tryptic region $Mnd2^{287\text{-}301}$ with one or two occupied phosphorylation sites. Since we were able to detect each of the tryptic peptides flanking the $Mnd2^{287\text{-}301}$ region in the reflectron mode MS analysis and confirm that they were unmodified, we concluded that the occupied phosphorylation sites are S^{293} and S^{300}. The ion at *m/z* 9838 was assigned to the largest tryptic peptide $Mnd2^{170\text{-}255}$ and contained an average of 4 occupied phosphorylation sites. The mass accuracy of this assignment was within 7 Da of the expected mass, which likely reflects an average of a mixture of the unmodified peptide (*m/z* 9519) and a mono-oxidized peptide (*m/z* 9535), since no other peptides with up to 10 missed cleavages could be closely matched to this ion. Calculation of the apex mass shift after phosphatase treatment indicated that $Mnd2^{170\text{-}255}$ contains an average of 4 occupied phosphorylation sites out of 8 potential serine or threonine residues. A comparison of these phosphopeptides in G1 phase shows that Mnd2 maintains partial phosphorylation (Figure 4.3 D). In summary, we find that Mnd2 is phosphorylated on at least 8 different sites during mitosis, and at least 4 sites during G1 phase.

Yeast harboring Mnd2 phosphorylation site mutations grow normally.

Cell cycle regulated phosphorylation is an important component of APC-mediated cell

Table 4.3.
Assignment of Mnd2 phosphopeptides.

Masses of the dephosphorylated peptides were used for assigning Mnd2 sequence to each MS ion, with the exception of *m/z* 1808.8 and *m/z* 2823.1 that were assigned by tandem MS sequencing. Mass of the phosphorylated peptide (m_p) was compared to the mass of the dephosphorylated peptide (m_{dp}) to determine the average number of phosphorylation sites occupied (Avg. no. HPO_3). The assigned Mnd2 peptide sequence, additional observed modifications after phosphatase treatment (Add. Mod), and the expected average mass (m) are shown. The mass accuracy is shown as the difference between the dephosphorylated peptides and the expected average mass ($m_{dp} - m$), with the exception of *m/z* 1808.8 and *m/z* 2823.1 whose error was calculated from the expected phosphorylated mass.

Observed Masses							
m_p	m_{dp}	Δm (= $m_p - m_{dp}$)	Avg. # HPO_3	Assigned Mnd2 Peptide Sequence	Add. Mod	Exp. Avg. Mass (m)	Error ($m_p - m$)
1808.8	--	--	1	^{258}IVPDDLLMRP**TS**L**S**R^{272}	--	1808.8	0.09
2823.1	--	--	1	^{140}AQNAEGNNEEDFRQHD**pS**REE DPR^{162}	--	2823.1	0.01
6618	6531	87	1	^{287}NPYDID**S**DNDGED**S**KVELDMN PDFEDDVGREHDYNSEYSQEPT SYGGITPDLASNWR^{343}	1 MeOx	6531	0
6688	6531	157	2	^{287}NPYDID**S**DNDGED**S**KVELDMN PDFEDDVGREHDYNSEYSQEPT SYGGITPDLASNWR^{343}	1 MeOx	6531	0
8393	8225	168	2	^{273}SLQQFVEEAHHLDRNPYDID**S**D NDGED**S**KVELDMNPDFEDDVGR EHDYNSEYSQEPTSYGGITPDLA SNWR^{343}	1 MeOx	8223	2
9838	9532	306	4	^{170}VILPHILQENEEYD**T**GEGV**T**GL H**S**MPND**S**MAILANN**S**ANN**S**QNE EV**S**EEDEI**S**YDYDAEFDHVVDED DNEEGEVPGEGVEGIEVQR^{255}	0 - 1 MeOx	9525	7

cycle regulation. Yeast strains harboring altered forms of the APC that cannot be modified by phosphorylation display growth defects associated with a delay in mitotic progression (Rudner and Murray, 2000). In order to determine if Mnd2 phosphorylation is critical to the progression of mitosis, we compared growth rates of an *mnd2Δ* strain in which the wild type form (WT) or phosphorylation site mutant forms of *MND2* (*mnd2-(S/T-A)* and *mnd2-(S/T-D)*), were introduced at the *TRP1* locus under control of the *MND2* promoter (see experimental procedures). Mnd2 phosphorylation site mutants were created by simultaneously mutating all 14 sites found or implicated by our MS analysis to alanine or aspartic acid (aspartic acid mutations are meant to mimic the phosphorylated state of Mnd2). The mutations to Mnd2 did not have a significant effect on APC binding compared to the WT form as determined in an *in vitro* binding assay (Figure 4.4 A). As a positive control for the growth rate of strains harboring an APC defect, we compared the growth rate of yeast lacking Apc10, which display a slow growth phenotype due to compromised APC processivity (Bonenfant et al., 2003; Passmore et al., 2003). Growth rates for all but the *apc10Δ* strain were undistinguishable at both 30°C and 37°C (Figure 4.4 B). This observation was not surprising since the *mnd2Δ* strain displays no significant difference in growth rate (Bonenfant et al., 2003; Page et al., 2005). We conclude that phosphorylation at the sites found in our MS analysis do not have a significant function in the proper progression of mitosis.

Mnd2 phosphorylation is required for progression through the first meiotic nuclear division.

Yeast lacking Mnd2 are incapable of sporulation and arrest after the completion of pre-meiotic S phase but before the first meiotic nuclear division

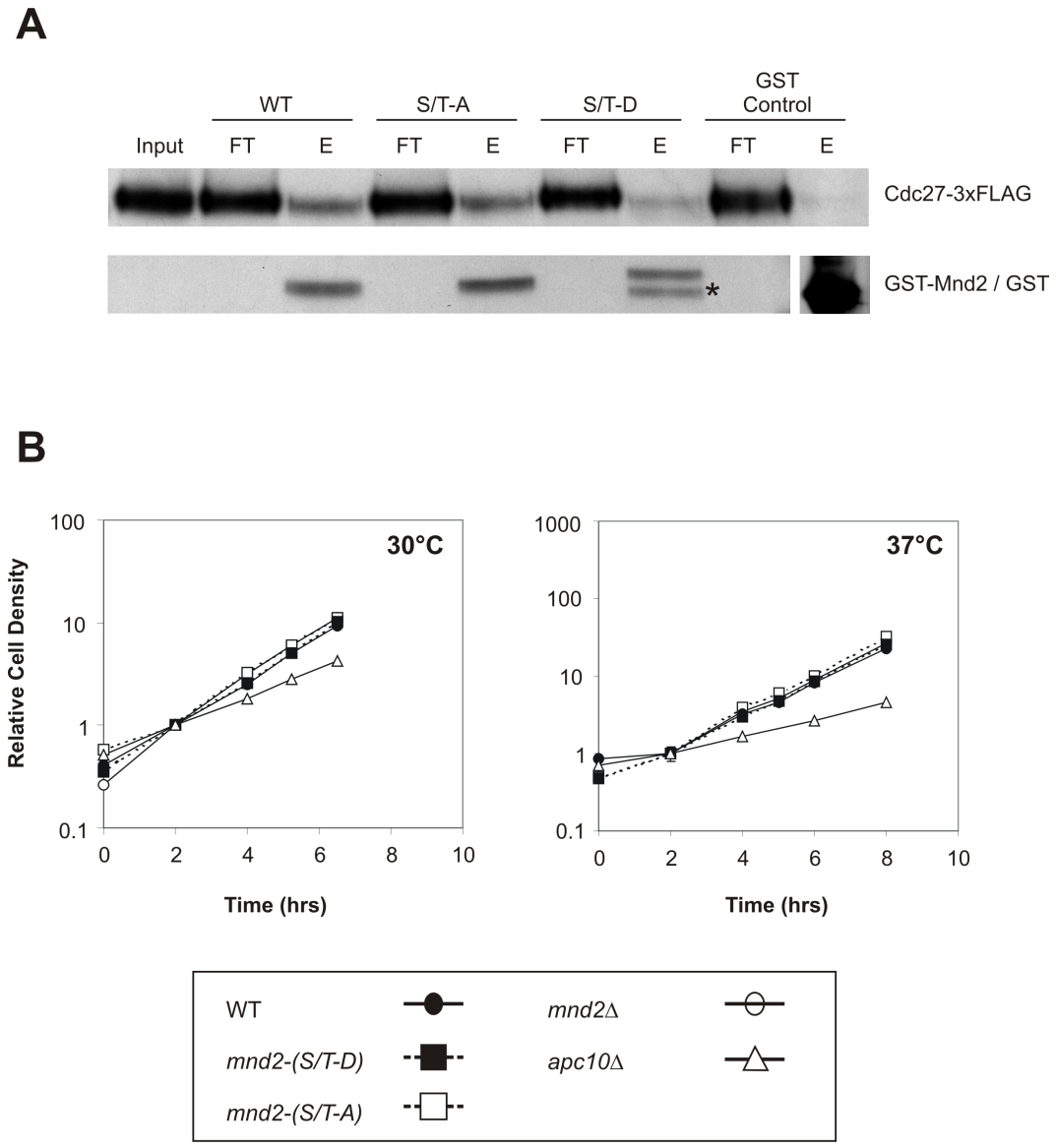

Figure 4.4. Yeast harboring Mnd2 phosphorylation site mutations grow normally. (A) *In vitro* binding assay between GST-Mnd2 WT, *mnd2-(S/T-A)*, *mnd2-(S/T-D)*, and GST. APC was purified from *CDC27-3XFLAG mnd2Δ* cells harvested from an asynchronous mid-log phase culture and incubated in batch with an excess of GST-Mnd2 fusion protein bound to GSH sepharose. Unbound protein was washed away with 100 bead-equivalent volumes of buffer and the bound protein was eluted in 1 bead-equivalent volume of SDS-PAGE loading buffer. The input (I), flow through (FT), and elution are shown after western blotting with anti-FLAG or ant-GST antibodies. (*) GST-Mnd2 breakdown product. (B) Logarithmic plots of vegetative growth rates relative to the 2 hour time point measured in YPD media for WT, *mnd2-(S/T-D)*, *mnd2-(S/T-A)*, *mnd2Δ*, and *apc10Δ* at 30°C (Left) and 37°C (Right).

(Oelschlaegel et al., 2005; Penkner et al., 2005; Rabitsch et al., 2001). In order to determine if Mnd2 phosphorylation was also required for sporulation, we compared the phenotypes WT, *mnd2Δ*, *mnd2-(S/T-A)*, and *mnd2-(S/T-D)* upon induction of sporulation. When comparing the kinetics of tetrad formation for each strain, we found that 85% of WT cells formed complete tetrads within 42 hours after plating to sporulation media, which was nearly identical to the sporulation percentage for cells harboring *MND2* at its natural genetic locus (Figure 4.5 A). In contrast, *mnd2Δ* strains were unable to form tetrads. Only 13% of cells harboring *mnd2-(S/T-A)* formed tetrads, while the percentage of tetrads increased to 42% of cells harboring *mnd2-(S/T-D)*. In addition, there was no appreciable accumulation of cells containing only two spores (dyads) as observed by light microscopy, which would have indicated arrest between the first and second nuclear division. The differences in tetrad formation between the WT and mutant strains was not due to a failure in meiotic entry since each strain completed pre-meiotic S phase as measured by flow cytometry (Figure 4.5 B).

Quantitation of tetrad formation cannot be used as an indicator for the ability of cells to complete meiotic nuclear divisions. Indeed, meiotic nuclear divisions and spore formation are not completely connected pathways, and it is possible to achieve nuclear divisions without forming spores, which has been reported for sub-populations of *ama1Δ* cells (Cooper et al., 2000). Cells that do not undergo the first meiotic nuclear division arrest with a single nucleus that can be visualized using fluorescence microscopy of DAPI-stained nuclei. In order to determine if meiotic nuclear divisions were compromised in *mnd2* phosphorylation mutants, we scored the percentages of non-tetrad forming (residual) cells that contained a single undivided nucleus after 48 hours on sporulation media. In strains harboring mutant or wild type Mnd2, the percentage of non-tetrad cells containing a single undivided nucleus was

greater than 90% (Figure 4.5 C). Since tetrads are formed at low levels in strains harboring *mnd2-(S/T-A)*, we also quantified the viability of tetrad spores. A high percentage of spore viability indicates that cells are capable of proper nuclear divisions that distribute a complete complement of the haploid genome to each spore. Low spore viability is observed when nuclear divisions are compromised such that individual spores are left with an incomplete complement of the haploid genome. Following tetrad dissection, 95% of WT spores were viable compared to 89% and 84% spore viability for *mnd2-(S/T-D)* and *mnd2-(S/T-A)* cells, respectively (Figure 4.5 C).

Mnd2 inhibits the ubiquitin ligase activity of APC^{Ama1} towards specific meiotic substrates including Pds1, Clb5, and Sgo1 (Oelschlaegel et al., 2005; Penkner et al., 2005). In particular, Pds1 and Clb5 fail to accumulate appreciably in sporulating *mnd2Δ* cells. In order to ascertain if the phosphorylation status of Mnd2 affects its function as an APC^{Ama1} inhibitor, we compared the protein stability of Clb5 in cell extracts taken from a sporulation time course. Sporulating cells were collected at 0, 24, and 48 hours and the percentage of tetrad forming cells and cells with replicated DNA were quantified to verify synchrony and meiotic entry of each strain (Figure 4.5 D top). Clb5 levels were low to immeasurable in the *mnd2Δ* strain compared to the WT strain (Figure 4.5 D bottom). Very little accumulation of Clb5 was observed for the *mnd2-(S/T-A)* strain, but was noticeably higher in the *mnd2-(S/T-D)* strain. A similar trend was observed for Pds1 (data not shown). Taken together, these data show that phosphorylation of Mnd2 is critical for efficient progression through the first meiotic nuclear division and for normal accumulation of the APC^{Ama1} substrate, Clb5. We conclude that phosphorylation of Mnd2 is involved in regulating the inhibition of APC^{Ama1} in early meiosis.

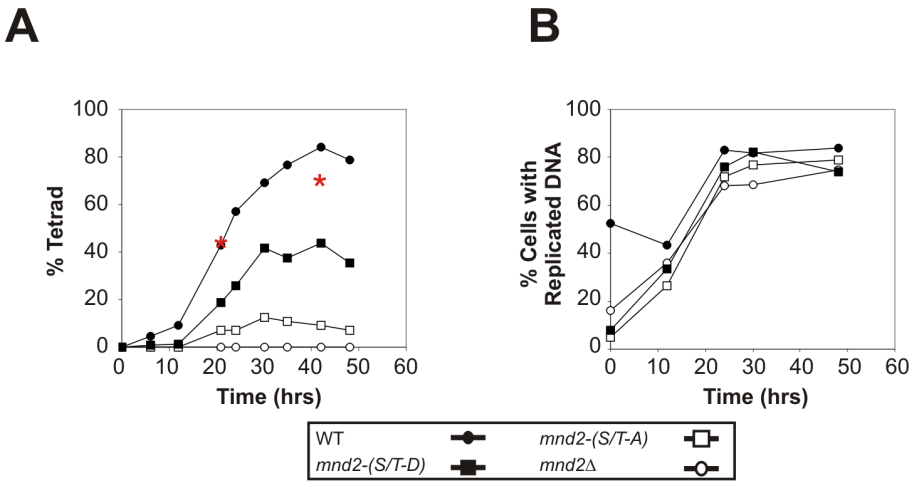

C

	DIC	DAPI	% Tetrad	% Residual Cells with Single Nucleus	Spore Viability
WT			80%	100%	95%
S/T-D			37%	93%	89%
S/T-A			7%	91%	84%
mnd2Δ			0%	84%	---

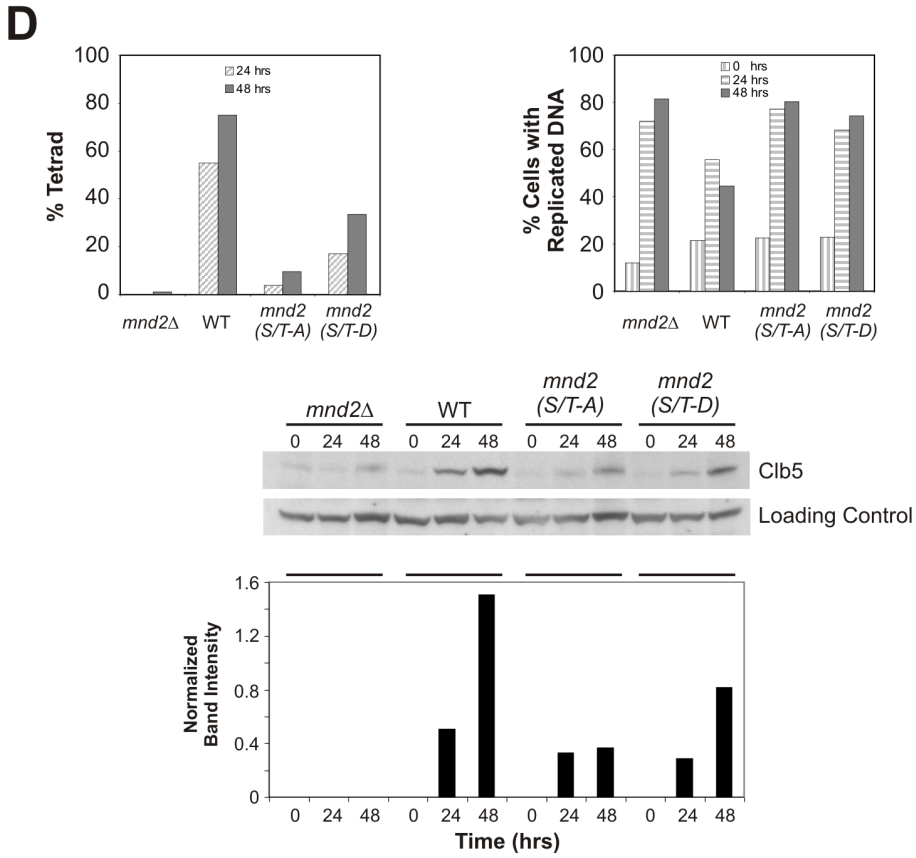

Figure 4.5. Phosphorylation of Mnd2 is necessary for efficient progression through the first meiotic nuclear division. (A) Kinetics of tetrad formation for WT, *mnd2-(S/T-D)*, *mnd2-(S/T-A)*, and *mnd2Δ* cells. Tetrad formation kinetics for a wild type strain in which MND2 is expressed from its normal locus is shown (*). (B) Kinetics of pre-meiotic S phase measured by flow cytometry. (C) DIC and fluorescence microscopy of DAPI-stained yeast 42 hours after plating on SPM. The percentage of tetrads formed, the percentage of non-tetrad (residual) cells with a single nucleus, and the percentage of viable spores are indicated to the right of each microscopy image. (D) Percentage of tetrad forming cells 24 and 48 hours after plating on SPM (top, left). Percentage of cells with replicated DNA at 0, 24, and 48 hours after plating on SPM (top, right). Western blot comparison of Clb5 levels in extracts prepared and quantified after lysis of cells harvested at 0, 24, and 48 hours after plating on SPM. A non-specific band detected in the western blot is shown as a loading control. Bar graph shows quantitation of Clb5 levels from the western blot. Normalized band intensities were calculated taking the ratio of Clb5 signal to the corresponding loading-control band for each lane. The data is shown after subtraction of the deletion strain Clb5 ratios for each corresponding time point.

Phosphorylation may be necessary to stabilize Mnd2 before meiotic entry.

Since phosphorylation of Mnd2 is not required for mitotic progression, yet it has a strong early meiotic requirement similar to an *mnd2* deletion, we asked whether or not the *mnd2* phosphorylation site mutants were differentially destabilized. We were unable to detect Mnd2 in western blots of mitotic whole cell extracts. Therefore, we conducted western blots with anti-Mnd2 antibody on the APC purified from 1L cell cultures via Cdc27-3xFLAG. The association of Mnd2 with the APC is extremely stable, even in buffers containing 450 mM NaCl that we typically use to purify APC (Hall et al., 2003).

We found that Mnd2 WT and phosphorylation site mutants were present in APC purifications at differential levels that were similar to the differences that we observed for the meiotic defect (Figure 4.6). The *mnd2-(S/T-A)* mutant was undetectable, although its binding was determined to be equivalent *in vitro* (Figure 4.4 A). In contrast, *mnd2-(S/T-D)* and Mnd2 WT were detected at levels representative of their differential progression through meiosis. Since each isoform is expressed from the same genetic locus under control of the same promoter, we conclude that the difference in Mnd2 abundance is not due to differences in protein expression. Alternatively, the difference in Mnd2 abundance in APC purifications could be due to differential sequestration of the different isoforms, however, there is no evidence to suggest this is a viable mechanism of Mnd2 regulation. Therefore, we hypothesize that the difference in Mnd2 abundance is due to differential stability of each isoform. Since the alanine mutant is the least stable, and the WT and aspartic acid mutant are more stable, we propose that phosphorylation is required to maintain the stability of Mnd2 during the mitotic cell cycle.

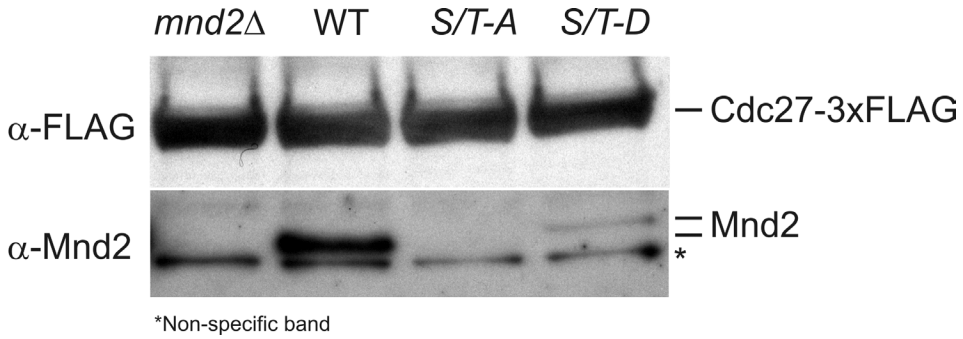

Figure 4.6. Phosphorylation of Mnd2 may be necessary for Mnd2 protein stability in mitosis. APC was purified from whole cell lysate (1L starting cell culture grown to OD600 = 1.0) through Cdc27-3xFLAG strains containing the indicated Mnd2 mutations. Purification from each strain was verified to be equivalent by anti-FLAG western blotting of Cdc27-3xFLAG (upper panel). Detection of co-precipitating Mnd2 isoforms was determined by western blotting with custom anti-Mnd2 rabbit polyclonal antibody (lower panel).

Discussion

We have used a mass spectrometric approach to discover and identify mitotic phosphorylation sites on the APC subunit, Mnd2. The phosphorylation status of Mnd2 appears to be generally similar to that of other phosphorylated yeast APC subunits (Cdc16, Cdc27, and Cdc23), in that it is higher in mitosis compared to G1 phase. Interestingly, none of the phosphopeptides observed contain the canonical cyclin dependent kinase recognition sequence, S/T-P, which suggests the involvement of other kinases. Mutation of Mnd2 phosphorylation sites has no effect on mitotic cell cycle progression, which is not surprising considering that Mnd2 has no required function during vegetative cell growth. However, there is a striking difference in the ability of Mnd2 phosphorylation site mutants to complete meiosis. The similarities in sporulation phenotype for the alanine and deletion mutant strains strongly suggest that phosphorylation is critical for Mnd2 function early in the meiotic program. Both strains complete pre-meiotic S phase and, like the deletion strain, the majority of alanine mutants fail to undergo the first meiotic nuclear division. The fact that mutation of each phosphorylation site to aspartic acid, which may mimic the phosphorylated state of Mnd2, recovers the sporulation phenotype to approximately 50% of the wild type strain further supports the conclusion that phosphorylation is necessary for Mnd2 function in early meiosis. In addition to a meiotic sporulation phenotype, we also find that *mnd2-(S/T-A)* mutants have lower levels of the APC^{Ama1} substrate, Clb5, which suggests that Mnd2 phosphorylation is necessary for some aspect of its inhibitory function rather than an effect unrelated to APC activity. In support of this hypothesis, we find that *mnd2-(S/T-A)* mutants appear to be destabilized during mitosis *in vivo*, which would explain why they share a meiotic phenotype similar to *mnd2Δ* cells.

We have also shown that the subunit, Apc1, is phosphorylated during mitosis. Preliminary experiments show that Apc1 is phosphorylated on a number of sites that are contained within a canonical CDK recognition sequence as well as some sites that are not (our unpublished results). Further work will focus on the characterization of these sites at different cell cycle stages and to determine the effects of mutating these sites on mitotic and meiotic progression.

Despite similarities to the *mnd2Δ* strain, some cells harboring *mnd2-(S/T-A)* are still capable of complete sporulation resulting in the formation of viable haploid spores. Thus, the possibility remains that other sites of phosphorylation specific to meiosis may be necessary, or the unphosphorylated form retains some low activity. The high percentage of spore viability in the phosphomutant strains also suggests that phosphorylation of Mnd2 at these sites is only necessary before the first meiotic nuclear division, since mutant cells that do form tetrads must be capable of completing normal meiotic nuclear divisions and spore formation. This observation is consistent with existing data that shows Mnd2 is necessary for the completion of recombination before the first meiotic nuclear division (Oelschlaegel et al., 2005; Penkner et al., 2005). In contrast, cells harboring *mnd2-(S/T-D)* are not capable of completely rescuing the sporulation phenotype, which may be due to insufficient mimicry of phosphorylation by the side chain of aspartic acid.

The kinase[s] that phosphorylates Mnd2 remain unknown. Indeed, the phosphorylation of Mnd2 during mitosis may not be caused by the same kinases responsible for its phosphorylation during meiosis. Therefore, the future goals of this research will address the kinase or kinases responsible for phosphorylating Mnd2. Currently, the primary kinases known to be involved in APC phosphorylation are CDK (Cdc28 in yeast) and polo-like kinase, Cdc5. However, none of the Mnd2 phosphopeptides that we observed contained

either a canonical CDK recognition sequence (S/T-P) or the polo box domain recognition sequence (S-pS/pT-P). Notably, many of the phosphorylation sites implicated by our MS analysis fell within regions of high D/E residue content, which could suggest phosphorylation by casein kinase 2 (Glover et al., 1998).

The molecular effect that phosphorylation of Mnd2 has on APC^{Ama1} inhibition is unknown. However, our evidence does suggest that phosphorylation or lack thereof does not effect Mnd2 binding to the APC since the phosphorylated form of Mnd2 co-purifies with the APC both before and after phosphatase treatment, and recombinant forms of the wild type, alanine, and aspartic acid phosphorylation site mutants are still capable of binding to the APC *in vitro*. Taken together, these observations do not support the hypothesis that Mnd2 phosphorylation controls APC^{Ama1} inhibition simply by altering the binding of the inhibitor to the complex. Rather, we suggest that Mnd2 phosphorylation is necessary to stabilize Mnd2 during mitosis. In this case, lack of phosphorylation would destabilize Mnd2, and upon meiotic entry, Ama1 could activate the APC prematurely similar to observations described for *mnd2Δ* cells (Oelschlaegel et al., 2005; Penkner et al., 2005).

We have shown that phosphorylation sites occupied differentially during the mitotic cell cycle can provide critical regulatory roles for the APC during meiosis. The fact that phosphorylation sites between the two types of nuclear division are shared in this way suggests that known phosphorylation sites within other APC subunits will also be important for meiosis. Although APC subunit phosphorylation is important for proper meiotic progression, the dynamics of phosphorylation at specific sites and by specific kinases is still poorly understood. Future experiments that characterize the dynamics of APC phosphorylation during meiosis will be invaluable to our understanding of APC regulation.

CHAPTER V

CONCLUSIONS AND GENERAL DISCUSSION

Summary

The anaphase-promoting complex (APC) E3 ubiquitin ligase is a key regulatory factor necessary for proper progression through mitotic and meiotic cell cycle transitions. At the inception of this work, very little was known about the role of the APC during meiosis. Moreover, nothing was known about the role of APC phosphorylation in the regulation of APC-mediated meiotic cell cycle transitions. In this thesis, I have used a variety of mass spectrometric methods to characterize APC subunit composition and APC post-translational modifications that exist during the cell cycle of *Saccharomyces cerevisiae*. I have demonstrated the association of two new subunits, Mnd2 and Swm1, which co-precipitate with the APC at stoichiometric levels throughout the cell cycle. Interestingly, both subunits are dispensable for mitosis, but required for meiosis in budding yeast. Furthermore, I show that the Mnd2 subunit is differentially phosphorylated during the mitotic cell cycle, while Swm1 is constantly modified by removal of methionine and N-terminal serine acetylation. Using mass spectrometry, I have identified the specific sites of Mnd2 phosphorylation and shown that they are necessary for progression beyond the first meiotic nuclear division. This work represents the first demonstration that APC phosphorylation is necessary for meiotic cell cycle transitions in any organism. However, a mechanism that describes phosphorylation in the context of Mnd2 as a meiotic APC inhibitor remains to be established. In this chapter, I relate observations that I have detailed in this thesis to existing literature data that describes Mnd2 function in early meiosis, with the goal of defining a possible mechanism for Mnd2 phosphorylation.

The role of Mnd2 as a meiotic APC inhibitor

Shortly after the discovery that Mnd2 and Swm1 were constitutive APC subunits during mitosis (Bonenfant et al., 2003; Passmore et al., 2003; Yoon et al., 2002) and meiosis (Bonenfant et al., 2003), reports on the function of both subunits began to emerge. Consistent with our observations (Bonenfant et al., 2003), these reports showed that mutants lacking *SWM1*, but not *MND2*, displayed growth defects (Page et al., 2005). They also showed that Swm1 was critical for maintaining structural integrity of the APC, such that the complex purified in the absence of Swm1 also lacked the TPR subunits Cdc16 and Cdc27 (Schwickart et al., 2004), and displayed lower catalytic activity (Page et al., 2005; Schwickart et al., 2004). In contrast, the requirement for Mnd2 in stabilizing APC structure or catalysis appeared to be negligible (Page et al., 2005).

A role for Mnd2 as an APC subunit was reported in early 2005 by two independent laboratories (Oelschlaegel et al., 2005; Penkner et al., 2005). Both laboratories reported that in yeast lacking *MND2*, cells could progress through pre-meiotic S phase, but failed to complete the first meiotic nuclear division, due to premature separation of sister chromatids in prophase I, caused by early APC activation by the meiosis-specific co-activator, Ama1. They went on to show that Mnd2 was necessary for accumulation of the anaphase inhibitor, Pds1, as well as Clb5, and the meiotic cohesin subunit, Rec8, during prophase I, consistent with a role as an APC inhibitor (Oelschlaegel et al., 2005). Finally, they showed that Mnd2 could specifically inhibit ubiquitination of Pds1 by APC^{Ama1} *in vitro* (Oelschlaegel et al., 2005). In this case, inhibition was specific for APC^{Ama1} complexes, but not APC^{Cdc20} or APC^{Cdh1}. The general conclusions from these studies are shown as an illustration (Figure 5.1).

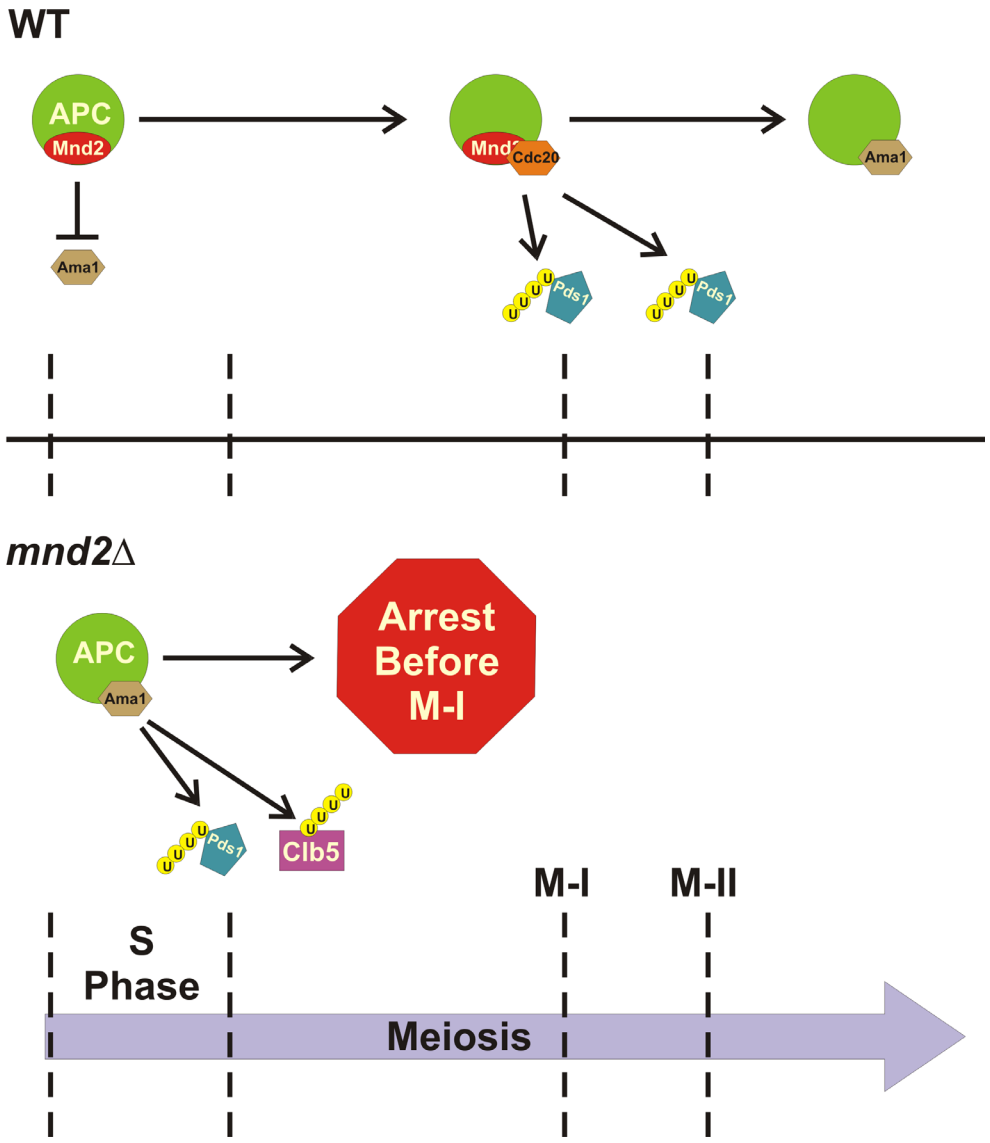

Figure 5.1. The role of Mnd2 as a meiotic APC inhibitor. (Top) Mechanism in wild type (WT) cells. Mnd2 inhibits premature ubiquitination and degradation of Pds1 until the APC can be activated normally by Cdc20. After the second nuclear division, Mnd2 is removed (by degradation through an unknown mechanism), allowing Ama1 to activate the APC in late meiosis, which is necessary for spore wall formation. (Bottom) Mechanism in *mnd2Δ* cells. In cells lacking Mnd2, Ama1 can activate the APC upon meiotic entry, which results in premature ubiquitination and degradation of Pds1 and Clb5 in prophase I. As a result, the cells arrest before the first meiotic nuclear division.

Mnd2 phosphorylation: necessary for protein stability?

Interestingly, both groups reported that Mnd2 was increasingly expressed and phosphorylated through the completion of both nuclear divisions as indicated by the appearance of a phosphatase-sensitive western blot band that they did not show (Oelschlaegel et al., 2005; Penkner et al., 2005). Although they did not investigate the role of phosphorylation directly, they did show that the band associated with phospho-Mnd2 is immediately apparent (at time 0) upon induction of the sporulation program, before pre-meiotic S phase. In addition, they found that Mnd2 was degraded sometime after anaphase II, although degradation was not required for completion of sporulation, since strains in which Mnd2 was constitutively expressed were still capable of complete sporulation. They also found that recombinant His-Mnd2 purified from bacterial cell lysates could effectively inhibit APC^{Ama1} in a dose-dependent fashion, suggesting that phosphorylation is not necessary for direct inhibition, at least *in vitro* (Oelschlaegel et al., 2005). Finally they showed that the levels of Ama1 were significantly lower in APC affinity purifications from wild type versus *mnd2Δ* cells, and apparently independent of Mnd2 phosphorylation, suggesting that Mnd2 might directly block an association between Ama1 and the APC independent of its phosphorylation status (Oelschlaegel et al., 2005).

In my research, I have found that Mnd2 phosphorylation is necessary for efficient progression beyond the first meiotic nuclear division. Furthermore, similar to previously published results (Oelschlaegel et al., 2005; Penkner et al., 2005), I find that there is no significant difference between the binding of phosphorylated or dephosphorylated Mnd2 to the APC, *in vitro* or *in vivo* (Chapter IV). Taken in context with the data from Oelschlagel et al. (2005), and Penker et al. (2005), these data suggest that phosphorylation of Mnd2

functions through an indirect rather than a direct regulatory mechanism that is critical for progression beyond the first meiotic nuclear division.

One intriguing hypothesis that I put forth now is that phosphorylation is necessary to stabilize Mnd2 before prophase I, thereby maintaining the inhibition of APC^{Ama1}, which allows cells to efficiently progress through the meiotic nuclear divisions. Indeed, others have found that phosphorylation can protect proteins from various forms of degradation including direct enzymatic proteolysis (Chen and Stracher, 1989; Litersky and Johnson, 1992), as well as ubiquitin-mediated proteolysis (Eckerdt et al., 2005; Hino et al., 2005). Consistent with this hypothesis, I found that Mnd2 levels are low in asynchronous mitotic cultures for the *S/T-A* phosphorylation site mutant, while not as low for the WT and *S/T-D* mutant *in vivo*. Furthermore the differential levels of the Mnd2 isoforms is proportional to the differences observed for sporulation of the corresponding yeast strains that harbor each isoform. This observation provides an explaination for the existence of phosphorylation on Mnd2 during mitosis, which until now has remained a mystery.

A mechanism for the role of mitotic Mnd2 phosphorylation is shown (Figure 5.2). I propose that Mnd2 phosphorylation is necessary to inhibit degradation of Mnd2 protein by some unknown mechanism during mitosis. Then, upon entry into pre-meiotic S phase, the active Mnd2 would be able to inhibit Ama1 from activating APC, and meiotic progression would occur normally. In the case of the alanine mutant, which mimics a constitutively dephosphorylated Mnd2 isoform, Mnd2 would be degraded, resulting in an *mnd2Δ* phenotype similar to what I've observed. Likewise, the aspartic acid mutant, which mimics a constitutively phosphorylated Mnd2 isoform, would be protected from degradation (as much as aspartic acid can mimic a phosphorylated serine or threonine), resulting in normal wild

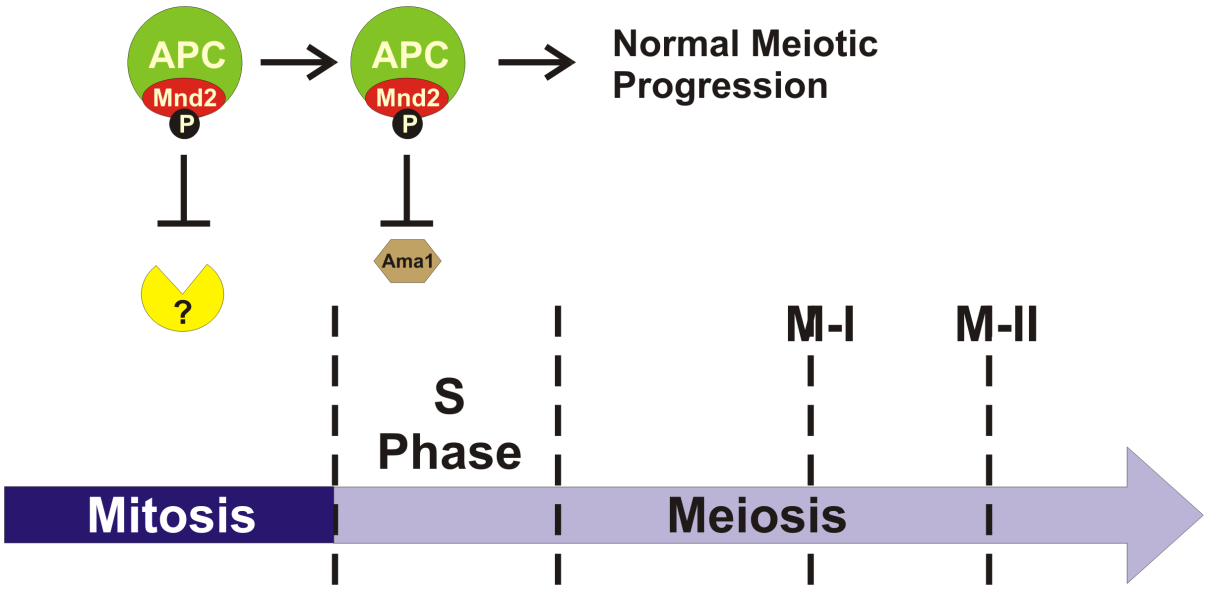

Figure 5.2. Hypothetical mechanism for Mnd2 phosphorylation in APC^{Ama1} inhibition. Mnd2 is phosphorylated during mitosis, G1 phase, and at the initiation of pre-meiotic S phase, which inhibits its degradation by an unknown mechanism. Mnd2 is thus protected and able to inhibit APC^{Ama1} complex which forms early in pre-meiotic S phase. Normal progression of meiosis continues, including timely ubiquitin-mediated proteolysis of Pds1 at both nuclear divisions, followed by spore formation.

type sporulation similar to what I've observed.

This hypothetical mechanism of Mnd2 regulation is intriguing for multiple reasons. First, it provides a reasonable explaination for why Mnd2 is phosphorylated during mitosis, when it clearly has no role in mitotic progression. Second, it provides a reasonable explaination for why Mnd2 is present on the APC during mitosis as opposed to being expressed in early meiosis. The explaination is that Ama1 becomes expressed immediately upon entry into meiosis. Since the decision to enter meiosis is made before pre-meiotic S phase, Mnd2 must be present ahead of time to ensure proper inhibition of APC^{Ama1}, and protective phosphorylation of Mnd2 would enable this to occur. Third, the hypothesis explains why both phosphorylated and dephosphorylated Mnd2 can bind the APC, but only the phosphorylated form can inhibit the APC. Fourth, regulation of Mnd2 by degradation has been shown to occur after the second meiotic nuclear division, shortly after the disappearance of a western blot band thought to be the phosphorylated form of Mnd2 *in vivo* (Oelschlaegel et al., 2005). Thus, Mnd2 degradation could be the primary mechanism by which Ama1 is allowed to activate the APC *in vivo*.

Should the stability hypothesis be supported by experimental evidence, it would be interesting to determine the proteins necessary for Mnd2 degradation. Recent evidence suggests that phosphorylation by PKA can block ubiquitination by the E3 ubiquitin ligase, SCF^{Skp1} (Hino et al., 2005). Interestingly, some Mnd2 phosphorylation sites discovered in my research fall within potential PKA recognition sequences, making this mechanis particularly attractive. In addition, regulation of an APC inhibitory protein, like Mnd2, by an SCF-dependent mechanism would be intriguing since the SCF has been shown to target other APC inhibitors such as Emi1 (Guardavaccaro et al., 2003; Peters, 2003). Furthermore, SKP1

and CDC53 (Cul1) components of the SCF are active during G1 phase, which would be the phase just before pre-meiotic S phase entry. In addition both SCF components are up-regulated early in prophase I (Chu S 1998), which would also fit the requirement for the observed *mnd2-(S/T-A)* phenotype.

APPENDIX

Matthew P. Torres
Department of Biochemistry and Biophysics
University of North Carolina at Chapel Hill
Chapel Hill, NC 27599-7260
Phone: (919) 843-4136
Fax: (919) 966-2852

February 20, 2007

American Chemical Society
PO Box 3337, Columbus, OH, 43210, USA

Attn: Permissions

I am completing a doctoral dissertation at the University of North Carolina at Chapel Hill entitled: "Regulation of the Anaphase-promoting Complex by Phosphorylation". I would like your permission to reprint as a chapter in my dissertation the following:

"Phosphatase-directed Phosphorylation-site Determination: A Synthesis of Methods for the Detection and Identification of Phosphopeptides" by Matthew Torres, Roopa Thapar, William Marzluff, and Christoph Borchers, *Journal of Proteome Research*, 2005 Sept.-Oct.; 4(5):1628-35.

The requested permission extends to any future revisions and editions of my dissertation, including non-exclusive world rights in all languages, and to the prospective publication of my dissertation by University Microfilms, Inc. These rights will in no way restrict republication of the material in any other form by you or by others authorized by you.

If these arrangements meet with your approval, please sign this letter where indicated below and Fax to me at the above-listed Fax number. Thank you very much.

Sincerely,

Matthew P. Torres

REFERENCES

Aebersold, R., and Mann, M. (2003). Mass spectrometry-based proteomics. Nature *422*, 198-207.

Agarwal, R., and Cohen-Fix, O. (2002). Phosphorylation of the mitotic regulator Pds1/securin by Cdc28 is required for efficient nuclear localization of Esp1/separase. Genes Dev *16*, 1371-1382.

Amon, A., Irniger, S., and Nasmyth, K. (1994). Closing the cell cycle circle in yeast: G2 cyclin proteolysis initiated at mitosis persists until the activation of G1 cyclins in the next cycle. Cell *77*, 1037-1050.

Amon, A., Tyers, M., Futcher, B., and Nasmyth, K. (1993). Mechanisms that help the yeast cell cycle clock tick: G2 cyclins transcriptionally activate G2 cyclins and repress G1 cyclins. Cell *74*, 993-1007.

Andersson, L., and Porath, J. (1986). Isolation of phosphoproteins by immobilized metal (Fe3+) affinity chromatography. Anal Biochem *154*, 250-254.

Annesley, T. M. (2003). Ion suppression in mass spectrometry. Clin Chem *49*, 1041-1044.

Bardin, A. J., Boselli, M. G., and Amon, A. (2003). Mitotic exit regulation through distinct domains within the protein kinase Cdc15. Mol Cell Biol *23*, 5018-5030.

Bashir, T., and Pagano, M. (2003). Aberrant ubiquitin-mediated proteolysis of cell cycle regulatory proteins and oncogenesis. Adv Cancer Res *88*, 101-144.

Baudat, F., Manova, K., Yuen, J. P., Jasin, M., and Keeney, S. (2000). Chromosome synapsis defects and sexually dimorphic meiotic progression in mice lacking Spo11. Mol Cell *6*, 989-998.

Baumeister, W., Walz, J., Zuhl, F., and Seemuller, E. (1998). The proteasome: paradigm of a self-compartmentalizing protease. Cell *92*, 367-380.

Beal, R., Deveraux, Q., Xia, G., Rechsteiner, M., and Pickart, C. (1996). Surface hydrophobic residues of multiubiquitin chains essential for proteolytic targeting. Proc Natl Acad Sci U S A *93*, 861-866.

Biemann, K., and Scoble, H. A. (1987). Characterization by tandem mass spectrometry of structural modifications in proteins. Science *237*, 992-998.

Blagoev, B., Kratchmarova, I., Ong, S. E., Nielsen, M., Foster, L. J., and Mann, M. (2003). A proteomics strategy to elucidate functional protein-protein interactions applied to EGF signaling. Nat Biotechnol *21*, 315-318.

Blanco, M. A., Pelloquin, L., and Moreno, S. (2001). Fission yeast mfr1 activates APC and coordinates meiotic nuclear division with sporulation. J Cell Sci *114*, 2135-2143.

Blanco, M. A., Sanchez-Diaz, A., de Prada, J. M., and Moreno, S. (2000). APC(ste9/srw1) promotes degradation of mitotic cyclins in G(1) and is inhibited by cdc2 phosphorylation. Embo J *19*, 3945-3955.

Bligh, S. W., Haley, T., and Lowe, P. N. (2003). Measurement of dissociation constants of inhibitors binding to Src SH2 domain protein by non-covalent electrospray ionization mass spectrometry. J Mol Recognit *16*, 139-148.

Bodnar, W. M., Blackburn, R. K., Krise, J. M., and Moseley, M. A. (2003). Exploiting the complementary nature of LC/MALDI/MS/MS and LC/ESI/MS/MS for increased proteome coverage. J Am Soc Mass Spectrom *14*, 971-979.

Bogdanov, B., and Smith, R. D. (2005). Proteomics by FTICR mass spectrometry: top down and bottom up. Mass Spectrom Rev *24*, 168-200.

Bolte, M., Steigemann, P., Braus, G. H., and Irniger, S. (2002). Inhibition of APC-mediated proteolysis by the meiosis-specific protein kinase Ime2. Proc Natl Acad Sci U S A *99*, 4385-4390.

Bonenfant, D., Schmelzle, T., Jacinto, E., Crespo, J. L., Mini, T., Hall, M. N., and Jenoe, P. (2003). Quantitation of changes in protein phosphorylation: a simple method based on stable isotope labeling and mass spectrometry. Proc Natl Acad Sci U S A *100*, 880-885.

Borchers, C. H., Marquez, V. E., Schroeder, G. K., Short, S. A., Snider, M. J., Speir, J. P., and Wolfenden, R. (2004). Fourier transform ion cyclotron resonance MS reveals the presence of a water molecule in an enzyme transition-state analogue complex. Proc Natl Acad Sci U S A *101*, 15341-15345.

Borchers, C. H., Thapar, R., Petrotchenko, E. V., Torres, M. P., Speir, J. P., Easterling, M., Dominski, Z., and Marzluff, W. F. (2006). Combined top-down and bottom-up proteomics identifies a phosphorylation site in stem-loop-binding proteins that contributes to high-affinity RNA binding. Proc Natl Acad Sci U S A *103*, 3094-3099.

Borden, K. L. (2000). RING domains: master builders of molecular scaffolds? J Mol Biol *295*, 1103-1112.

Borden, K. L., and Freemont, P. S. (1996). The RING finger domain: a recent example of a sequence-structure family. Curr Opin Struct Biol *6*, 395-401.

Bornsen, K. O. (2000). Influence of salts, buffers, detergents, solvents, and matrices on MALDI-MS protein analysis in complex mixtures. Methods Mol Biol *146*, 387-404.

Brancia, F. L. (2006). Recent developments in ion-trap mass spectrometry and related technologies. Expert Rev Proteomics *3*, 143-151.

Burbee, D. G., Forgacs, E., Zochbauer-Muller, S., Shivakumar, L., Fong, K., Gao, B., Randle, D., Kondo, M., Virmani, A., Bader, S.*, et al.* (2001). Epigenetic inactivation of RASSF1A in lung and breast cancers and malignant phenotype suppression. J Natl Cancer Inst *93*, 691-699.

Burton, J. L., and Solomon, M. J. (2001). D box and KEN box motifs in budding yeast Hsl1p are required for APC-mediated degradation and direct binding to Cdc20p and Cdh1p. Genes Dev *15*, 2381-2395.

Burton, J. L., Tsakraklides, V., and Solomon, M. J. (2005). Assembly of an APC-Cdh1-substrate complex is stimulated by engagement of a destruction box. Mol Cell *18*, 533-542.

Byrdwell, W. C. (2001). Atmospheric pressure chemical ionization mass spectrometry for analysis of lipids. Lipids *36*, 327-346.

Carroll, C. W., and Morgan, D. O. (2002). The Doc1 subunit is a processivity factor for the anaphase-promoting complex. Nat Cell Biol *4*, 880-887.

Castro, A., Arlot-Bonnemains, Y., Vigneron, S., Labbe, J. C., Prigent, C., and Lorca, T. (2002a). APC/Fizzy-Related targets Aurora-A kinase for proteolysis. EMBO Rep *3*, 457-462.

Castro, A., Bernis, C., Vigneron, S., Labbe, J. C., and Lorca, T. (2005). The anaphase-promoting complex: a key factor in the regulation of cell cycle. Oncogene *24*, 314-325.

Castro, A., Vigneron, S., Bernis, C., Labbe, J. C., Prigent, C., and Lorca, T. (2002b). The D-Box-activating domain (DAD) is a new proteolysis signal that stimulates the silent D-Box sequence of Aurora-A. EMBO Rep *3*, 1209-1214.

Chait, B. T. (2006). Chemistry. Mass spectrometry: bottom-up or top-down? Science *314*, 65-66.

Chalmers, M. J., Mackay, C. L., Hendrickson, C. L., Wittke, S., Walden, M., Mischak, H., Fliser, D., Just, I., and Marshall, A. G. (2005). Combined top-down and bottom-up mass spectrometric approach to characterization of biomarkers for renal disease. Anal Chem *77*, 7163-7171.

Chang, E. J., Archambault, V., McLachlin, D. T., Krutchinsky, A. N., and Chait, B. T. (2004). Analysis of protein phosphorylation by hypothesis-driven multiple-stage mass spectrometry. Anal Chem *76*, 4472-4483.

Chau, V., Tobias, J. W., Bachmair, A., Marriott, D., Ecker, D. J., Gonda, D. K., and Varshavsky, A. (1989). A multiubiquitin chain is confined to specific lysine in a targeted short-lived protein. Science *243*, 1576-1583.

Chen, M., and Stracher, A. (1989). In situ phosphorylation of platelet actin-binding protein by cAMP-dependent protein kinase stabilizes it against proteolysis by calpain. J Biol Chem *264*, 14282-14289.

Ciosk, R., Zachariae, W., Michaelis, C., Shevchenko, A., Mann, M., and Nasmyth, K. (1998). An ESP1/PDS1 complex regulates loss of sister chromatid cohesion at the metaphase to anaphase transition in yeast. Cell *93*, 1067-1076.

Clancy, M. J. (1998). Meiosis: step-by-step through sporulation. Curr Biol *8*, R461-463.

Cohen-Fix, O., and Koshland, D. (1997). The anaphase inhibitor of Saccharomyces cerevisiae Pds1p is a target of the DNA damage checkpoint pathway. Proc Natl Acad Sci U S A *94*, 14361-14366.

Cohen-Fix, O., Peters, J. M., Kirschner, M. W., and Koshland, D. (1996). Anaphase initiation in Saccharomyces cerevisiae is controlled by the APC-dependent degradation of the anaphase inhibitor Pds1p. Genes Dev *10*, 3081-3093.

Cooper, K. F., Mallory, M. J., Egeland, D. B., Jarnik, M., and Strich, R. (2000). Ama1p is a meiosis-specific regulator of the anaphase promoting complex/cyclosome in yeast. Proc Natl Acad Sci U S A *97*, 14548-14553.

Craig, A. G., Hoeger, C. A., Miller, C. L., Goedken, T., Rivier, J. E., and Fischer, W. H. (1994). Monitoring protein kinase and phosphatase reactions with matrix-assisted laser desorption/ionization mass spectrometry and capillary zone electrophoresis: comparison of the detection efficiency of peptide-phosphopeptide mixtures. Biol Mass Spectrom *23*, 519-528.

Dammann, R., Li, C., Yoon, J. H., Chin, P. L., Bates, S., and Pfeifer, G. P. (2000). Epigenetic inactivation of a RAS association domain family protein from the lung tumour suppressor locus 3p21.3. Nat Genet *25*, 315-319.

Das, A. K., Cohen, P. W., and Barford, D. (1998). The structure of the tetratricopeptide repeats of protein phosphatase 5: implications for TPR-mediated protein-protein interactions. Embo J *17*, 1192-1199.

Dirick, L., Bohm, T., and Nasmyth, K. (1995). Roles and regulation of Cln-Cdc28 kinases at the start of the cell cycle of Saccharomyces cerevisiae. Embo J *14*, 4803-4813.

Dominski, Z., Yang, X. C., Raska, C. S., Santiago, C., Borchers, C. H., Duronio, R. J., and Marzluff, W. F. (2002). 3' end processing of Drosophila melanogaster histone pre-mRNAs: requirement for phosphorylated Drosophila stem-loop binding protein and coevolution of the histone pre-mRNA processing system. Mol Cell Biol *22*, 6648-6660.

Dreijerink, K., Braga, E., Kuzmin, I., Geil, L., Duh, F. M., Angeloni, D., Zbar, B., Lerman, M. I., Stanbridge, E. J., Minna, J. D*., et al.* (2001). The candidate tumor suppressor gene, RASSF1A, from human chromosome 3p21.3 is involved in kidney tumorigenesis. Proc Natl Acad Sci U S A *98*, 7504-7509.

Dreisewerd, K. (2003). The desorption process in MALDI. Chem Rev *103*, 395-426.

Dube, P., Herzog, F., Gieffers, C., Sander, B., Riedel, D., Muller, S. A., Engel, A., Peters, J. M., and Stark, H. (2005). Localization of the coactivator Cdh1 and the cullin subunit Apc2 in a cryo-electron microscopy model of vertebrate APC/C. Mol Cell *20*, 867-879.

Eckerdt, F., Yuan, J., Saxena, K., Martin, B., Kappel, S., Lindenau, C., Kramer, A., Naumann, S., Daum, S., Fischer, G., *et al.* (2005). Polo-like kinase 1-mediated phosphorylation stabilizes Pin1 by inhibiting its ubiquitination in human cells. J Biol Chem *280*, 36575-36583.

Edwards, E., and thomas-Oates, J. (2005). Hyphenating liquid phase separation techniques with mass spectrometry: on-line or off-line. Analyst *130*, 13-17.

Evans, T., Rosenthal, E. T., Youngblom, J., Distel, D., and Hunt, T. (1983). Cyclin: a protein specified by maternal mRNA in sea urchin eggs that is destroyed at each cleavage division. Cell *33*, 389-396.

Eytan, E., Moshe, Y., Braunstein, I., and Hershko, A. (2006). Roles of the anaphase-promoting complex/cyclosome and of its activator Cdc20 in functional substrate binding. Proc Natl Acad Sci U S A *103*, 2081-2086.

Fang, G. (2002). Checkpoint protein BubR1 acts synergistically with Mad2 to inhibit anaphase-promoting complex. Mol Biol Cell *13*, 755-766.

Fang, G., Yu, H., and Kirschner, M. W. (1998a). The checkpoint protein MAD2 and the mitotic regulator CDC20 form a ternary complex with the anaphase-promoting complex to control anaphase initiation. Genes Dev *12*, 1871-1883.

Fang, G., Yu, H., and Kirschner, M. W. (1998b). Direct binding of CDC20 protein family members activates the anaphase-promoting complex in mitosis and G1. Mol Cell *2*, 163-171.

Feldman, R. M., Correll, C. C., Kaplan, K. B., and Deshaies, R. J. (1997). A complex of Cdc4p, Skp1p, and Cdc53p/cullin catalyzes ubiquitination of the phosphorylated CDK inhibitor Sic1p. Cell *91*, 221-230.

Felix, M. A., Labbe, J. C., Doree, M., Hunt, T., and Karsenti, E. (1990). Triggering of cyclin degradation in interphase extracts of amphibian eggs by cdc2 kinase. Nature *346*, 379-382.

Fenn, J. B., Mann, M., Meng, C. K., Wong, S. F., and Whitehouse, C. M. (1989). Electrospray ionization for mass spectrometry of large biomolecules. Science *246*, 64-71.

Ficarro, S. B., McCleland, M. L., Stukenberg, P. T., Burke, D. J., Ross, M. M., Shabanowitz, J., Hunt, D. F., and White, F. M. (2002). Phosphoproteome analysis by mass spectrometry and its application to Saccharomyces cerevisiae. Nat Biotechnol *20*, 301-305.

Garcia, M. C. (2005). The effect of the mobile phase additives on sensitivity in the analysis of peptides and proteins by high-performance liquid chromatography-electrospray mass spectrometry. J Chromatogr B Analyt Technol Biomed Life Sci *825*, 111-123.

Garcia, M. C., Hogenboom, A. C., Zappey, H., and Irth, H. (2002). Effect of the mobile phase composition on the separation and detection of intact proteins by reversed-phase liquid chromatography-electrospray mass spectrometry. J Chromatogr A *957*, 187-199.

Gavin, A. C., and Superti-Furga, G. (2003). Protein complexes and proteome organization from yeast to man. Curr Opin Chem Biol *7*, 21-27.

Gelbart, M. E., Rechsteiner, T., Richmond, T. J., and Tsukiyama, T. (2001). Interactions of Isw2 chromatin remodeling complex with nucleosomal arrays: analyses using recombinant yeast histones and immobilized templates. Mol Cell Biol *21*, 2098-2106.

Ghislain, M., Udvardy, A., and Mann, C. (1993). S. cerevisiae 26S protease mutants arrest cell division in G2/metaphase. Nature *366*, 358-362.

Glotzer, M., Murray, A. W., and Kirschner, M. W. (1991). Cyclin is degraded by the ubiquitin pathway. Nature *349*, 132-138.

Glover, D. M., Hagan, I. M., and Tavares, A. A. (1998). Polo-like kinases: a team that plays throughout mitosis. Genes Dev *12*, 3777-3787.

Gmachl, M., Gieffers, C., Podtelejnikov, A. V., Mann, M., and Peters, J. M. (2000). The RING-H2 finger protein APC11 and the E2 enzyme UBC4 are sufficient to ubiquitinate substrates of the anaphase-promoting complex. Proc Natl Acad Sci U S A *97*, 8973-8978.

Golan, A., Yudkovsky, Y., and Hershko, A. (2002). The cyclin-ubiquitin ligase activity of cyclosome/APC is jointly activated by protein kinases Cdk1-cyclin B and Plk. J Biol Chem *277*, 15552-15557.

Gonnet, F., Lemaitre, G., Waksman, G., and Tortajada, J. (2003). MALDI/MS peptide mass fingerprinting for proteome analysis: identification of hydrophobic proteins attached to eucaryote keratinocyte cytoplasmic membrane using different matrices in concert. Proteome Sci *1*, 2.

Greenberg, R., Groves, M. L., and Dower, H. J. (1984). Human beta-casein. Amino acid sequence and identification of phosphorylation sites. J Biol Chem *259*, 5132-5138.

Gross, J. H. (2004). Mass spectrometry : a textbook (Berlin ; London, Springer).

Grossberger, R., Gieffers, C., Zachariae, W., Podtelejnikov, A. V., Schleiffer, A., Nasmyth, K., Mann, M., and Peters, J. M. (1999). Characterization of the DOC1/APC10 subunit of the yeast and the human anaphase-promoting complex. J Biol Chem *274*, 14500-14507.

Gruhler, A., Olsen, J. V., Mohammed, S., Mortensen, P., Faergeman, N. J., Mann, M., and Jensen, O. N. (2005). Quantitative phosphoproteomics applied to the yeast pheromone signaling pathway. Mol Cell Proteomics *4*, 310-327.

Guardavaccaro, D., Kudo, Y., Boulaire, J., Barchi, M., Busino, L., Donzelli, M., Margottin-Goguet, F., Jackson, P. K., Yamasaki, L., and Pagano, M. (2003). Control of meiotic and mitotic progression by the F box protein beta-Trcp1 in vivo. Dev Cell *4*, 799-812.

Gygi, S. P., Rist, B., Gerber, S. A., Turecek, F., Gelb, M. H., and Aebersold, R. (1999). Quantitative analysis of complex protein mixtures using isotope-coded affinity tags. Nat Biotechnol *17*, 994-999.

Haglund, K., Di Fiore, P. P., and Dikic, I. (2003). Distinct monoubiquitin signals in receptor endocytosis. Trends Biochem Sci *28*, 598-603.

Haigler, H. T., McKanna, J. A., and Cohen, S. (1979). Direct visualization of the binding and internalization of a ferritin conjugate of epidermal growth factor in human carcinoma cells A-431. J Cell Biol *81*, 382-395.

Hall, M. C., Torres, M. P., Schroeder, G. K., and Borchers, C. H. (2003). Mnd2 and Swm1 are core subunits of the Saccharomyces cerevisiae anaphase-promoting complex. J Biol Chem *278*, 16698-16705.

Hall, M. C., Warren, E. N., and Borchers, C. H. (2004). Multi-Kinase Phosphorylation of the APC/C Activator Cdh1 Revealed by Mass Spectrometry. Cell Cycle *3*.

Han, D. K., Eng, J., Zhou, H., and Aebersold, R. (2001). Quantitative profiling of differentiation-induced microsomal proteins using isotope-coded affinity tags and mass spectrometry. Nat Biotechnol *19*, 946-951.

Harper, J. W., Burton, J. L., and Solomon, M. J. (2002). The anaphase-promoting complex: it's not just for mitosis any more. Genes Dev *16*, 2179-2206.

Henry, K. D., Williams, E. R., Wang, B. H., McLafferty, F. W., Shabanowitz, J., and Hunt, D. F. (1989). Fourier-transform mass spectrometry of large molecules by electrospray ionization. Proc Natl Acad Sci U S A *86*, 9075-9078.

Herlihy, W. C., Royal, N. J., Biemann, K., Putney, S. D., and Schimmel, P. R. (1980). Mass spectra of partial protein hydrolysates as a multiple phase check for long polypeptides deduced from DNA sequences: NH2-terminal segment of alanine tRNA synthetase. Proc Natl Acad Sci U S A *77*, 6531-6535.

Hershko, A. (2005). The ubiquitin system for protein degradation and some of its roles in the control of the cell division cycle. Cell Death Differ *12*, 1191-1197.

Hershko, A., Ganoth, D., Sudakin, V., Dahan, A., Cohen, L. H., Luca, F. C., Ruderman, J. V., and Eytan, E. (1994). Components of a system that ligates cyclin to ubiquitin and their regulation by the protein kinase cdc2. J Biol Chem *269*, 4940-4946.

Hicke, L. (2001a). A new ticket for entry into budding vesicles-ubiquitin. Cell *106*, 527-530.

Hicke, L. (2001b). Protein regulation by monoubiquitin. Nat Rev Mol Cell Biol *2*, 195-201.

Hilioti, Z., Chung, Y. S., Mochizuki, Y., Hardy, C. F., and Cohen-Fix, O. (2001). The anaphase inhibitor Pds1 binds to the APC/C-associated protein Cdc20 in a destruction box-dependent manner. Curr Biol *11*, 1347-1352.

Hillenkamp, F., and Karas, M. (1990). Mass spectrometry of peptides and proteins by matrix-assisted ultraviolet laser desorption/ionization. Methods Enzymol *193*, 280-295.

Hino, S., Tanji, C., Nakayama, K. I., and Kikuchi, A. (2005). Phosphorylation of beta-catenin by cyclic AMP-dependent protein kinase stabilizes beta-catenin through inhibition of its ubiquitination. Mol Cell Biol *25*, 9063-9072.

Hirschberg, D., Jagerbrink, T., Samskog, J., Gustafsson, M., Stahlberg, M., Alvelius, G., Husman, B., Carlquist, M., Jornvall, H., and Bergman, T. (2004). Detection of phosphorylated peptides in proteomic analyses using microfluidic compact disk technology. Anal Chem *76*, 5864-5871.

Ho, Y., Gruhler, A., Heilbut, A., Bader, G. D., Moore, L., Adams, S. L., Millar, A., Taylor, P., Bennett, K., Boutilier, K.*, et al.* (2002). Systematic identification of protein complexes in Saccharomyces cerevisiae by mass spectrometry. Nature *415*, 180-183.

Hochstrasser, M. (1996). Ubiquitin-dependent protein degradation. Annu Rev Genet *30*, 405-439.

Hollfelder, F., and Herschlag, D. (1995). The nature of the transition state for enzyme-catalyzed phosphoryl transfer. Hydrolysis of O-aryl phosphorothioates by alkaline phosphatase. Biochemistry *34*, 12255-12264.

Holliday, R. (1964). The Induction of Mitotic Recombination by Mitomycin C in Ustilago and Saccharomyces. Genetics *50*, 323-335.

Hu, Q., Noll, R. J., Li, H., Makarov, A., Hardman, M., and Graham Cooks, R. (2005). The Orbitrap: a new mass spectrometer. J Mass Spectrom *40*, 430-443.

Huibregtse, J. M., Scheffner, M., Beaudenon, S., and Howley, P. M. (1995). A family of proteins structurally and functionally related to the E6-AP ubiquitin-protein ligase. Proc Natl Acad Sci U S A *92*, 2563-2567.

Huibregtse, J. M., Scheffner, M., and Howley, P. M. (1993). Localization of the E6-AP regions that direct human papillomavirus E6 binding, association with p53, and ubiquitination of associated proteins. Mol Cell Biol *13*, 4918-4927.

Huibregtse, J. M., Yang, J. C., and Beaudenon, S. L. (1997). The large subunit of RNA polymerase II is a substrate of the Rsp5 ubiquitin-protein ligase. Proc Natl Acad Sci U S A *94*, 3656-3661.

Hunt, D. F., Buko, A. M., Ballard, J. M., Shabanowitz, J., and Giordani, A. B. (1981). Sequence analysis of polypeptides by collision activated dissociation on a triple quadrupole mass spectrometer. Biomed Mass Spectrom *8*, 397-408.

Hunt, D. F., Yates, J. R., 3rd, Shabanowitz, J., Winston, S., and Hauer, C. R. (1986). Protein sequencing by tandem mass spectrometry. Proc Natl Acad Sci U S A *83*, 6233-6237.

Hurley, J. H., and Emr, S. D. (2006). The ESCRT complexes: structure and mechanism of a membrane-trafficking network. Annu Rev Biophys Biomol Struct *35*, 277-298.

Hwang, L. H., and Murray, A. W. (1997). A novel yeast screen for mitotic arrest mutants identifies DOC1, a new gene involved in cyclin proteolysis. Mol Biol Cell *8*, 1877-1887.

Ibarrola, N., Kalume, D. E., Gronborg, M., Iwahori, A., and Pandey, A. (2003). A proteomic approach for quantitation of phosphorylation using stable isotope labeling in cell culture. Anal Chem *75*, 6043-6049.

Irniger, S., and Nasmyth, K. (1997). The anaphase-promoting complex is required in G1 arrested yeast cells to inhibit B-type cyclin accumulation and to prevent uncontrolled entry into S-phase. J Cell Sci *110 (Pt 13)*, 1523-1531.

Janek, K., Wenschuh, H., Bienert, M., and Krause, E. (2001). Phosphopeptide analysis by positive and negative ion matrix-assisted laser desorption/ionization mass spectrometry. Rapid Commun Mass Spectrom *15*, 1593-1599.

Jaspersen, S. L., Charles, J. F., and Morgan, D. O. (1999). Inhibitory phosphorylation of the APC regulator Hct1 is controlled by the kinase Cdc28 and the phosphatase Cdc14. Curr Biol *9*, 227-236.

Jaspersen, S. L., Charles, J. F., Tinker-Kulberg, R. L., and Morgan, D. O. (1998). A late mitotic regulatory network controlling cyclin destruction in Saccharomyces cerevisiae. Mol Biol Cell *9*, 2803-2817.

Jaspersen, S. L., and Morgan, D. O. (2000). Cdc14 activates cdc15 to promote mitotic exit in budding yeast. Curr Biol *10*, 615-618.

Johnson, R. S., Martin, S. A., Biemann, K., Stults, J. T., and Watson, J. T. (1987). Novel fragmentation process of peptides by collision-induced decomposition in a tandem mass spectrometer: differentiation of leucine and isoleucine. Anal Chem *59*, 2621-2625.

Jonscher, K. R., and Yates, J. R., 3rd (1997). The quadrupole ion trap mass spectrometer--a small solution to a big challenge. Anal Biochem *244*, 1-15.

Karas, M., and Hillenkamp, F. (1988). Laser desorption ionization of proteins with molecular masses exceeding 10,000 daltons. Anal Chem *60*, 2299-2301.

Katis, V. L., Galova, M., Rabitsch, K. P., Gregan, J., and Nasmyth, K. (2004). Maintenance of cohesin at centromeres after meiosis I in budding yeast requires a kinetochore-associated protein related to MEI-S332. Curr Biol *14*, 560-572.

Katzmann, D. J., Odorizzi, G., and Emr, S. D. (2002). Receptor downregulation and multivesicular-body sorting. Nat Rev Mol Cell Biol *3*, 893-905.

Katzmann, D. J., and Wendland, B. (2005). Analysis of Ubiquitin-Dependent Protein Sorting Within the Endocytic Pathway in Saccharomyces cerevisiae. Methods Enzymol *399*, 192-211.

Kim, E. E., and Wyckoff, H. W. (1991). Reaction mechanism of alkaline phosphatase based on crystal structures. Two-metal ion catalysis. J Mol Biol *218*, 449-464.

King, R. W., Deshaies, R. J., Peters, J. M., and Kirschner, M. W. (1996). How proteolysis drives the cell cycle. Science *274*, 1652-1659.

King, R. W., Peters, J. M., Tugendreich, S., Rolfe, M., Hieter, P., and Kirschner, M. W. (1995). A 20S complex containing CDC27 and CDC16 catalyzes the mitosis-specific conjugation of ubiquitin to cyclin B. Cell *81*, 279-288.

Kitajima, T. S., Kawashima, S. A., and Watanabe, Y. (2004). The conserved kinetochore protein shugoshin protects centromeric cohesion during meiosis. Nature *427*, 510-517.

Kitajima, T. S., Miyazaki, Y., Yamamoto, M., and Watanabe, Y. (2003). Rec8 cleavage by separase is required for meiotic nuclear divisions in fission yeast. Embo J *22*, 5643-5653.

Klein, F., Mahr, P., Galova, M., Buonomo, S. B., Michaelis, C., Nairz, K., and Nasmyth, K. (1999). A central role for cohesins in sister chromatid cohesion, formation of axial elements, and recombination during yeast meiosis. Cell *98*, 91-103.

Konishi, Y., and Tominaga, A. (2006). PU.1 is degraded in differentiation of erythrocytes through a proteasome-dependent pathway. DNA Cell Biol *25*, 340-345.

Kotani, S., Tanaka, H., Yasuda, H., and Todokoro, K. (1999). Regulation of APC activity by phosphorylation and regulatory factors. J Cell Biol *146*, 791-800.

Kotani, S., Tugendreich, S., Fujii, M., Jorgensen, P. M., Watanabe, N., Hoog, C., Hieter, P., and Todokoro, K. (1998). PKA and MPF-activated polo-like kinase regulate anaphase-promoting complex activity and mitosis progression. Mol Cell *1*, 371-380.

Kraft, C., Herzog, F., Gieffers, C., Mechtler, K., Hagting, A., Pines, J., and Peters, J. M. (2003). Mitotic regulation of the human anaphase-promoting complex by phosphorylation. Embo J *22*, 6598-6609.

Kraft, C., Vodermaier, H. C., Maurer-Stroh, S., Eisenhaber, F., and Peters, J. M. (2005). The WD40 propeller domain of Cdh1 functions as a destruction box receptor for APC/C substrates. Mol Cell *18*, 543-553.

Kramer, E. R., Scheuringer, N., Podtelejnikov, A. V., Mann, M., and Peters, J. M. (2000). Mitotic regulation of the APC activator proteins CDC20 and CDH1. Mol Biol Cell *11*, 1555-1569.

Kratzer, R., Eckerskorn, C., Karas, M., and Lottspeich, F. (1998). Suppression effects in enzymatic peptide ladder sequencing using ultraviolet - matrix assisted laser desorption/ionization - mass spectormetry. Electrophoresis *19*, 1910-1919.

Kudo, N. R., Wassmann, K., Anger, M., Schuh, M., Wirth, K. G., Xu, H., Helmhart, W., Kudo, H., McKay, M., Maro, B.*, et al.* (2006). Resolution of chiasmata in oocytes requires separase-mediated proteolysis. Cell *126*, 135-146.

Kuntzel, H., Schulz, A., and Ehbrecht, I. M. (1996). Cell cycle control and initiation of DNA replication in Saccharomyces cerevisiae. Biol Chem *377*, 481-487.

Lahav-Baratz, S., Sudakin, V., Ruderman, J. V., and Hershko, A. (1995). Reversible phosphorylation controls the activity of cyclosome-associated cyclin-ubiquitin ligase. Proc Natl Acad Sci U S A *92*, 9303-9307.

Laugesen, S., and Roepstorff, P. (2003). Combination of two matrices results in improved performance of MALDI MS for peptide mass mapping and protein analysis. J Am Soc Mass Spectrom *14*, 992-1002.

Leverson, J. D., Joazeiro, C. A., Page, A. M., Huang, H., Hieter, P., and Hunter, T. (2000). The APC11 RING-H2 finger mediates E2-dependent ubiquitination. Mol Biol Cell *11*, 2315-2325.

Link, A. J., Eng, J., Schieltz, D. M., Carmack, E., Mize, G. J., Morris, D. R., Garvik, B. M., and Yates, J. R., 3rd (1999). Direct analysis of protein complexes using mass spectrometry. Nat Biotechnol *17*, 676-682.

Litersky, J. M., and Johnson, G. V. (1992). Phosphorylation by cAMP-dependent protein kinase inhibits the degradation of tau by calpain. J Biol Chem *267*, 1563-1568.

Littlepage, L. E., and Ruderman, J. V. (2002). Identification of a new APC/C recognition domain, the A box, which is required for the Cdh1-dependent destruction of the kinase Aurora-A during mitotic exit. Genes Dev *16*, 2274-2285.

Liu, B., Liang, M. H., Kuo, Y. L., Liao, W., Boros, I., Kleinberger, T., Blancato, J., and Giam, C. Z. (2003). Human T-lymphotropic virus type 1 oncoprotein tax promotes unscheduled degradation of Pds1p/securin and Clb2p/cyclin B1 and causes chromosomal instability. Mol Cell Biol *23*, 5269-5281.

Liu, J., Furukawa, M., Matsumoto, T., and Xiong, Y. (2002). NEDD8 modification of CUL1 dissociates p120(CAND1), an inhibitor of CUL1-SKP1 binding and SCF ligases. Mol Cell *10*, 1511-1518.

Loo, J. A., Berhane, B., Kaddis, C. S., Wooding, K. M., Xie, Y., Kaufman, S. L., and Chernushevich, I. V. (2005). Electrospray ionization mass spectrometry and ion mobility analysis of the 20S proteasome complex. J Am Soc Mass Spectrom *16*, 998-1008.

Loo, J. A., Edmonds, C. G., and Smith, R. D. (1990). Primary sequence information from intact proteins by electrospray ionization tandem mass spectrometry. Science *248*, 201-204.

Loo, J. A., Quinn, J. P., Ryu, S. I., Henry, K. D., Senko, M. W., and McLafferty, F. W. (1992). High-resolution tandem mass spectrometry of large biomolecules. Proc Natl Acad Sci U S A *89*, 286-289.

Loughrey Chen, S., Huddleston, M. J., Shou, W., Deshaies, R. J., Annan, R. S., and Carr, S. A. (2002). Mass spectrometry-based methods for phosphorylation site mapping of hyperphosphorylated proteins applied to Net1, a regulator of exit from mitosis in yeast. Mol Cell Proteomics *1*, 186-196.

Lucero, P., Penalver, E., Vela, L., and Lagunas, R. (2000). Monoubiquitination is sufficient to signal internalization of the maltose transporter in Saccharomyces cerevisiae. J Bacteriol *182*, 241-243.

Lupas, A., Baumeister, W., and Hofmann, K. (1997). A repetitive sequence in subunits of the 26S proteasome and 20S cyclosome (anaphase-promoting complex). Trends Biochem Sci *22*, 195-196.

Maniatis, T. (1999). A ubiquitin ligase complex essential for the NF-kappaB, Wnt/Wingless, and Hedgehog signaling pathways. Genes Dev *13*, 505-510.

Mann, M., Ong, S. E., Gronborg, M., Steen, H., Jensen, O. N., and Pandey, A. (2002). Analysis of protein phosphorylation using mass spectrometry: deciphering the phosphoproteome. Trends Biotechnol *20*, 261-268.

March, R. E., Hughes, R. J., and Todd, J. F. J. (1989). Quadrupole storage mass spectrometry (New York, Wiley).

Marshall, A. G., Hendrickson, C. L., and Jackson, G. S. (1998). Fourier transform ion cyclotron resonance mass spectrometry: a primer. Mass Spectrom Rev *17*, 1-35.

Marston, A. L., Tham, W. H., Shah, H., and Amon, A. (2004). A genome-wide screen identifies genes required for centromeric cohesion. Science *303*, 1367-1370.

McDonald, C. M., Cooper, K. F., and Winter, E. (2005). The Ama1-directed anaphase-promoting complex regulates the Smk1 mitogen-activated protein kinase during meiosis in yeast. Genetics *171*, 901-911.

McDonald, E. R., 3rd, and El-Deiry, W. S. (2001). Checkpoint genes in cancer. Ann Med *33*, 113-122.

McGrew, J. T., Goetsch, L., Byers, B., and Baum, P. (1992). Requirement for ESP1 in the nuclear division of Saccharomyces cerevisiae. Mol Biol Cell *3*, 1443-1454.

McLafferty, F. W. (1981a). Tandem mass spectrometry. Science *214*, 280-287.

McLafferty, F. W. (1981b). Tandem mass spectrometry in trace toxicant analysis. Biomed Mass Spectrom *8*, 446-448.

McLuckey, S. A., Van Berkel, G. J., Goeringer, D. E., and Glish, G. L. (1994). Ion trap mass spectrometry. Using high-pressure ionization. Anal Chem *66*, 737A-743A.

Mendenhall, M. D. (1993). An inhibitor of p34CDC28 protein kinase activity from Saccharomyces cerevisiae. Science *259*, 216-219.

Mendenhall, M. D., al-Jumaily, W., and Nugroho, T. T. (1995). The Cdc28 inhibitor p40SIC1. Prog Cell Cycle Res *1*, 173-185.

Mendenhall, M. D., Jones, C. A., and Reed, S. I. (1987). Dual regulation of the yeast CDC28-p40 protein kinase complex: cell cycle, pheromone, and nutrient limitation effects. Cell *50*, 927-935.

Michalides, R. J., van de Brekel, M., and Balm, F. (2002). Defects in G1-S cell cycle control in head and neck cancer: a review. Head Neck *24*, 694-704.

Millea, K. M., Krull, I. S., Cohen, S. A., Gebler, J. C., and Berger, S. J. (2006). Integration of multidimensional chromatographic protein separations with a combined "top-down" and "bottom-up" proteomic strategy. J Proteome Res *5*, 135-146.

Morgan, D. O. (1999). Regulation of the APC and the exit from mitosis. Nat Cell Biol *1*, E47-53.

Murray, A. W. (1989). Cyclin synthesis and degradation and the embryonic cell cycle. J Cell Sci Suppl *12*, 65-76.

Murray, A. W. (2004). Recycling the cell cycle: cyclins revisited. Cell *116*, 221-234.

Murray, A. W., and Kirschner, M. W. (1989). Cyclin synthesis drives the early embryonic cell cycle. Nature *339*, 275-280.

Murray, A. W., Solomon, M. J., and Kirschner, M. W. (1989). The role of cyclin synthesis and degradation in the control of maturation promoting factor activity. Nature *339*, 280-286.

Musacchio, A., and Hardwick, K. G. (2002). The spindle checkpoint: structural insights into dynamic signalling. Nat Rev Mol Cell Biol *3*, 731-741.

Nau, H., and Riordan, J. F. (1975). Gas chromatography-mass spectrometry for probing the structure and mechanism of action of enzyme active sites. The role of Glu-270 in carboxypeptidase A. Biochemistry *14*, 5285-5294.

Nemeth-Cawley, J. F., Tangarone, B. S., and Rouse, J. C. (2003). "Top Down" characterization is a complementary technique to peptide sequencing for identifying protein species in complex mixtures. J Proteome Res *2*, 495-505.

Nousiainen, M., Sillje, H. H., Sauer, G., Nigg, E. A., and Korner, R. (2006). Phosphoproteome analysis of the human mitotic spindle. Proc Natl Acad Sci U S A *103*, 5391-5396.

O'Brien, P. J., and Herschlag, D. (1999). Catalytic promiscuity and the evolution of new enzymatic activities. Chem Biol *6*, R91-R105.

Oda, Y., Huang, K., Cross, F. R., Cowburn, D., and Chait, B. T. (1999). Accurate quantitation of protein expression and site-specific phosphorylation. Proc Natl Acad Sci U S A *96*, 6591-6596.

Oelschlaegel, T., Schwickart, M., Matos, J., Bogdanova, A., Camasses, A., Havlis, J., Shevchenko, A., and Zachariae, W. (2005). The yeast APC/C subunit Mnd2 prevents premature sister chromatid separation triggered by the meiosis-specific APC/C-Ama1. Cell *120*, 773-788.

Ohta, T., Michel, J. J., Schottelius, A. J., and Xiong, Y. (1999). ROC1, a homolog of APC11, represents a family of cullin partners with an associated ubiquitin ligase activity. Mol Cell *3*, 535-541.

Olsen, J. V., Blagoev, B., Gnad, F., Macek, B., Kumar, C., Mortensen, P., and Mann, M. (2006). Global, in vivo, and site-specific phosphorylation dynamics in signaling networks. Cell *127*, 635-648.

Olsen, J. V., Ong, S. E., and Mann, M. (2004). Trypsin cleaves exclusively C-terminal to arginine and lysine residues. Mol Cell Proteomics *3*, 608-614.

Ong, S. E., Foster, L. J., and Mann, M. (2003). Mass spectrometric-based approaches in quantitative proteomics. Methods *29*, 124-130.

Orlicky, S., Tang, X., Willems, A., Tyers, M., and Sicheri, F. (2003). Structural basis for phosphodependent substrate selection and orientation by the SCFCdc4 ubiquitin ligase. Cell *112*, 243-256.

Page, A. M., Aneliunas, V., Lamb, J. R., and Hieter, P. (2005). In vivo characterization of the nonessential budding yeast anaphase-promoting complex/cyclosome components Swm1p, Mnd2p and Apc9p. Genetics *170*, 1045-1062.

Page, A. M., and Hieter, P. (1999). The anaphase-promoting complex: new subunits and regulators. Annu Rev Biochem *68*, 583-609.

Passmore, L. A., Booth, C. R., Venien-Bryan, C., Ludtke, S. J., Fioretto, C., Johnson, L. N., Chiu, W., and Barford, D. (2005). Structural analysis of the anaphase-promoting complex reveals multiple active sites and insights into polyubiquitylation. Mol Cell *20*, 855-866.

Passmore, L. A., McCormack, E. A., Au, S. W., Paul, A., Willison, K. R., Harper, J. W., and Barford, D. (2003). Doc1 mediates the activity of the anaphase-promoting complex by contributing to substrate recognition. Embo J *22*, 786-796.

Patton, E. E., Willems, A. R., Sa, D., Kuras, L., Thomas, D., Craig, K. L., and Tyers, M. (1998). Cdc53 is a scaffold protein for multiple Cdc34/Skp1/F-box proteincomplexes that regulate cell division and methionine biosynthesis in yeast. Genes Dev *12*, 692-705.

Penkner, A. M., Prinz, S., Ferscha, S., and Klein, F. (2005). Mnd2, an essential antagonist of the anaphase-promoting complex during meiotic prophase. Cell *120*, 789-801.

Peters, J. M. (1998). SCF and APC: the Yin and Yang of cell cycle regulated proteolysis. Curr Opin Cell Biol *10*, 759-768.

Peters, J. M. (1999). Subunits and substrates of the anaphase-promoting complex. Exp Cell Res *248*, 339-349.

Peters, J. M. (2002). The anaphase-promoting complex: proteolysis in mitosis and beyond. Mol Cell *9*, 931-943.

Peters, J. M. (2003). Emi1 proteolysis: how SCF(beta-Trcp1) helps to activate the anaphase-promoting complex. Mol Cell *11*, 1420-1421.

Peters, J. M. (2006). The anaphase promoting complex/cyclosome: a machine designed to destroy. Nat Rev Mol Cell Biol *7*, 644-656.

Peters, J. M., King, R. W., Hoog, C., and Kirschner, M. W. (1996). Identification of BIME as a subunit of the anaphase-promoting complex. Science *274*, 1199-1201.

Petronczki, M., Siomos, M. F., and Nasmyth, K. (2003). Un menage a quatre: the molecular biology of chromosome segregation in meiosis. Cell *112*, 423-440.

Pfleger, C. M., and Kirschner, M. W. (2000). The KEN box: an APC recognition signal distinct from the D box targeted by Cdh1. Genes Dev *14*, 655-665.

Pfleger, C. M., Lee, E., and Kirschner, M. W. (2001). Substrate recognition by the Cdc20 and Cdh1 components of the anaphase-promoting complex. Genes Dev *15*, 2396-2407.

Phizicky, E., Bastiaens, P. I., Zhu, H., Snyder, M., and Fields, S. (2003). Protein analysis on a proteomic scale. Nature *422*, 208-215.

Pickart, C. M. (2001). Mechanisms underlying ubiquitination. Annu Rev Biochem *70*, 503-533.

Posewitz, M. C., and Tempst, P. (1999). Immobilized gallium(III) affinity chromatography of phosphopeptides. Anal Chem *71*, 2883-2892.

Pray, T. R., Parlati, F., Huang, J., Wong, B. R., Payan, D. G., Bennett, M. K., Issakani, S. D., Molineaux, S., and Demo, S. D. (2002). Cell cycle regulatory E3 ubiquitin ligases as anticancer targets. Drug Resist Updat *5*, 249-258.

Puig, O., Caspary, F., Rigaut, G., Rutz, B., Bouveret, E., Bragado-Nilsson, E., Wilm, M., and Seraphin, B. (2001). The tandem affinity purification (TAP) method: a general procedure of protein complex purification. Methods *24*, 218-229.

Rabitsch, K. P., Gregan, J., Schleiffer, A., Javerzat, J. P., Eisenhaber, F., and Nasmyth, K. (2004). Two fission yeast homologs of Drosophila Mei-S332 are required for chromosome segregation during meiosis I and II. Curr Biol *14*, 287-301.

Rabitsch, K. P., Toth, A., Galova, M., Schleiffer, A., Schaffner, G., Aigner, E., Rupp, C., Penkner, A. M., Moreno-Borchart, A. C., Primig, M.*, et al.* (2001). A screen for genes required for meiosis and spore formation based on whole-genome expression. Curr Biol *11*, 1001-1009.

Raffaelli, A., and Saba, A. (2003). Atmospheric pressure photoionization mass spectrometry. Mass Spectrom Rev *22*, 318-331.

Raiborg, C., Rusten, T. E., and Stenmark, H. (2003). Protein sorting into multivesicular endosomes. Curr Opin Cell Biol *15*, 446-455.

Ranish, J. A., Yi, E. C., Leslie, D. M., Purvine, S. O., Goodlett, D. R., Eng, J., and Aebersold, R. (2003). The study of macromolecular complexes by quantitative proteomics. Nat Genet *33*, 349-355.

Raska, C. S., Parker, C. E., Dominski, Z., Marzluff, W. F., Glish, G. L., Pope, R. M., and Borchers, C. H. (2002). Direct MALDI-MS/MS of phosphopeptides affinity-bound to immobilized metal ion affinity chromatography beads. Anal Chem *74*, 3429-3433.

Reed, S. I. (2003). Ratchets and clocks: the cell cycle, ubiquitylation and protein turnover. Nat Rev Mol Cell Biol *4*, 855-864.

Reggiori, F., and Pelham, H. R. (2002). A transmembrane ubiquitin ligase required to sort membrane proteins into multivesicular bodies. Nat Cell Biol *4*, 117-123.

Reimann, J. D., Freed, E., Hsu, J. Y., Kramer, E. R., Peters, J. M., and Jackson, P. K. (2001a). Emi1 is a mitotic regulator that interacts with Cdc20 and inhibits the anaphase promoting complex. Cell *105*, 645-655.

Reimann, J. D., Gardner, B. E., Margottin-Goguet, F., and Jackson, P. K. (2001b). Emi1 regulates the anaphase-promoting complex by a different mechanism than Mad2 proteins. Genes Dev *15*, 3278-3285.

Roepstorff, P., and Fohlman, J. (1984). Proposal for a common nomenclature for sequence ions in mass spectra of peptides. Biomed Mass Spectrom *11*, 601.

Romanienko, P. J., and Camerini-Otero, R. D. (2000). The mouse Spo11 gene is required for meiotic chromosome synapsis. Mol Cell *6*, 975-987.

Rostom, A. A., and Robinson, C. V. (1999). Disassembly of intact multiprotein complexes in the gas phase. Curr Opin Struct Biol *9*, 135-141.

Rudner, A. D., Hardwick, K. G., and Murray, A. W. (2000). Cdc28 activates exit from mitosis in budding yeast. J Cell Biol *149*, 1361-1376.

Rudner, A. D., and Murray, A. W. (2000). Phosphorylation by Cdc28 activates the Cdc20-dependent activity of the anaphase-promoting complex. J Cell Biol *149*, 1377-1390.

Salah, S. M., and Nasmyth, K. (2000). Destruction of the securin Pds1p occurs at the onset of anaphase during both meiotic divisions in yeast. Chromosoma *109*, 27-34.

Scheffner, M., Huibregtse, J. M., Vierstra, R. D., and Howley, P. M. (1993). The HPV-16 E6 and E6-AP complex functions as a ubiquitin-protein ligase in the ubiquitination of p53. Cell *75*, 495-505.

Scheffner, M., Nuber, U., and Huibregtse, J. M. (1995). Protein ubiquitination involving an E1-E2-E3 enzyme ubiquitin thioester cascade. Nature *373*, 81-83.

Schiller, J., Suss, R., Fuchs, B., Muller, M., Petkovic, M., Zschornig, O., and Waschipky, H. (2006). The suitability of different DHB isomers as matrices for the MALDI-TOF MS analysis of phospholipids: which isomer for what purpose? Eur Biophys J.

Schneper, L., Duvel, K., and Broach, J. R. (2004). Sense and sensibility: nutritional response and signal integration in yeast. Curr Opin Microbiol *7*, 624-630.

Schwab, M., Lutum, A. S., and Seufert, W. (1997). Yeast Hct1 is a regulator of Clb2 cyclin proteolysis. Cell *90*, 683-693.

Schwab, M., Neutzner, M., Mocker, D., and Seufert, W. (2001). Yeast Hct1 recognizes the mitotic cyclin Clb2 and other substrates of the ubiquitin ligase APC. Embo J *20*, 5165-5175.

Schwacha, A., and Kleckner, N. (1995). Identification of double Holliday junctions as intermediates in meiotic recombination. Cell *83*, 783-791.

Schwickart, M., Havlis, J., Habermann, B., Bogdanova, A., Camasses, A., Oelschlaegel, T., Shevchenko, A., and Zachariae, W. (2004). Swm1/Apc13 is an evolutionarily conserved subunit of the anaphase-promoting complex stabilizing the association of Cdc16 and Cdc27. Mol Cell Biol *24*, 3562-3576.

Schwob, E., Bohm, T., Mendenhall, M. D., and Nasmyth, K. (1994). The B-type cyclin kinase inhibitor p40SIC1 controls the G1 to S transition in S. cerevisiae. Cell *79*, 233-244.

Schwob, E., and Nasmyth, K. (1993). CLB5 and CLB6, a new pair of B cyclins involved in DNA replication in Saccharomyces cerevisiae. Genes Dev *7*, 1160-1175.

Scigelova, M., and Makarov, A. (2006). Orbitrap mass analyzer - overview and applications in proteomics. Proteomics *6 Suppl 2*, 16-21.

Sechi, S., and Chait, B. T. (1998). Modification of cysteine residues by alkylation. A tool in peptide mapping and protein identification. Anal Chem *70*, 5150-5158.

Seeger, M., Hartmann-Petersen, R., Wilkinson, C. R., Wallace, M., Samejima, I., Taylor, M. S., and Gordon, C. (2003). Interaction of the anaphase-promoting complex/cyclosome and proteasome protein complexes with multiubiquitin chain-binding proteins. J Biol Chem *278*, 16791-16796.

Seufert, W., Futcher, B., and Jentsch, S. (1995). Role of a ubiquitin-conjugating enzyme in degradation of S- and M-phase cyclins. Nature *373*, 78-81.

Shahgholi, M., Garcia, B. A., Chiu, N. H., Heaney, P. J., and Tang, K. (2001). Sugar additives for MALDI matrices improve signal allowing the smallest nucleotide change (A:T) in a DNA sequence to be resolved. Nucleic Acids Res *29*, E91.

Shirayama, M., Toth, A., Galova, M., and Nasmyth, K. (1999). APC(Cdc20) promotes exit from mitosis by destroying the anaphase inhibitor Pds1 and cyclin Clb5. Nature *402*, 203-207.

Shirayama, M., Zachariae, W., Ciosk, R., and Nasmyth, K. (1998). The Polo-like kinase Cdc5p and the WD-repeat protein Cdc20p/fizzy are regulators and substrates of the anaphase promoting complex in Saccharomyces cerevisiae. Embo J *17*, 1336-1349.

Shivakumar, L., Minna, J., Sakamaki, T., Pestell, R., and White, M. A. (2002). The RASSF1A tumor suppressor blocks cell cycle progression and inhibits cyclin D1 accumulation. Mol Cell Biol *22*, 4309-4318.

Shou, W. Z., and Naidong, W. (2005). Simple means to alleviate sensitivity loss by trifluoroacetic acid (TFA) mobile phases in the hydrophilic interaction chromatography-electrospray tandem mass spectrometric (HILIC-ESI/MS/MS) bioanalysis of basic compounds. J Chromatogr B Analyt Technol Biomed Life Sci *825*, 186-192.

Shteinberg, M., Protopopov, Y., Listovsky, T., Brandeis, M., and Hershko, A. (1999). Phosphorylation of the cyclosome is required for its stimulation by Fizzy/cdc20. Biochem Biophys Res Commun *260*, 193-198.

Sigismund, S., Polo, S., and Di Fiore, P. P. (2004). Signaling through monoubiquitination. Curr Top Microbiol Immunol *286*, 149-185.

Sigrist, S., Jacobs, H., Stratmann, R., and Lehner, C. F. (1995). Exit from mitosis is regulated by Drosophila fizzy and the sequential destruction of cyclins A, B and B3. Embo J *14*, 4827-4838.

Sigrist, S. J., and Lehner, C. F. (1997). Drosophila fizzy-related down-regulates mitotic cyclins and is required for cell proliferation arrest and entry into endocycles. Cell *90*, 671-681.

Song, M. S., and Lim, D. S. (2004). Control of APC-Cdc20 by the tumor suppressor RASSF1A. Cell Cycle *3*, 574-576.

Song, M. S., Song, S. J., Ayad, N. G., Chang, J. S., Lee, J. H., Hong, H. K., Lee, H., Choi, N., Kim, J., Kim, H.*, et al.* (2004). The tumour suppressor RASSF1A regulates mitosis by inhibiting the APC-Cdc20 complex. Nat Cell Biol *6*, 129-137.

Spellman, P. T., Sherlock, G., Zhang, M. Q., Iyer, V. R., Anders, K., Eisen, M. B., Brown, P. O., Botstein, D., and Futcher, B. (1998). Comprehensive identification of cell cycle-regulated genes of the yeast Saccharomyces cerevisiae by microarray hybridization. Mol Biol Cell *9*, 3273-3297.

Stapels, M. D., and Barofsky, D. F. (2004). Complementary use of MALDI and ESI for the HPLC-MS/MS analysis of DNA-binding proteins. Anal Chem *76*, 5423-5430.

Stapels, M. D., Cho, J. C., Giovannoni, S. J., and Barofsky, D. F. (2004). Proteomic analysis of novel marine bacteria using MALDI and ESI mass spectrometry. J Biomol Tech *15*, 191-198.

Steen, H., Jebanathirajah, J. A., Rush, J., Morrice, N., and Kirschner, M. W. (2006). Phosphorylation analysis by mass spectrometry: myths, facts, and the consequences for qualitative and quantitative measurements. Mol Cell Proteomics *5*, 172-181.

Steen, H., Jebanathirajah, J. A., Springer, M., and Kirschner, M. W. (2005). Stable isotope-free relative and absolute quantitation of protein phosphorylation stoichiometry by MS. Proc Natl Acad Sci U S A *102*, 3948-3953.

Stensballe, A., Andersen, S., and Jensen, O. N. (2001). Characterization of phosphoproteins from electrophoretic gels by nanoscale Fe(III) affinity chromatography with off-line mass spectrometry analysis. Proteomics *1*, 207-222.

Stensballe, A., and Jensen, O. N. (2004). Phosphoric acid enhances the performance of Fe(III) affinity chromatography and matrix-assisted laser desorption/ionization tandem mass spectrometry for recovery, detection and sequencing of phosphopeptides. Rapid Commun Mass Spectrom *18*, 1721-1730.

Stern, B. M., and Murray, A. W. (2001). Lack of tension at kinetochores activates the spindle checkpoint in budding yeast. Curr Biol *11*, 1462-1467.

Stewart, A. F., Bonsing, J., Beattie, C. W., Shah, F., Willis, I. M., and Mackinlay, A. G. (1987). Complete nucleotide sequences of bovine alpha S2- and beta-casein cDNAs: comparisons with related sequences in other species. Mol Biol Evol *4*, 231-241.

Strader, M. B., Verberkmoes, N. C., Tabb, D. L., Connelly, H. M., Barton, J. W., Bruce, B. D., Pelletier, D. A., Davison, B. H., Hettich, R. L., Larimer, F. W., and Hurst, G. B. (2004). Characterization of the 70S Ribosome from Rhodopseudomonas palustris using an integrated "top-down" and "bottom-up" mass spectrometric approach. J Proteome Res *3*, 965-978.

Stults, J. T. (1995). Matrix-assisted laser desorption/ionization mass spectrometry (MALDI-MS). Curr Opin Struct Biol *5*, 691-698.

Sudakin, V., Chan, G. K., and Yen, T. J. (2001). Checkpoint inhibition of the APC/C in HeLa cells is mediated by a complex of BUBR1, BUB3, CDC20, and MAD2. J Cell Biol *154*, 925-936.

Sudakin, V., Ganoth, D., Dahan, A., Heller, H., Hershko, J., Luca, F. C., Ruderman, J. V., and Hershko, A. (1995). The cyclosome, a large complex containing cyclin-selective ubiquitin ligase activity, targets cyclins for destruction at the end of mitosis. Mol Biol Cell *6*, 185-197.

Swaminathan, S., Amerik, A. Y., and Hochstrasser, M. (1999). The Doa4 deubiquitinating enzyme is required for ubiquitin homeostasis in yeast. Mol Biol Cell *10*, 2583-2594.

Swanson, K. A., Hicke, L., and Radhakrishnan, I. (2006). Structural basis for monoubiquitin recognition by the Ede1 UBA domain. J Mol Biol *358*, 713-724.

Terrell, J., Shih, S., Dunn, R., and Hicke, L. (1998). A function for monoubiquitination in the internalization of a G protein-coupled receptor. Mol Cell *1*, 193-202.

Thapar, R., Marzluff, W. F., and Redinbo, M. R. (2004). Electrostatic contribution of serine phosphorylation to the Drosophila SLBP--histone mRNA complex. Biochemistry *43*, 9401-9412.

Thornton, B. R., Chen, K. C., Cross, F. R., Tyson, J. J., and Toczyski, D. P. (2004). Cycling without the cyclosome: modeling a yeast strain lacking the APC. Cell Cycle *3*, 629-633.

Thornton, B. R., Ng, T. M., Matyskiela, M. E., Carroll, C. W., Morgan, D. O., and Toczyski, D. P. (2006). An architectural map of the anaphase-promoting complex. Genes Dev *20*, 449-460.

Thornton, B. R., and Toczyski, D. P. (2003). Securin and B-cyclin/CDK are the only essential targets of the APC. Nat Cell Biol *5*, 1090-1094.

Thornton, B. R., and Toczyski, D. P. (2006). Precise destruction: an emerging picture of the APC. Genes Dev *20*, 3069-3078.

Thrower, J. S., Hoffman, L., Rechsteiner, M., and Pickart, C. M. (2000). Recognition of the polyubiquitin proteolytic signal. Embo J *19*, 94-102.

Tinker-Kulberg, R. L., and Morgan, D. O. (1999). Pds1 and Esp1 control both anaphase and mitotic exit in normal cells and after DNA damage. Genes Dev *13*, 1936-1949.

Toth, A., Rabitsch, K. P., Galova, M., Schleiffer, A., Buonomo, S. B., and Nasmyth, K. (2000). Functional genomics identifies monopolin: a kinetochore protein required for segregation of homologs during meiosis i. Cell *103*, 1155-1168.

Tyers, M. (1996). The cyclin-dependent kinase inhibitor p40SIC1 imposes the requirement for Cln G1 cyclin function at Start. Proc Natl Acad Sci U S A *93*, 7772-7776.

Tyers, M., and Jorgensen, P. (2000). Proteolysis and the cell cycle: with this RING I do thee destroy. Curr Opin Genet Dev *10*, 54-64.

Tyers, M., and Mann, M. (2003). From genomics to proteomics. Nature *422*, 193-197.

Ufano, S., San-Segundo, P., del Rey, F., and Vazquez de Aldana, C. R. (1999). SWM1, a developmentally regulated gene, is required for spore wall assembly in Saccharomyces cerevisiae. Mol Cell Biol *19*, 2118-2129.

Uhlmann, F., Lottspeich, F., and Nasmyth, K. (1999). Sister-chromatid separation at anaphase onset is promoted by cleavage of the cohesin subunit Scc1. Nature *400*, 37-42.

Veenstra, T. D. (2006). Global and targeted quantitative proteomics for biomarker discovery. J Chromatogr B Analyt Technol Biomed Life Sci.

Visintin, R., Craig, K., Hwang, E. S., Prinz, S., Tyers, M., and Amon, A. (1998). The phosphatase Cdc14 triggers mitotic exit by reversal of Cdk-dependent phosphorylation. Mol Cell *2*, 709-718.

Visintin, R., Hwang, E. S., and Amon, A. (1999). Cfi1 prevents premature exit from mitosis by anchoring Cdc14 phosphatase in the nucleolus. Nature *398*, 818-823.

Visintin, R., Prinz, S., and Amon, A. (1997). CDC20 and CDH1: a family of substrate-specific activators of APC-dependent proteolysis. Science *278*, 460-463.

Vodermaier, H. C., Gieffers, C., Maurer-Stroh, S., Eisenhaber, F., and Peters, J. M. (2003). TPR Subunits of the Anaphase-Promoting Complex Mediate Binding to the Activator Protein CDH1. Curr Biol *13*, 1459-1468.

Washburn, M. P., Wolters, D., and Yates, J. R., 3rd (2001). Large-scale analysis of the yeast proteome by multidimensional protein identification technology. Nat Biotechnol *19*, 242-247.

Watanabe, Y., and Nurse, P. (1999). Cohesin Rec8 is required for reductional chromosome segregation at meiosis. Nature *400*, 461-464.

Watanabe, Y., Yokobayashi, S., Yamamoto, M., and Nurse, P. (2001). Pre-meiotic S phase is linked to reductional chromosome segregation and recombination. Nature *409*, 359-363.

Wendt, K. S., Vodermaier, H. C., Jacob, U., Gieffers, C., Gmachl, M., Peters, J. M., Huber, R., and Sondermann, P. (2001). Crystal structure of the APC10/DOC1 subunit of the human anaphase-promoting complex. Nat Struct Biol *8*, 784-788.

Whitehouse, M. W., and Cleland, L. G. (1985). Reactive oxygen species and drug therapy for inflammatory diseases. Agents Actions Suppl *17*, 177-188.

Wilm, M., Shevchenko, A., Houthaeve, T., Breit, S., Schweigerer, L., Fotsis, T., and Mann, M. (1996). Femtomole sequencing of proteins from polyacrylamide gels by nano-electrospray mass spectrometry. Nature *379*, 466-469.

Wittenberg, C., and Reed, S. I. (1988). Control of the yeast cell cycle is associated with assembly/disassembly of the Cdc28 protein kinase complex. Cell *54*, 1061-1072.

Wolters, D. A., Washburn, M. P., and Yates, J. R., 3rd (2001). An automated multidimensional protein identification technology for shotgun proteomics. Anal Chem *73*, 5683-5690.

Wu, G., Xu, G., Schulman, B. A., Jeffrey, P. D., Harper, J. W., and Pavletich, N. P. (2003). Structure of a beta-TrCP1-Skp1-beta-catenin complex: destruction motif binding and lysine specificity of the SCF(beta-TrCP1) ubiquitin ligase. Mol Cell *11*, 1445-1456.

Xhou, W., Merrick, B. A., Khaledi, M. G., and Tomer, K. B. (2000). Detection and sequencing of phosphopeptides affinity bound to immobilized metal ion beads by matrix-assisted laser desorption/ionization mass spectrometry. J Am Soc Mass Spectrom *11*, 273-282.

Yam, C. H., Fung, T. K., and Poon, R. Y. (2002). Cyclin A in cell cycle control and cancer. Cell Mol Life Sci *59*, 1317-1326.

Yamasaki, L., and Pagano, M. (2004). Cell cycle, proteolysis and cancer. Curr Opin Cell Biol *16*, 623-628.

Yates, J. R., 3rd, Carmack, E., Hays, L., Link, A. J., and Eng, J. K. (1999). Automated protein identification using microcolumn liquid chromatography-tandem mass spectrometry. Methods Mol Biol *112*, 553-569.

Yeong, F. M., Lim, H. H., Wang, Y., and Surana, U. (2001). Early expressed Clb proteins allow accumulation of mitotic cyclin by inactivating proteolytic machinery during S phase. Mol Cell Biol *21*, 5071-5081.

Yoon, H. J., Feoktistova, A., Chen, J. S., Jennings, J. L., Link, A. J., and Gould, K. L. (2006). Role of Hcn1 and its phosphorylation in fission yeast anaphase-promoting complex/cyclosome function. J Biol Chem *281*, 32284-32293.

Yoon, H. J., Feoktistova, A., Wolfe, B. A., Jennings, J. L., Link, A. J., and Gould, K. L. (2002). Proteomics analysis identifies new components of the fission and budding yeast anaphase-promoting complexes. Curr Biol *12*, 2048-2054.

Yost, R. A., and Boyd, R. K. (1990). Tandem mass spectrometry: quadrupole and hybrid instruments. Methods Enzymol *193*, 154-200.

Zachariae, W. (2004). Destruction with a box: substrate recognition by the anaphase-promoting complex. Mol Cell *13*, 2-3.

Zachariae, W., and Nasmyth, K. (1999). Whose end is destruction: cell division and the anaphase-promoting complex. Genes Dev *13*, 2039-2058.

Zachariae, W., Schwab, M., Nasmyth, K., and Seufert, W. (1998a). Control of cyclin ubiquitination by CDK-regulated binding of Hct1 to the anaphase promoting complex. Science *282*, 1721-1724.

Zachariae, W., Shevchenko, A., Andrews, P. D., Ciosk, R., Galova, M., Stark, M. J., Mann, M., and Nasmyth, K. (1998b). Mass spectrometric analysis of the anaphase-promoting complex from yeast: identification of a subunit related to cullins. Science *279*, 1216-1219.

Zachariae, W., Shin, T. H., Galova, M., Obermaier, B., and Nasmyth, K. (1996). Identification of subunits of the anaphase-promoting complex of Saccharomyces cerevisiae. Science *274*, 1201-1204.

Zhao, X., Muller, E. G., and Rothstein, R. (1998). A suppressor of two essential checkpoint genes identifies a novel protein that negatively affects dNTP pools. Mol Cell *2*, 329-340.

Zheng, L., Dominski, Z., Yang, X. C., Elms, P., Raska, C. S., Borchers, C. H., and Marzluff, W. F. (2003). Phosphorylation of stem-loop binding protein (SLBP) on two threonines triggers degradation of SLBP, the sole cell cycle-regulated factor required for regulation of histone mRNA processing, at the end of S phase. Mol Cell Biol *23*, 1590-1601.

Zhu, H., Bilgin, M., and Snyder, M. (2003). Proteomics. Annu Rev Biochem *72*, 783-812.

Zhu, Q., Wani, G., Wang, Q. E., El-mahdy, M., Snapka, R. M., and Wani, A. A. (2005). Deubiquitination by proteasome is coordinated with substrate translocation for proteolysis in vivo. Exp Cell Res *307*, 436-451.

Zur, A., and Brandeis, M. (2002). Timing of APC/C substrate degradation is determined by fzy/fzr specificity of destruction boxes. Embo J *21*, 4500-4510.